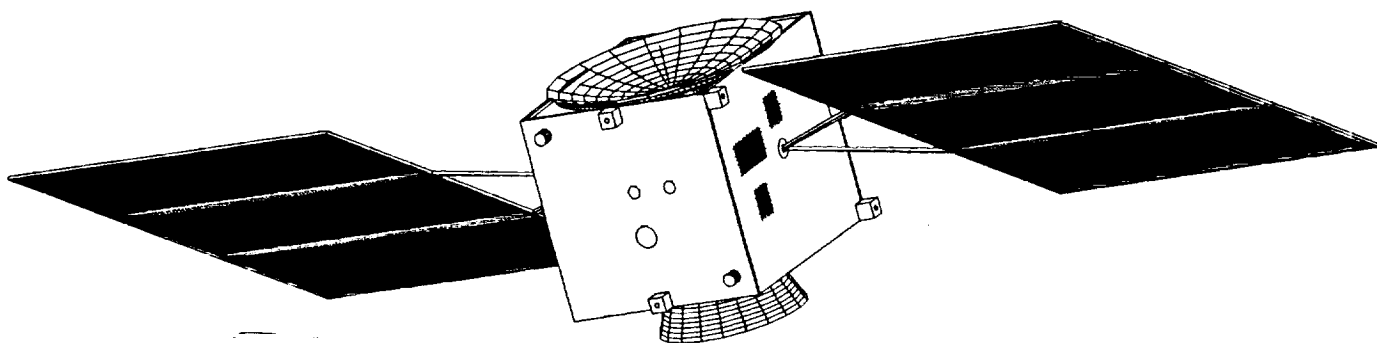


Near Earth Asteroid Rendezvous

IN-12-CR
204279
146P

Design Project for AE 4871

15 December, 1992
Naval Postgraduate School
Monterey, California



(NASA-CR-195518) NEAR EARTH
ASTEROID RENDEZVOUS (Naval
Postgraduate School) 146 p

N94-24808

Unclas

G3/12 0204279

Abstract

The AE4871 Spacecraft Design Course is the capstone design class for the M.S. in Astronautics at the Naval Postgraduate School. The Fall 92 class designed a spacecraft for the Near Earth Asteroid Rendezvous Mission (NEAR). The NEAR mission uses a robotic spacecraft to conduct up-close reconnaissance of a Near-Earth asteroid. Such a mission will provide information on Solar System formation and possible space resources. The spacecraft is intended to complete a NEAR mission as a relatively low-budget program while striving to gather as much information about the target asteroid as possible. A complete mission analysis and detailed spacecraft design were completed. Mission analysis includes orbit comparison and selection, payload and telemetry requirements, spacecraft configuration, and launch vehicle selection. Spacecraft design includes all major subsystems: structure, electrical power, attitude control, propulsion, payload integration, and thermal control. The resulting spacecraft demonstrates the possibility to meet the NEAR Mission requirements using existing technology, "off-the-shelf" components and a relatively low-cost launch vehicle.

TABLE OF CONTENTS

I. INTRODUCTION.....	1
A. Mission and Spacecraft Description	1
1. Near Earth Asteroid Rendezvous	1
2. Target Asteroids.....	2
3. Overall Design Criteria	3
B. Mission Phases	4
II. ORBITAL DYNAMICS	6
A. Selection of Orbits	6
B. Detailed Analysis	7
1. Launch/Injection	7
2. Cruise	7
3. Rendezvous/Capture.....	9
4. Operational Orbits.....	14
C. Perturbations/Station Keeping.....	15
D. Solar Eclipse.....	16
1. Launch/Injection	16
2. Operations.....	16
III. LAUNCH VEHICLE.....	17
A. Mission Requirements.....	17
B. Tradeoffs	17
C. Hardware Description	18
D. Performance.....	19
IV. STRUCTURE SUBSYSTEM	20
A. Requirements.....	20
B. Structural Component Design/Sizing	20
1. Central Tube Assembly	21
2. Interface Rings	22
3. Strut Assemblies.....	22
4. Equipment Panels.....	23
5. Decks	23
6. Structure Summary.....	25
V. SPACECRAFT CONFIGURATION	26
A. Propellant Tank Layout.....	26
1. Oxidizer Tanks/Central Tube Assembly	26
2. Fuel and N2 Tank/Center Deck Configuration.....	27
B. Equipment/Instrumentation Configuration	27
1. Plus Z Face.....	28
2. Minus Z Face	29
3. Plus Y Face	29
4. Minus Y Face.....	29
5. Plus X Face	31
6. Minus X Face.....	31
C. Solar Array Configuration.....	32
1. Deployed Configuration	32
2. Launch Configuration	33

D. Internal Packing.....	33
VI. PAYLOAD	36
A. Functional Description.....	36
1. Overview.....	36
2. Science Payload Subsystem	36
3. RF Communications Subsystem.....	37
4. Command and Data Handling Subsystem	38
5. Summary of Payload Subsystem Operation	38
B. Subsystem Design and Hardware Description.....	41
1. Science Payload Subsystem	41
2. Communications and Data Handling Subsystems	44
3. Command and Data Handling Subsystem	47
VII. ELECTRICAL POWER SUBSYSTEM (EPS).....	49
A. Functional Requirements	49
1. Overview.....	49
2. Power Requirements.....	49
B. EPS Description.....	51
1. General	51
2. Solar Array	52
3. Battery	52
4. Power Conditioning and Distribution	53
C. EPS Component Design, Analysis, and Selection.....	55
1. Battery	55
2. Solar Array Design.....	56
3. Frame Selection.....	59
4. Solar Array Drive Assembly (SADA) Selection.....	59
5. Power Conditioning and Distribution	59
VIII. ATTITUDE CONTROL	61
A. Functional Requirements	61
1. Operational Requirements.....	62
2. Designs Concept and Tradeoffs	62
B. System Description	63
C. Component Description	65
1. Reaction Wheel Assemblies (RWA's)	65
2. Sun Sensors.....	65
3. Fiber Optic Gyros (FOGS).....	66
4. Star Camera	67
D. System Integration and Performance	67
1. Moments of Inertia.....	68
2. Spin Stabilization.....	68
3. Acquisition Sequence	69
4. Three-axis Stabilization.....	69
IX. PROPULSION SUBSYSTEM.....	77
A. Functional Requirements	77
B. Design and Hardware.....	77
1. 468-N Thruster.....	77
2. 4.5-N Thrusters.....	79
3. Propellant Tanks	80
4. Miscellaneous.....	80
C. Performance.....	81
X. THERMAL CONTROL SUBSYSTEM	82

A. Functional Requirement	82
B. Design	82
C. Components.....	84
1. Multi-layer Insulation (MLI)	84
2. Optical Solar Reflectors (OSR).....	84
3. Heaters.....	85
D. Thermal analysis and Performance.....	85
E. PC-ITAS Node Analysis Initial Conditions and Assumptions.....	86
F. Conclusions	89
XI. CONCLUSION.....	90
APPENDIX A - STRUCTURAL CALCULATIONS	91
APPENDIX B - ORBITAL MECHANICS CALCULATIONS	97
APPENDIX C - LINK BUDGET CALCULATIONS.....	109
APPENDIX D - ELECTRICAL POWER SUBSYSTEM.....	124
APPENDIX E - ATTITUDE CONTROL CALCULATIONS	130
APPENDIX F - PROPULSION CALCULATIONS	134
APPENDIX G - MASS BUDGET SPREADSHEET	135
REFERENCES	140

I. INTRODUCTION

This design project was completed as part of course AE4871, Advanced Spacecraft Design, at the Naval Postgraduate School. The purpose of the mission is to send a satellite into a Near Earth Asteroid Rendezvous (NEAR) that will allow as much useful information about the asteroid as possible to be relayed to scientists on Earth, while keeping the cost down by using proven technology and low mass components. Cost efficiency is also achieved by designing a flexible spacecraft bus which is capable of performing follow-on missions.

The project focused on the design of a satellite to study near-earth asteroids, in order to compete in the AIAA / Lockheed Corporation Graduate Team Space Design Competition of 1993 (Design Competition). Each student participating in the course was assigned a primary and secondary area of responsibility. This report compiles the design proposals of the student team and provides a solid foundation for more detailed design.

A. MISSION AND SPACECRAFT DESCRIPTION

1. Near Earth Asteroid Rendezvous

The purpose of the mission is to send a satellite into a Near Earth Asteroid Rendezvous (NEAR) that will allow as much useful information about the asteroid as possible to be relayed to scientists on earth, while keeping the cost to reasonable levels by using components of proven heritage and low mass. NEAR missions will also promote relatively low-budget programs that will ensure that manufacturing proficiency and technical advance are retained while agency funding levels are reduced. The design team strove to create a satellite that would be compatible with a large variety of missions, so that cost could be further reduced by using the same bus for follow-on missions to multiple asteroids. The specific mission requirements, target asteroids and some other

information are included in the Design Competition rules and supplementary data package; these data are included in the report where they are used.

2. Target Asteroids

Four target asteroids were specifically delineated in the supplementary data package for consideration by the design team. Interplanetary trajectory solutions were provided for each and these solutions were used as the basis for the design, principally because solutions that would provide enhanced mission capabilities were out of the bounds of the software available during the term of this project. Orbital mechanics issues are more fully developed later; Table 1 lists the four target asteroids and their characteristics.

Asteroid	Seleucus	1982 XB	McAuliffe	Orpheus
Max. Solar Dist. (AU)	2.750	2.640	2.460	1.600
Max. Earth Dist. (AU)	3.430	3.600	2.180	2.580
C3 (km ² /sec ²)	36.880	27.799	38.745	17.72
Δv (km/s)	1.804	1.458	1.336	1.458
Payload Max (kg)	605	725	580	895
Launcher	Atlas IIA	Delta II	Atlas IIA	Delta II

Table 1. Asteroids Listed in the Supplementary Data Package

One of the most difficult decisions in the project focused on launcher selection. When the design was begun, a maximum solar distance of 2 AU was assumed for solar array sizing. It was thought that transfer trajectories could be found that would allow the satellite to reach the asteroid such that one year would be spent on station within 2 AU of the sun. With this assumption the team nearly completed the design of a spacecraft with a 605 kg launch mass that could satisfy any of these four missions using a Delta II launch vehicle providing 36.880 km²/sec². The C3 of 38.745 km²/sec² required for the McAuliffe mission would have been achieved by off loading some fuel, since the Δv requirement for that mission is relatively low.

When software limitations precluded adequate trajectory solutions for the transfer orbit to the asteroids, the transfer orbit data discussed in the Orbital Mechanics section were adopted,

along with the asteroid ephemerides listed in Table 1. Note that the maximum solar distance for each asteroid is the apoapsis of the asteroid orbit, except for Seleucus, where 2.75 AU is the solar range at the anticipated end of the mission. The solar arrays required for operation at a solar range of 2.75 AU have roughly twice the area of those needed at 2 AU. The bus was designed to be as small as possible while still providing a large Δv , so the extra weight requirement of the array forced the satellite mass from 605 kg to 725 kg when fully fueled for a Δv of 1.85 km/sec. As Table 1 shows, the Delta II can satisfy the 1982 XB and Orpheus missions where a lower C3 is required, but the more expensive Atlas IIA is required for the Seleucus and McAuliffe missions. The team still feels that with more study, trajectories can be found that will reduce the solar range enough to allow smaller solar arrays and Delta II launch for all four missions.

3. Overall Design Criteria

The spacecraft must be able to reach the asteroid within three years after launch and remain on station in the vicinity of the asteroid for a period of at least one year. The launch must occur between 1996 and 2006, with a ten day launch window. The spacecraft must be able to perform mid-course and rendezvous maneuvers, with a total Δv capability of 1.85 km/sec. It should also be able to maneuver in the asteroid vicinity. This design chose to orbit the asteroid, both to reduce fuel consumption and to lower the sensor range. The satellite must be capable of communicating via the NASA Deep Space Network (DSN) and autonomous operation for seven days, except during critical maneuvers.

Sensors should be capable of inferring mechanical and chemical properties of the asteroid. To achieve this science goal images in six colors with 6m per pixel pair resolution or better are required along with 300 m resolution approach and departure images, which are fully described in the Payload section. The payload will include a visible imager, an IR spectrometer, a laser altimeter and a magnetometer. A gamma-ray spectrometer is listed in the list of payload articles in the supplementary data package, but it was not included in this design because of the requirements

it imposes on the mission. The gamma-ray spectrometer weighs 16 kg and requires one month of cumulative time at an altitude of less than 1 asteroid body radius in order to achieve low levels of data error.

B. MISSION PHASES

The mission is broken into six phases of flight, starting with the *Launch Phase*, which is the period from booster ignition until spacecraft-booster separation. All systems are dormant, but the battery is functioning to maintain bus loads. The spacecraft will enter the earth's shadow shortly after launch for a period not to exceed 30 minutes. The battery is specifically designed to provide the requisite power for this period. The solar arrays will remain stowed and the spacecraft will be spinning with the momentum imparted by the launch system. Also during this phase, the Delta 3rd stage will fire for the transfer orbit insertion. The *Post-Eclipse Phase* begins when the spacecraft separates from the launch vehicle, exits the earth's shadow and begins to transfer to the asteroid. During this phase the satellite will be spinning with one-third of the solar array area exposed, so that the battery will be relieved while the spacecraft undergoes the transition to three-axis stabilization. The reaction wheel system will be started and the spin will be removed by thrusters. The solar arrays will be deployed once the attitude is controlled.

When the solar arrays are deployed and charging the batteries, the *Cruise Phase* has begun. The bulk of the mission will be spent in this phase as the spacecraft makes the transit to the rendezvous. A mid-course trajectory burn is performed in this phase if required. When the satellite approaches rendezvous, the *Acquisition Phase* is entered. As the spacecraft approaches the asteroid, images will be relayed that will allow a refined orbital solution so that the spacecraft can make a proper transition into an asteroid satellite. Once in orbit, the satellite is in the *Mission Phase*, which has two sub-phases: *Science Phase* and *Communication Phase*.

The Mission Phase has two parts because the satellite activity has two distinct categories. In the Science Phase, the +x face of the satellite is pointing at the asteroid to gather data while the

solar arrays continue to point the sun. When enough data is collected or when commanded from earth, the satellite will slew to point the High Gain Antenna (HGA) at earth because the data are transmitted much faster using the HGA link to the NASA Deep Space Network. The Science Phase requires much less power than the Communication Phase, so the battery supplements the power requirements of the Communication Phase. Throughout the mission, the satellite will continuously transition from the Science Phase to the Communication Phase of flight as it continues to send home information.

II. ORBITAL DYNAMICS

A. SELECTION OF ORBITS

The orbits of the NEAR spacecraft were determined from the mission, spacecraft and science requirements of the specification, as stated in Section, and the required asteroid targets. The four asteroid targets as designated in the supplementary data package are 1982XB, Orpheus, McAuliffe, and Seleucus. The parameters of each asteroid are shown in Table 2 and Table 3. Each of the targets was picked as a near earth asteroid that could be reached in the designated 3 years with the limited C3 of $40 \text{ km}^2/\text{sec}^2$ and the total delta-v of 1.85 km/sec. Unless otherwise stated, all coordinates are in reference to the solar ecliptic plane and the position of the autumnal equinox of 1950.

Asteroid	a (km)	e	Ω (deg)	ω (deg)	i (deg)	r_p (AU)	r_a (AU)	Period (days)
Orpheus	1.209	0.3226	189.14	301.57	2.688	0.819	1.599	485.75
McAuliffe	1.879	0.3695	106.90	15.59	4.777	1.185	2.573	940.6
1982XB	1.836	0.4467	74.53	16.78	3.874	1.016	2.655	908.4
Seleucus	2.033	0.4571	218.13	349.19	5.930	1.103	2.962	1058.5

Table 2. Asteroid Ephemerides

Asteroid	Mass (kg)	Gravitational Parameter (km^3/sec^2)	Radius (km)	Sphere of Influence (km)
Orpheus	8.042e11	5.364e-8	0.4	7.95
McAuliffe	2.171e13	1.448e-6	1.2	46.14
1982XB	1.005e14	6.705e-6	2.0	83.20
Seleucus	1.005e14	6.705e-6	2.0	92.14

Table 3. Asteroid Physical Characteristics

Note the mass of the asteroids is an estimated mass based on the assumptions that all the asteroid targets are spherical with a density of 3 gm/cm^3 . Lack of accurate data on the asteroids prevents better estimates of mass.

B. DETAILED ANALYSIS

The analysis of the orbits was made with the a few necessary assumptions. Because the shape of the asteroid is unknown, a perfectly spherical shape is assumed so that the only perturbing force is the gravitational pull of the sun. This analysis also assumes that the orbital parameters given in the supplementary data package are accurate. The orbital parameters in the package were used as valid and engineered to derive the relevant information since adequate software could not be found in the short amount of time available for the design. The last assumption is that the ten day launch window starts on the date given in the supplementary data package for the given C3 and that it ends ten days later with a C3 of 40.5 km²/sec².

1. Launch/Injection

The launch of the NEAR spacecraft to any one of the target asteroids is constrained by the practicality of a minimum Δv trajectory. Table 4 shows the trajectory parameters for launch.

Asteroid	Date of Launch	C3 km ² /sec ²	Velocity at Infinity (km/sec)			Heliocentric Velocity (km/sec)			Δv Injection (km/sec)	DLA (deg)	RLA (deg)
			x	y	z	x	y	z			
Orpheus	3/9/98	17.72	-3.136	-2.163	1.791	-8.252	-31.694	1.791	4.003	10.679	220.705
McAuliffe	1/15/99	38.745	-5.3	-2.634	1.926	-32.449	-16.046	1.926	4.862	6.607	210.995
1982XB	12/8/00	27.799	-4.648	0.702	2.388	-34.347	6.5	2.388	4.422	27.938	183.794
Seleucus	4/27/03	36.88	-4.39	2.894	21.406	-27.548	2.894	35.007	4.789	8.536	300.401

C3 = injection energy. Also, square of the velocity at infinity.

DLA = declination of launch asymptote; Earth equator and equinox of 1950 coordinates.

RLA = right ascension of launch asymptote; Earth equator and equinox of 1950 coordinates.

Table 4. Launch/Injection Orbital Parameters

2. Cruise

The cruise trajectory takes the NEAR spacecraft from launch and transfer orbit injection at earth to rendezvous/capture at the asteroid. The cruise orbit is divided into two phases of trajectory for all targets except 1982XB. Phase 1 trajectory takes the NEAR spacecraft from injection to the mid-course maneuver point, where a Δv burn puts the spacecraft on its final trajectory to the asteroid. Phase 2 trajectory takes the spacecraft from the mid-course maneuver

point to rendezvous/capture with the asteroid. Tables 5 and 6 list the Phase 1 and 2 transfer orbit parameters. Figures 1 through 4 show the cruise orbits from launch until arrival at the asteroid in the x-y, z-x, z-y planes.

The trajectory of the cruise orbit goes through maximum and minimum distances from the sun, distance from earth, sun angle and declination of Earth from the spacecraft. These variations affect the design of other parts of the NEAR spacecraft and are shown in Tables 7 and 8.

Asteroid	a (AU)	e	Ω (deg)	ω (deg)	i (deg)	Period of Transfer (days)	Mid-Course Δv (km/sec)	Mid-Course Date
Orpheus	1.250	0.205	171.080	0	3.130	220	1.228	10/15/98
McAuliffe	1.810	0.457	116.542	0	3.046	305	1.123	11/16/99
1982XB	1.542	0.362	78.585	0	3.908	757	N/A	N/A
Seleucus	1.657	0.392	219.29	0	4.742	400	0.603	6/1/04

Table 5. Phase 1 Cruise Orbit Parameters

Asteroid	a (AU)	e	Ω (deg)	ω (deg)	i (deg)	Period of Transfer (days)
Orpheus	1.182	0.307	-171.904	-57.014	2.707	175
McAuliffe	1.934	0.387	106.883	15.115	4.71	640
Seleucus	1.72	0.359	-140.637	-10.677	5.563	345

Table 6. Phase 2 Cruise Orbit Parameters

Asteroid	Distances (AU)				Angles (deg)			
	Max. Sun	Min. Sun	Max. Earth	Min. Earth	Max. Sun	Min. Sun	Max. Earth Declination	Min. Earth Declination
Orpheus	1.489	0.994	1.132	0	89.671	0	32.316	0
McAuliffe	2.445	0.983	3.293	0	90.000	10.174	18.002	0
1982XB	2.1	0.984	3.08	0	82.457	0	26.891	-7.589
Seleucus	2.306	1.008	3.304	0	89.996	0	28.369	-0.204

Table 7. Phase 1 Cruise Orbit Maxima and Minima

Asteroid	Distances (AU)				Angles (deg)			
	Max. Sun	Min. Sun	Max. Earth	Min. Earth	Max. Sun	Min. Sun	Max. Earth Declination	Min. Earth Declination
Orpheus	1.497	0.826	1.557	1.154	54.544	39.144	0.029	-1.773
McAuliffe	2.684	1.187	3.560	1.586	24.414	0.267	0.944	-4.553
Seleucus	2.305	1.106	3.216	0.571	64.719	8.197	-0.156	-14.414

Table 8. Phase 2 Cruise Orbit Maxima and Minima

3. Rendezvous/Capture

Rendezvous and capture with the asteroid begins with the acquisition of the asteroid 10 days before the encounter. After acquisition navigational corrections are made and the spacecraft approaches the asteroid for capture. Given the small orbital velocities about the asteroids, the limited Δv available and the small gravitational pull of the asteroid the NEAR spacecraft crosses near the asteroid (i.e. on the order of the desired orbital altitude). Also, the relative velocity of the spacecraft with respect to the asteroid must be small and less than or equal to the Δv available for capture. Tables 9 and 10 and show the rendezvous and capture parameters.

Asteroid	Relative Velocity (km/sec)			Relative Velocity (km/sec)	DAP (deg)	RAP (deg)	Phase Angle (deg)	Rendezvous Δv (km/sec)
	x	y	z					
Orpheus	0.19	0.13	0.03	0.230	6.293	35.307	88	0.230
McAuliffe	-0.20	-0.08	-0.02	0.213	-4.346	202.017	94	0.213
1982XB	1.08	0.98	0	1.458	-0.160	42.074	105	1.458
Seleucus	-0.43	1.07	-0.34	1.201	-16.257	111.612	92	1.201

Relative Velocity Components = the Cartesian velocity vector of the S/C with respect to the asteroid.

DAP = declination of arrival V_{inf}

RAP = right ascension of arrival V_{inf}

Phase Angle = Sun-asteroid-spacecraft angle on approach to the asteroid.

Table 9. Rendezvous Parameters

Asteroid	Velocity of Arrival (km/sec)	Asteroid Velocity at Arrival (km/sec)	ϕ_2 (deg)	θ (deg)	Circular Orbit Velocity (km/sec)
Orpheus	37.506	37.735	0.053	8.632	0.110 (4 km)
McAuliffe	32.041	31.828	0.068	10.066	0.455 (6 km)
1982XB	31.497	32.942	0.351	7.607	0.915 (6 km)
Seleucus	32.989	34.170	0.389	10.727	0.915 (6 km)

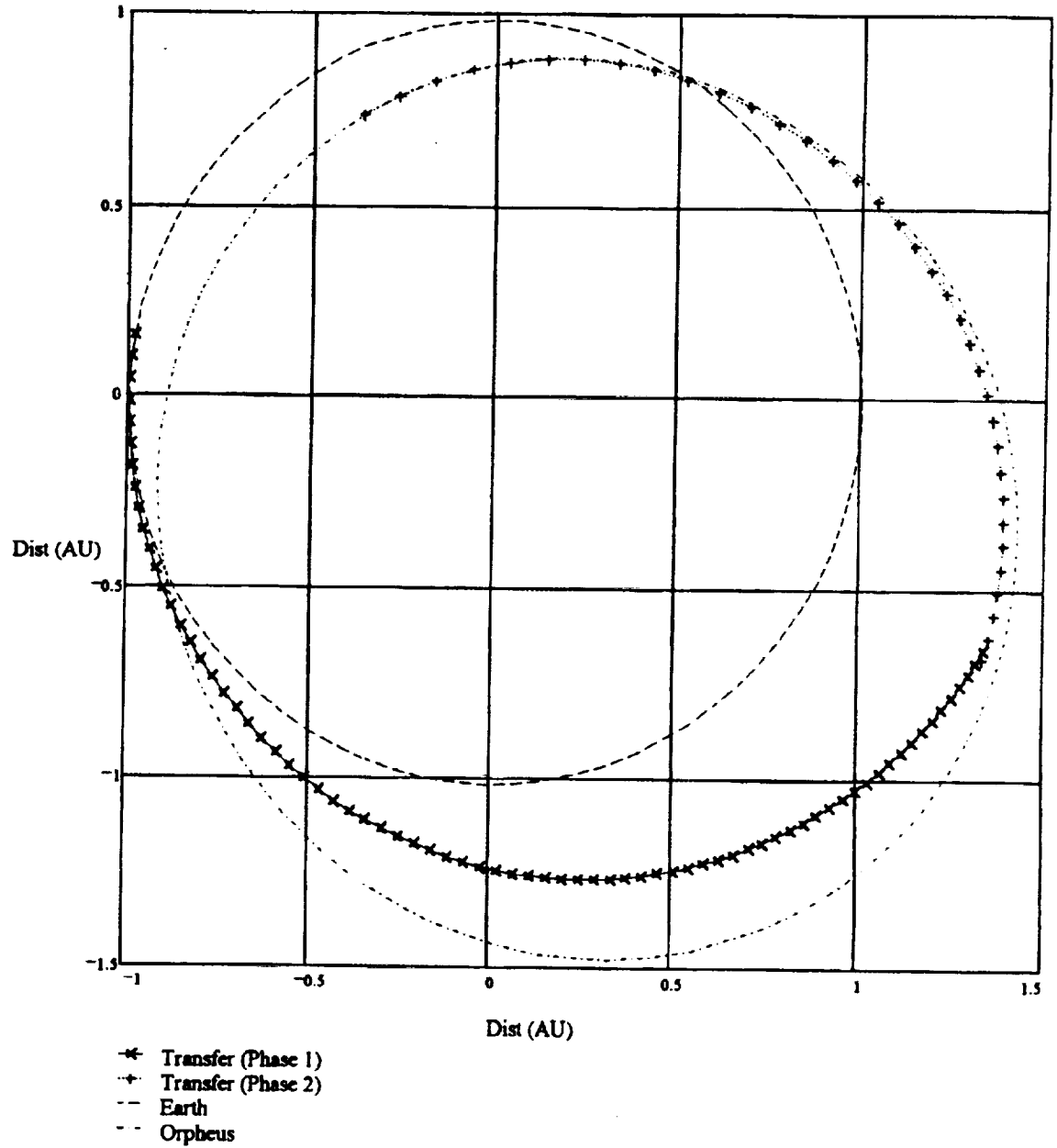
ϕ_2 = angle between spacecraft arrival velocity vector and asteroid orbital velocity vector.

θ = angle between V_{inf} vector and asteroid orbital velocity vector.

Table 10. Capture Parameters

ORPHEUS TRANSFER ORBIT (X-Y Plane)

Transfer Time tics in 3 day increments for Phase 1 and 5 day increments for Phase 2



1.42693

Figure 1. Orpheus Cruise Trajectory (x-y plane)

McAULIFFE TRANSFER ORBIT (X-Y Plane)
 Transfer Time tics in 30 day increments

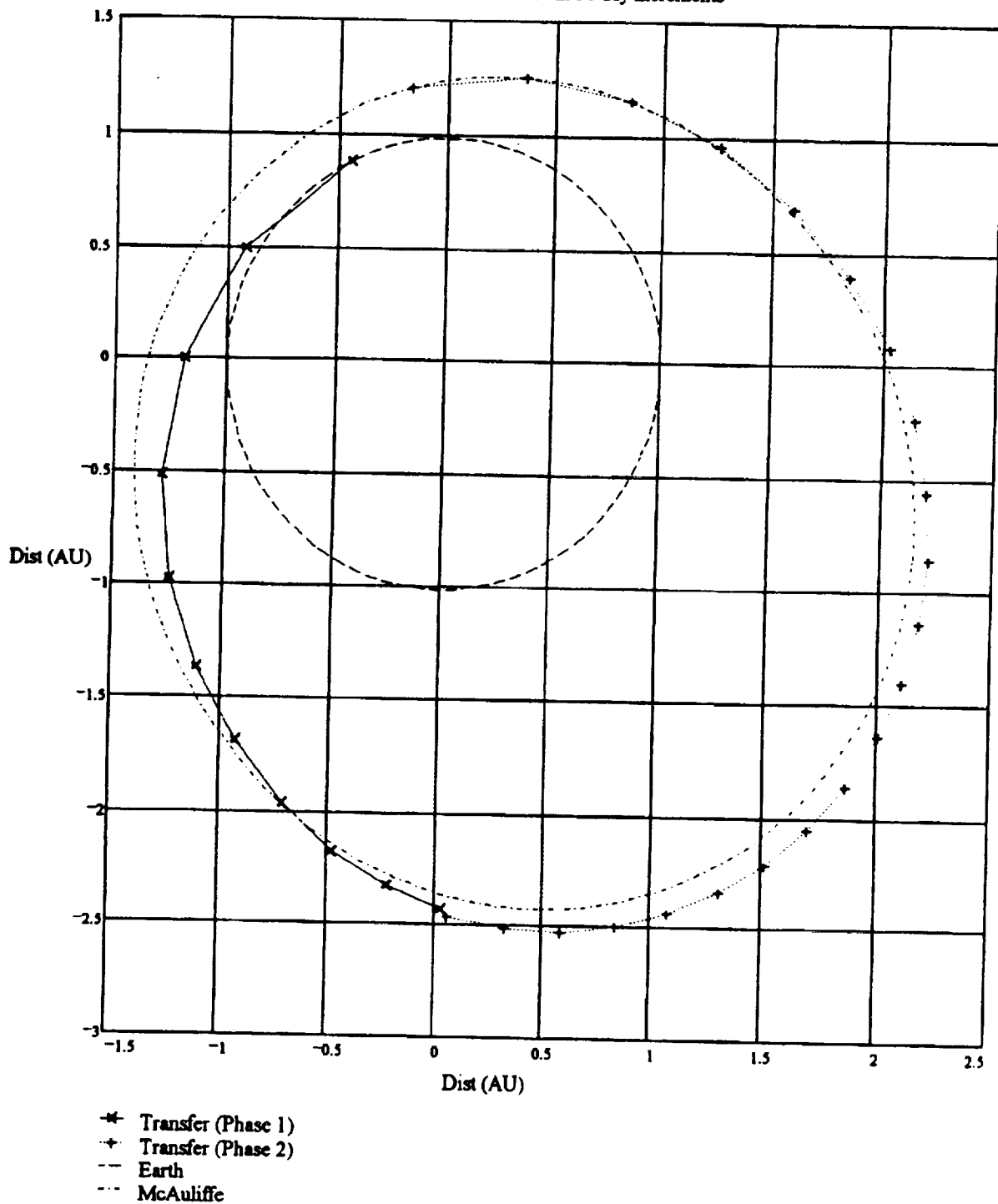


Figure 2. McAuliffe Cruise Trajectory (x-y plane)

1982XB TRANSFER ORBIT (X-Y Plane)
Transfer Time tics in 15 day increments

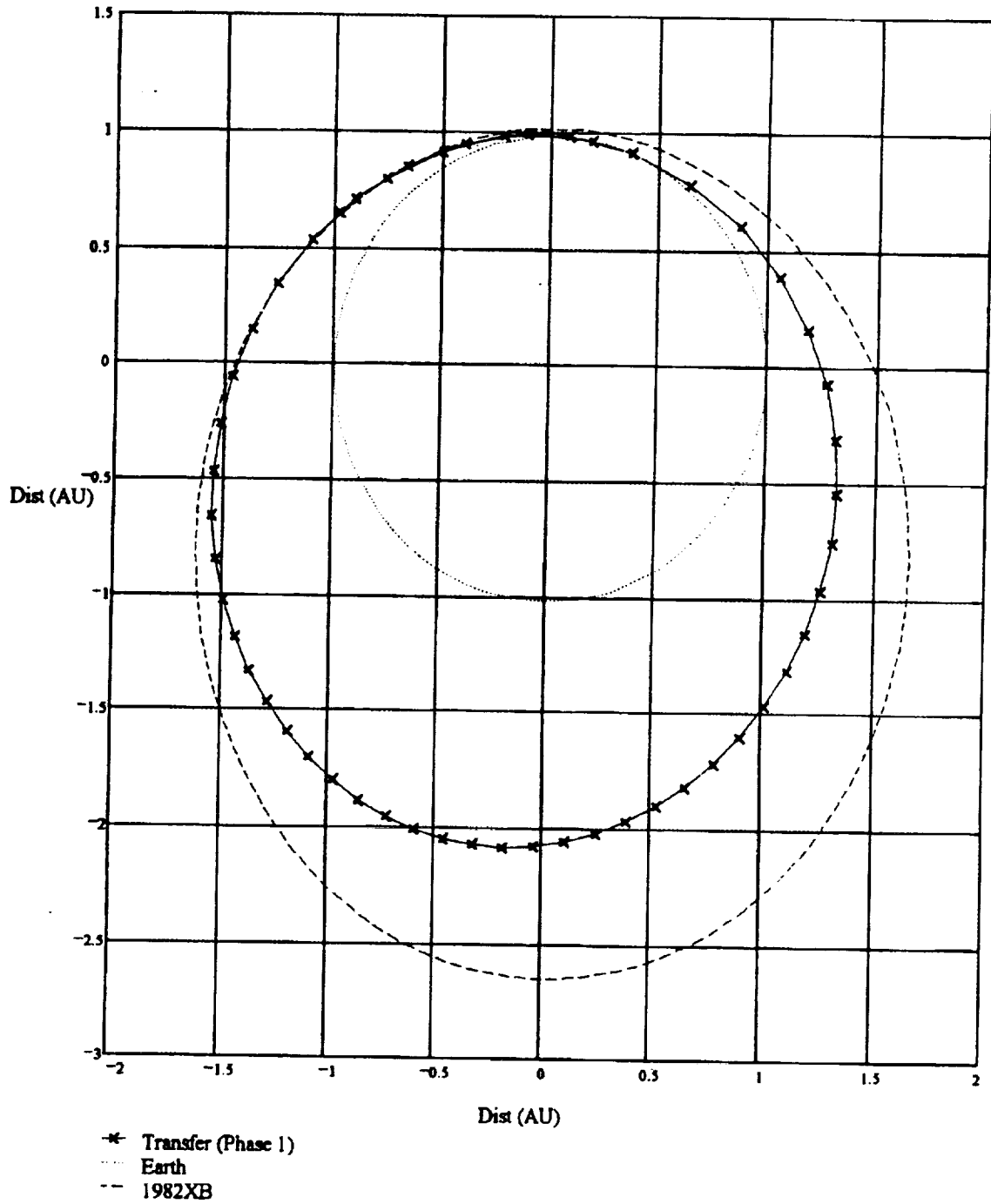


Figure 3. 1982XB Cruise Trajectory (x-y plane)

SELEUCUS TRANSFER ORBIT (X-Y Plane)
 Transfer Time tics in 15 day increments

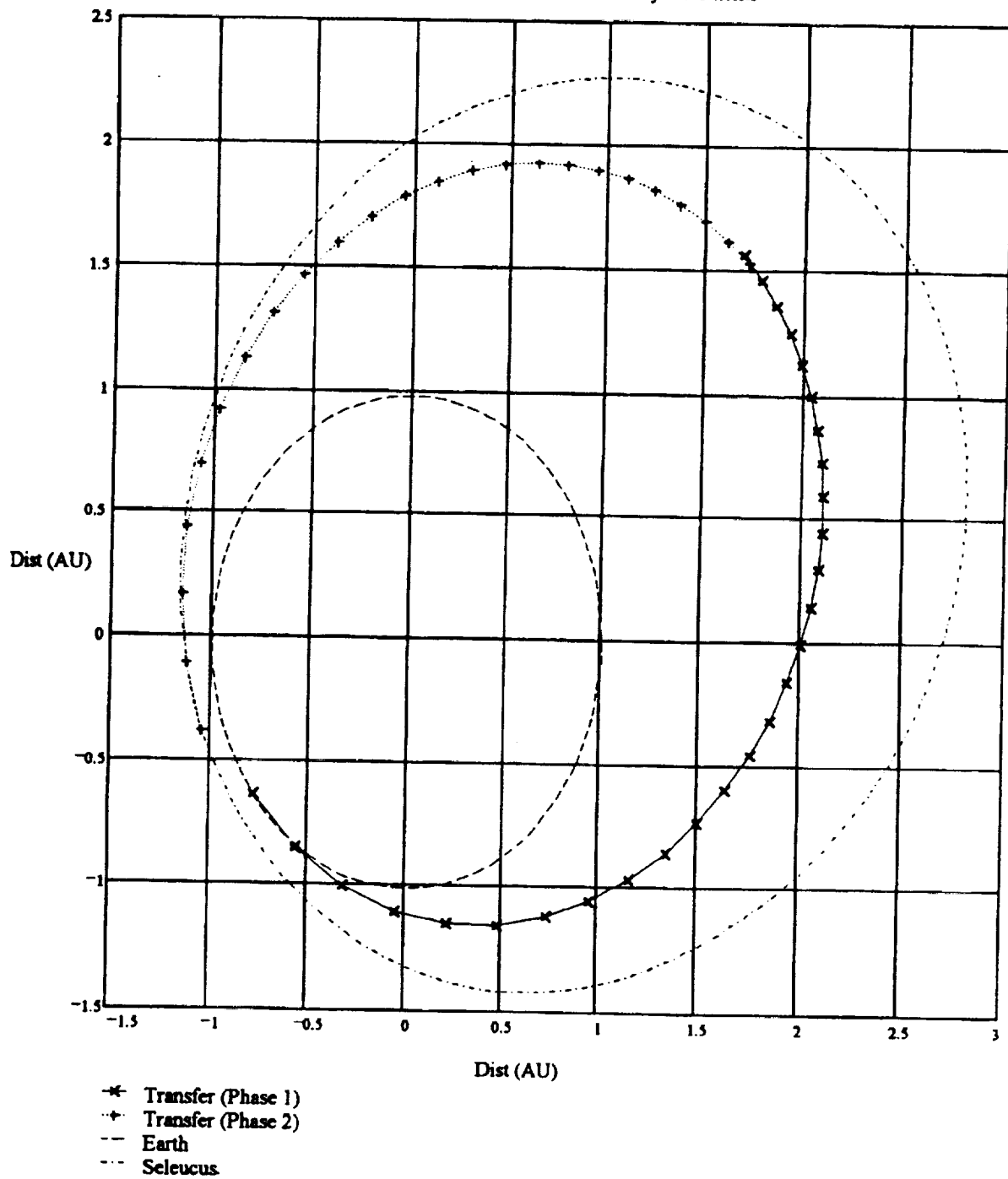


Figure 4. Seleucus Cruise Trajectory (x-y plane)

4. Operational Orbits

The asteroid operational orbits were chosen to maximize science operations during the one year of operations and to provide a optimal margin of safety in light of the requirement to be able to operate autonomously for 7 days. Analysis of the orbits was conducted using the Artificial Satellite Analysis Program (ASAP) Version 2.0. The following assumptions were made.

- All the target asteroids are spherical in shape.
- The density of the asteroids is 3 gm/cm^3 .
- The asteroid's spin axis inclination is equal to the inclination of its orbit with the ecliptic.
- The maximum solar eclipse period the spacecraft could withstand is 1.5 hours due to battery limitations.

The orbital analysis for the satellite on-station around the asteroid results in orbits with three characteristics: 1) The plane of the orbit is normal to the Earth-Asteroid line which simplifies communications with Earth since the instrument panel is at right angles to the high gain antenna. 2) The orbit altitude is 6 km for all asteroids with the exception of Orpheus, which is 4 km due to its smaller size. These altitudes allow the science mission to meet its requirements while still providing a margin of safety of $\pm 1 \text{ km}$. These altitudes also keep perturbations within an acceptable level. 3) The orbital plane is canted slightly from the sun terminator line on the asteroid to allow optimal lighting for imaging.

Table 11 lists the initial orbital parameters. Upon arrival at the asteroid the orbit can be adjusted to correct for the actual conditions and to allow for images and spectra to be taken at small phase angles. These adjustment are made at a very small Δv cost (on the order of 0.1-1.0 m/sec Δv per maneuver).

Asteroid	a (km)	e	Ω (deg)	ω (deg)	i (deg)	Altitude (km)	Period (hr.)
Orpheus	6.4	0	169.0	0	91.0	4	70
McAuliffe	7.2	0	-70.0	0	89.0	6	28
1982XB	8.0	0	32.0	0	86.0	6	15.2
Seleucus	8.0	0	194.0	0	194.0	6	15.2

Table 11. Initial Operational Orbit Parameters

During the one year of operations the NEAR spacecraft goes through maximum and minimums in distance from the sun, distance from earth, sun angle and declination of Earth from the spacecraft. These variations affect the design of other parts of the NEAR spacecraft and are shown in Table 12.

Asteroid	Distances (AU)				Angles (deg)			
	Max. Sun	Min. Sun	Max. Earth	Min. Earth	Max. Sun	Min. Sun	Max. Earth Declination	Min. Earth Declination
Orpheus	1.599	0.819	2.583	1.560	38.391	1.106	1.725	-1.237
McAuliffe	2.463	1.185	2.176	1.209	32.219	1.733	4.615	0.063
1982XB	2.642	1.131	3.597	0.667	60.066	0.761	9.065	-0.511
Seleucus	2.749	1.103	3.427	1.099	54.858	1.541	5.211	-1.871

Table 12. Operational Orbit Maxima and Minima

C. PERTURBATIONS/STATION KEEPING

Perturbations of the asteroid operational altitudes were analyzed using ASAP. The perturbations while in orbit around any of the target asteroids derive mainly from the forces of solar gravitation and solar wind. The solar wind, being the weaker of the two forces, acts to reduce the effect of the solar gravitational pull. The overall effect on the orbit around the asteroid is to turn the initial circular orbit into an eccentric one. This gradually reduces the periapsis altitude until it drops below the margin level of nominal altitude, 1 km. At this point a Δv correction is made to put the orbit back to a circular orbit of an altitude of 6 km. Corrections for altitude will be required every 15 days for Orpheus and McAuliffe and every 30 days for 1982XB and Seleucus. Δv 's for all the asteroids while conducting these maneuvers range from 0.01 to 0.1 m/sec. This gives a total Δv requirement for station keeping in the range of 0.25 to 1.25 m/sec for the entire one year of station-keeping.

D. SOLAR ECLIPSE

Solar eclipse by either the Earth at launch or the asteroid during operations is a concern as the design of the NEAR spacecraft only allows for 1.5 hours of battery operating time. The selection of the respective trajectories and orbits is heavily influenced by this limitation.

1. Launch/Injection

Solar eclipse during the launch/injection is limited to approximately 24 minutes from the time of entry into the Earth's shadow to the exit from it. Entry into eclipse occurs after launch and before interplanetary trajectory insertion. Insertion into the cruise trajectory occurs approximately 6 minutes after entry into the Earth's shadow.

2. Operations

Solar eclipse while on station at the asteroid is determined by the angle between the sun and the orbit plane (the "Beta" angle). With the orbit plane held perpendicular to the asteroid-earth line for the duration of operations at the asteroid, the Beta angle varies. For eclipse to occur the absolute value of the Beta angle must be less than the critical for the given orbit altitude, but even then the orbit is only partially eclipse. Critical angles for the orbit altitudes chosen are 5.2, 8.6, 14.5 and 14.5 degrees for Orpheus, McAuliffe, 1982XB and Seleucus respectively. For the orbits chosen, no eclipse periods are predicted for any of the target asteroids.

III. LAUNCH VEHICLE

A. MISSION REQUIREMENTS

The launch vehicle must be capable of providing a C3 value of $40 \text{ km}^2/\text{s}^2$, with the earliest launch date of 1996. Given the estimated size of the spacecraft (605-725 kg), four launchers that are readily available to the US. market are capable of this performance. These include the Delta II 7925, Atlas-Centaur II, Titan II-G SLV, and Ariane IV. Other expendable launch vehicles (ELV's) are either too small (e.g., Pegasus, Scout, Conestoga, etc.) or too large (e.g., Titan III/IV, etc.).

B. TRADEOFFS

Of the four launchers chosen, two were eliminated by factors other than cost or performance. The Ariane series, while completely capable of fulfilling the mission, was eliminated due to the political sensitivity of launching an American satellite on a French rocket when American launchers are available.

The second launcher eliminated was the Titan II-G SLV. This launcher is a refurbished intercontinental ballistic missile from the 1960's. These missiles, which are currently stored in a warehouse at Norton Air Force Base in Riverside, California, are shipped to the Martin Marietta plant in Denver, Colorado for overhaul. Liaison with the Air Force Titan II program office at Los Angeles AFB indicates that the first available vehicle could not be launched until FY97 due to refurbishing time and an earlier request by the Air Force SDI office to use a Titan II-G for the SDI Clementine mission. Therefore, the Titan II-G couldn't meet the earliest launch requirement. Currently, the Titan II-G is only launched from Vandenberg AFB, CA. The launch azimuths available from Vandenberg extend westward from NNW to South, so the advantage of launching eastward from Cape Canaveral to gain the rotational velocity of the Earth is lost. To achieve the

required C3 value, solid strap-on motors would be needed. A comparison of costs shows the basic refurbished Titan II-G listed at \$42.7 million (Baker, 1992). Add the hardware and integration costs of strap-ons, and the total cost is roughly \$50 million. For this amount, a brand new Delta II could be purchased. Finally, only 3 Titan II's have been launched since the Gemini program in the 1960's, so the question of reliability must be raised. For these reasons, the Titan II-G SLV was eliminated.

Of the two remaining launchers, the Delta II 7925 is the obvious choice for cost reduction. Obtaining current Delta II cost data is difficult due to ongoing litigation between the Air Force and McDonnell Douglas regarding release of this information. However, comparison with past cost figures and estimates by Air Force program personnel yields an approximate cost of \$54.1 million for the Delta II 7925 (Roddy, 1992). In comparison, the cost figure for the Atlas-Centaur II is \$71 million (Ginser, 1992). The Delta II 7925 with the standard 9.5-foot (2.9 m) fairing is capable of lifting 570 kg to required C3 value. If the smaller 8-foot fairing is used on the Delta, this figure increases to 588 kg. In comparison, the Atlas-Centaur II is capable of lifting 732 kg. For the missions listed in the design guidelines, the Delta II is capable of the performance required for two missions, at greatly reduced cost. The Delta II has had over 200 launches since 1960 and has had a 98% success rate over the past 12 years. For these reasons, the Delta II 7925 was chosen as the launch vehicle for this design.

C. HARDWARE DESCRIPTION

The Delta II 7925 is a three-stage launch vehicle manufactured by McDonnell Douglas. The first stage liquid-propellant booster is powered by a Rocketdyne RS-27 main engine, assisted by nine externally-mounted Hercules graphite epoxy motors. The second stage consists of the restartable Aerojet AJ10-118K engine and a guidance and control electronics suite that controls guidance stabilization for the first two stages. The third stage consists of a STAR-48B solid rocket

motor supported at the base on a spin table that mounts to the upper portion of the second stage. Prior to third-stage deployment, the stage and spacecraft are spun up using spin rockets. The spacecraft is housed inside a 9.5-foot diameter aluminum fairing, which incorporates acoustic absorption blankets on its interior. The fairing is jettisoned 24 seconds after second-stage ignition.

The spacecraft is attached to the third stage via the 3712C payload attach fitting (PAF) manufactured by McDonnell Douglas. A short adapter tube is mounted to the PAF to prevent the spacecraft thruster nozzle from striking the top of the STAR-48B motor. The PAF provides mounts for four separation spring actuators, two electrical disconnects, an event sequencing system, and a nutation control system. The spacecraft is separated from the third stage by bolt cutters severing the PAF attachment bolts, and separation springs which impart a separation velocity of 2 to 8 ft/sec. Following separation, a yo-yo weight tumble system despins the third stage and changes the momentum vector direction of the third stage to stage to ensure the spacecraft does not recontact the third stage (McDonnell Douglas, 1987).

D. PERFORMANCE

The Delta II 7925 will provide $27.90 \text{ km}^2/\text{s}^2$ with a 725 kg payload. The proposed satellite design will have a launch mass of 725 kg with an onboard Δv capability of 1.85 km/sec, which is the minimum requirement for a mission to Seleucus. The Delta will provide the necessary C3 for the 1982XB and Orpheus missions, but the Atlas IIA - capable of a C3 of $40 \text{ km}^2/\text{sec}^2$ with a 725 kg payload - is needed for the missions to McAuliffe and Seleucus. The satellite is designed for a 37 inch diameter launcher interface, since both the Delta and the Atlas rockets have the same diameter interface with their adapters. By designing the spacecraft to fit inside the envelope of the Delta II, compatibility with the larger Atlas IIA is assured. But because of cost, missions using the Delta II are heavily favored.

IV. STRUCTURE SUBSYSTEM

A. REQUIREMENTS

The structure subsystem must 1) provide mechanical support to all other subsystems, 2) meet subsystem position and alignment requirements and 3) protect subsystems from launch loads; all while fitting inside launch vehicle and configuration constraints. The structure subsystem design began with the size and launch environment requirements of the Delta II launch vehicle. The structure is required to produce fundamental frequencies above 35 Hz in the thrust axis, and 15 Hz in the lateral axis. Delta flight dynamic excitations are superimposed on steady-state accelerations to produce combined accelerations used in the spacecraft structural design.

	Lateral	Axial
Minimum Natural Frequencies	15Hz	35Hz
Limit Loads at S/C C.G.	± 3.0 g	6.0 ± 0.3 g

Table 13. Spacecraft Design Factors

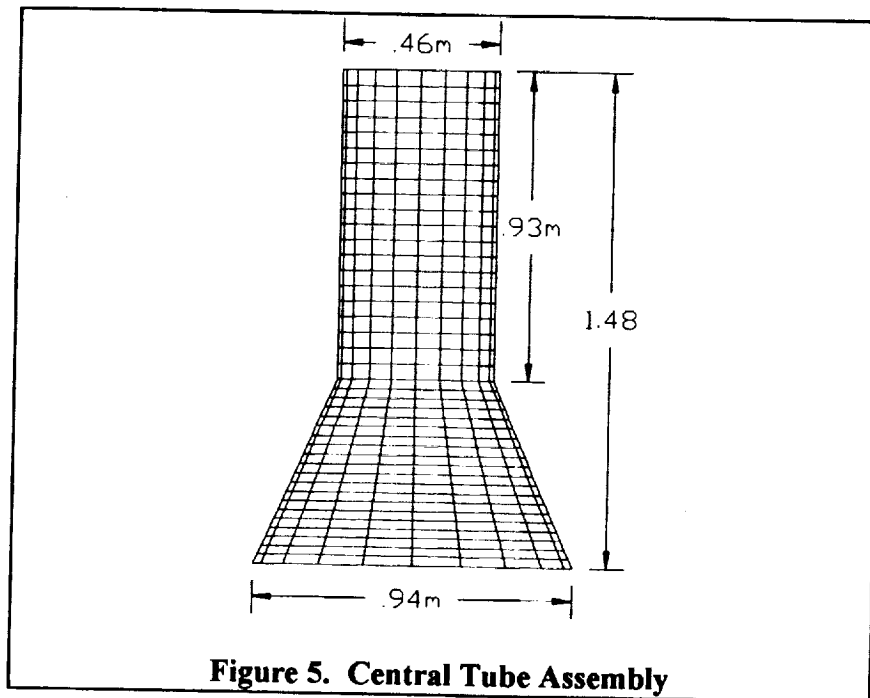
B. STRUCTURAL COMPONENT DESIGN/SIZING

The basic structure was chosen to be a central tube assembly as the primary load carrying member supporting two main side equipment panels, three decks, and two lighter sides via a supporting network of strut assemblies. Factors considered in deciding on structural configuration included simplicity (cost), thermal control, launch vehicle constraints and design team experience. Aluminum was chosen as the basic material for the structure due to its strength-to-weight ratio, ease of manufacturing and cost. The structure was designed to support a spacecraft separation mass of 725 kilograms with a minimum margin of safety of 20% and a design load factor of 1.5.

All calculations were entered into a spreadsheet program to provide the ability to do iterations and for flexibility during later stages of development. 6061-T6 Aluminum properties were used in all calculations. Calculations and spreadsheet outputs are found in Appendix A. A brief description of each component and its design follows.

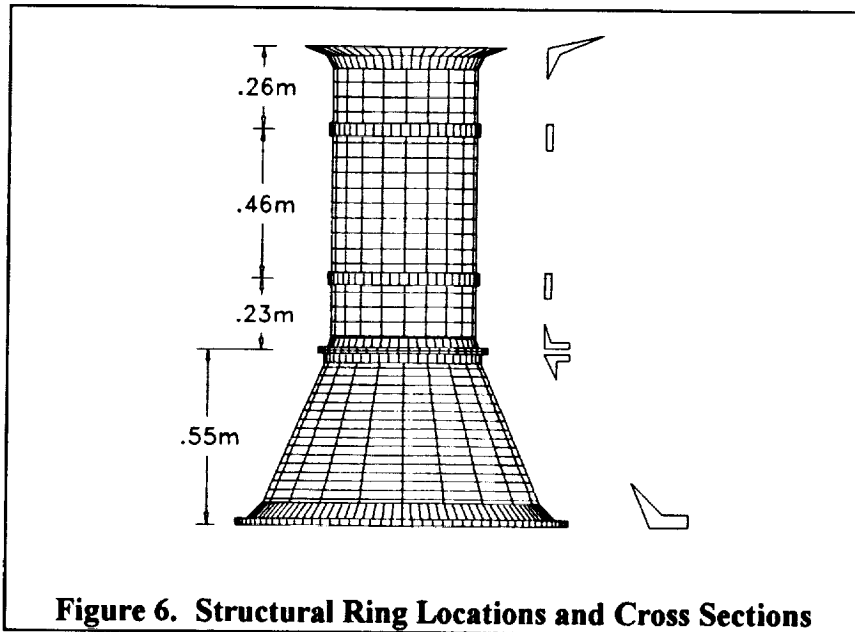
1. Central Tube Assembly

The Central Tube Assembly provides the load path for all subsystems and is also a framework for mounting hardware. The assembly consists of a thrust cone connected to the Delta II launch interface and a central cylindrical shell. The Central Tube has a fundamental frequency above 40 Hz and a margin of safety of 0.40. Both components are made of 2mm thick aluminum. Central Tube Assembly dimensions are shown in Figure 5.



2. Interface Rings

Six ring assemblies are used to connect the central tube to thrust cone, the thrust cone to the launch vehicle, and the high gain antenna to the central tube assembly. The rings also provide hardened mounting points for the internal oxidizer tanks and struts. Ring locations and cross sections are shown below:



3. Strut Assemblies

A series of 8 struts connect each corner of the spacecraft to mounting points on the central tube. They are designed as load paths for the equipment panels during launch and also provide axial mounts for the fuel tanks. Each strut is a 1.095m long tube of 3 cm radius. The struts are 3mm thick and designed to support 20 kg under maximum design loads. Each strut has a fundamental frequency above 60 Hz and margin of safety of 1.14. Strut locations and orientation are depicted in Figure 7.

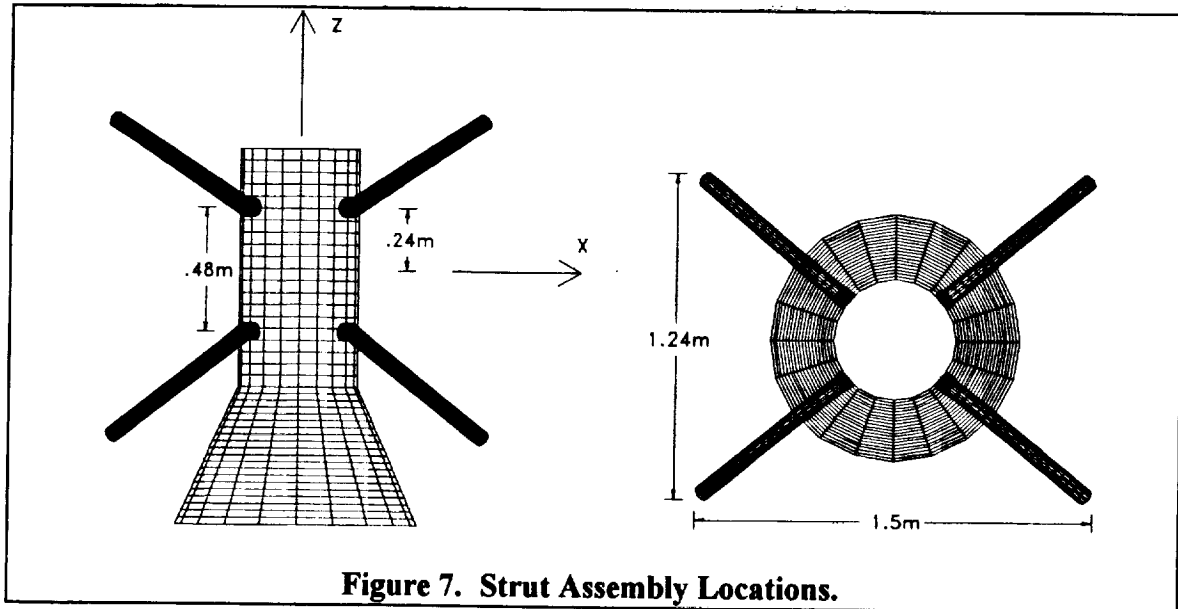


Figure 7. Strut Assembly Locations.

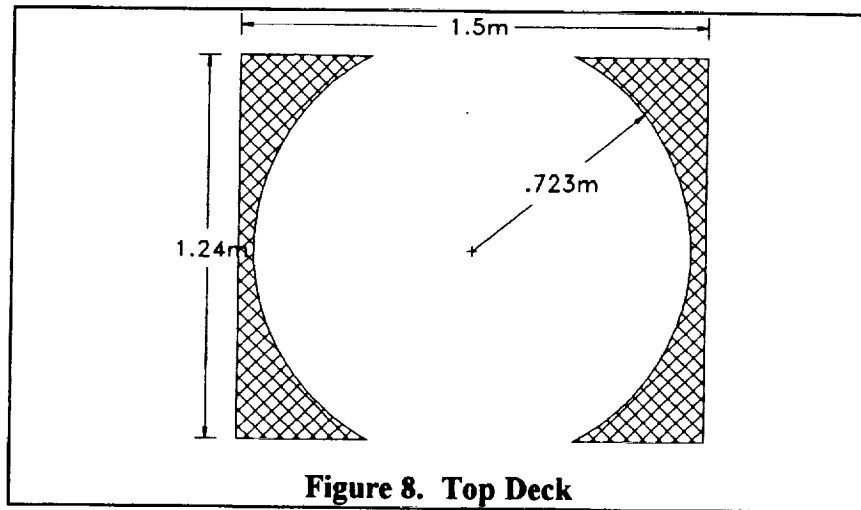
4. Equipment Panels

The four sides of the spacecraft are made of aluminum honeycomb sandwich material. The panels on the solar array sides (plus and minus y faces) are designed to support a component mass of 90kg. Each has a 3 cm thick core, a face skin thickness of 0.5 mm and fundamental frequency above 60 Hz. The remaining two sides are designed for 10kg total mass each. Their primary function is to provide mounting points for wiring, plumbing, insulation and payload instruments. Each has a 2 cm thick core and a face skin thickness of 0.5 mm and a fundamental frequency above 40 Hz. Each of the four panels is connected to the strut assembly at all four corners.

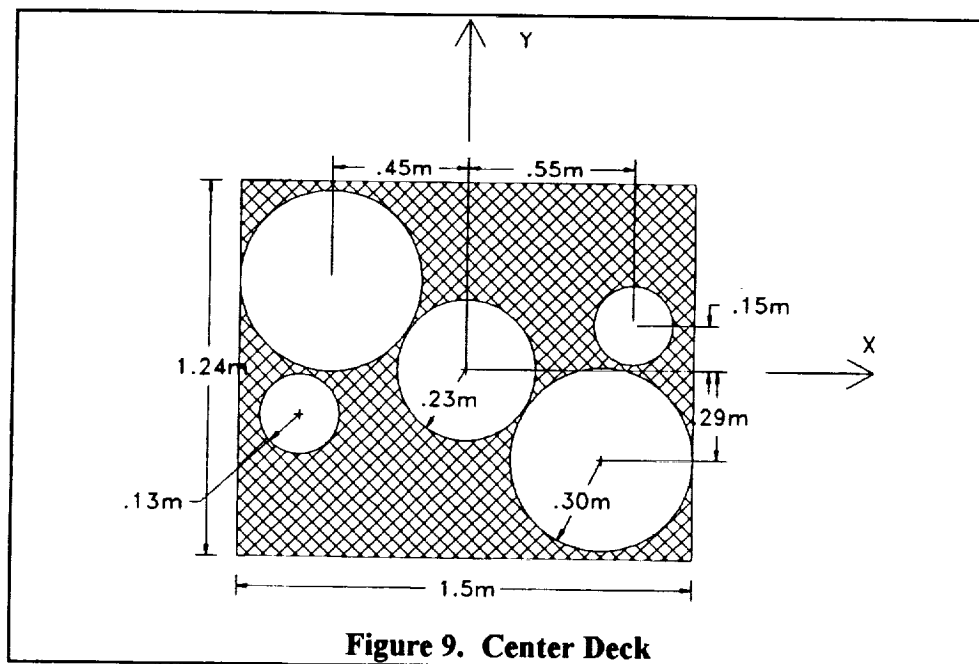
5. Decks

The horizontal components of the structure consists of three aluminum honeycomb decks; top, bottom and center. All three are constructed of aluminum honeycomb sandwich material, with 2 cm cores and face skin thicknesses of 0.5 mm. Each deck has a fundamental frequency above 100 Hz. The top and bottom decks are designed primarily to close the spacecraft interior for thermal control and as secondary mounting surfaces for internal wiring. The top deck is sized to

provide some lateral support for the high gain antenna and actually consists of two separate parts, as shown in Figure 8.



The center deck is used for lateral support of the fuel and nitrogen tanks and also as a mounting surface for wiring, plumbing and small components. It is designed to support a total mass of 10kg in the axial direction. Its size and orientation are shown in Figure 9. The bottom deck is designed to seal around the thrust cone for thermal control. Its dimensions are shown in Figure 10.



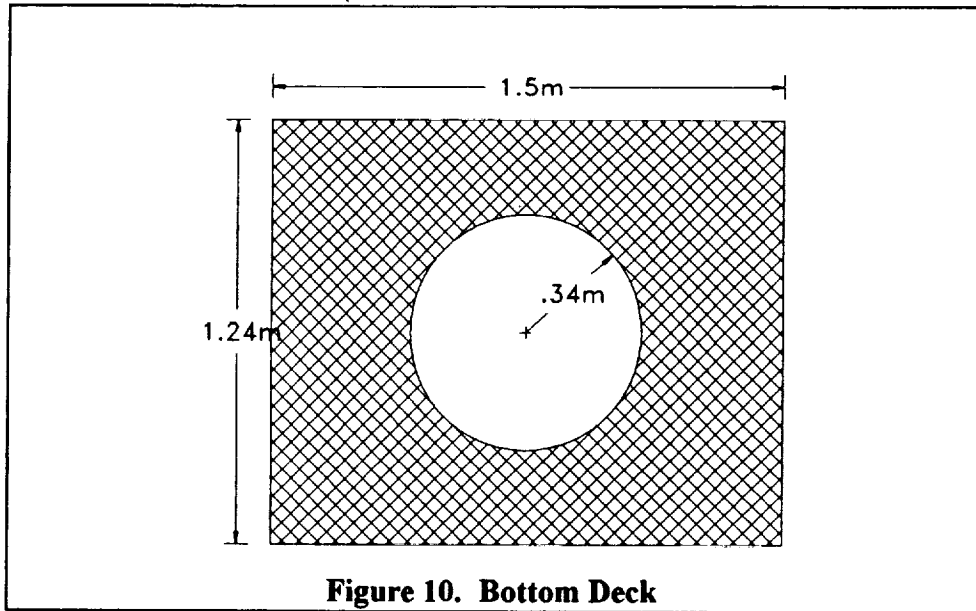


Figure 10. Bottom Deck

6. Structure Summary

Total structure subsystem mass is calculated to be 76.9 kg or 10.6 percent of the spacecraft separation mass. Mass values for components constructed of honeycomb were calculated by assuming the core mass was 30 percent of the face skin mass. A complete mass breakdown of the structure subsystem can be found in Appendix G. Internal structural configuration is shown in Figure 11.

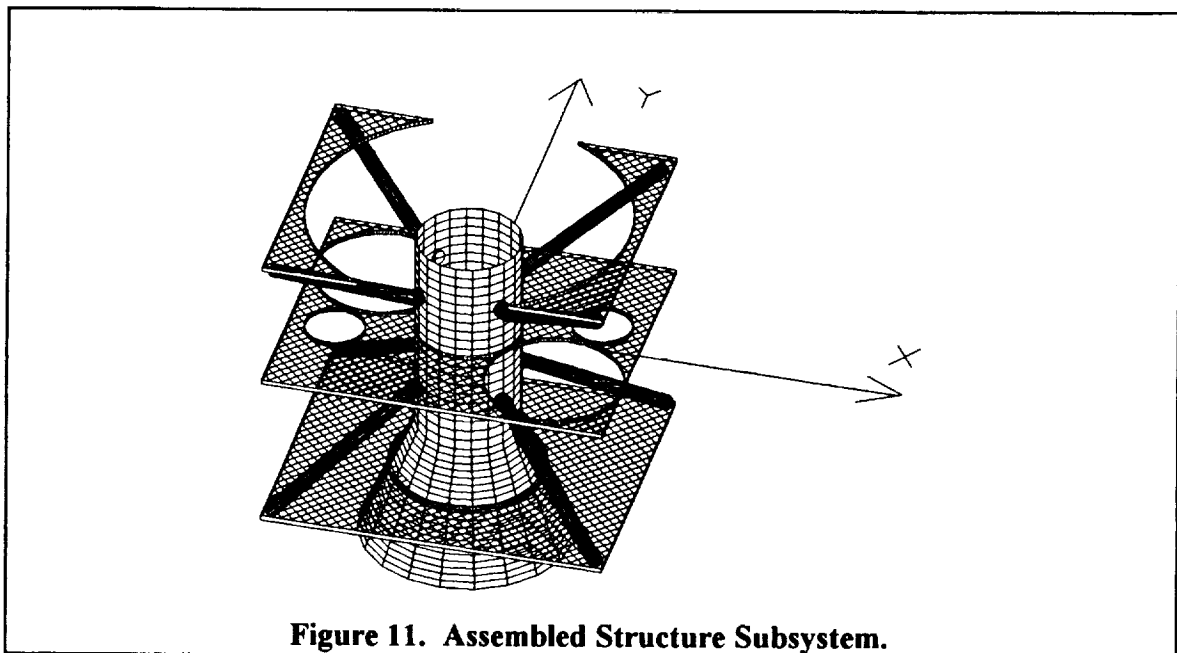


Figure 11. Assembled Structure Subsystem.

V. SPACECRAFT CONFIGURATION

The primary considerations in designing the NEAR spacecraft configuration were size constraints for the Delta II launch vehicle, power and communication requirements, internal packing, and structural integrity. In order to minimize moments of inertia and provide an easily recognizable body coordinate system, the spacecraft origin was chosen to be centered on the solar array axis and the propellant tanks were clustered symmetrically about the origin. From here the spacecraft was designed outward to the launch vehicle size constraint. The axes of the spacecraft coordinate system were chosen such that the positive Z axis is along the centerline of the Central Tube Assembly through the parabolic antenna, the positive X axis is perpendicular to the instrument face, and the positive Y axis is along the solar array axis which forms a right hand coordinate system. Unless otherwise noted, references to planes, axes, etc., in this section refer to the spacecraft coordinate system.

A detailed accounting of individual component, subsystem, and total system mass, dimensions, and moments of inertia was completed using a computer-based spreadsheet program. This method proved quite flexible in handling design changes. The spreadsheet for this spacecraft has all necessary formulas embedded in it, allowing for future refinement as component information is updated. The spreadsheet and its results are located in Appendix G.

A. PROPELLANT TANK LAYOUT

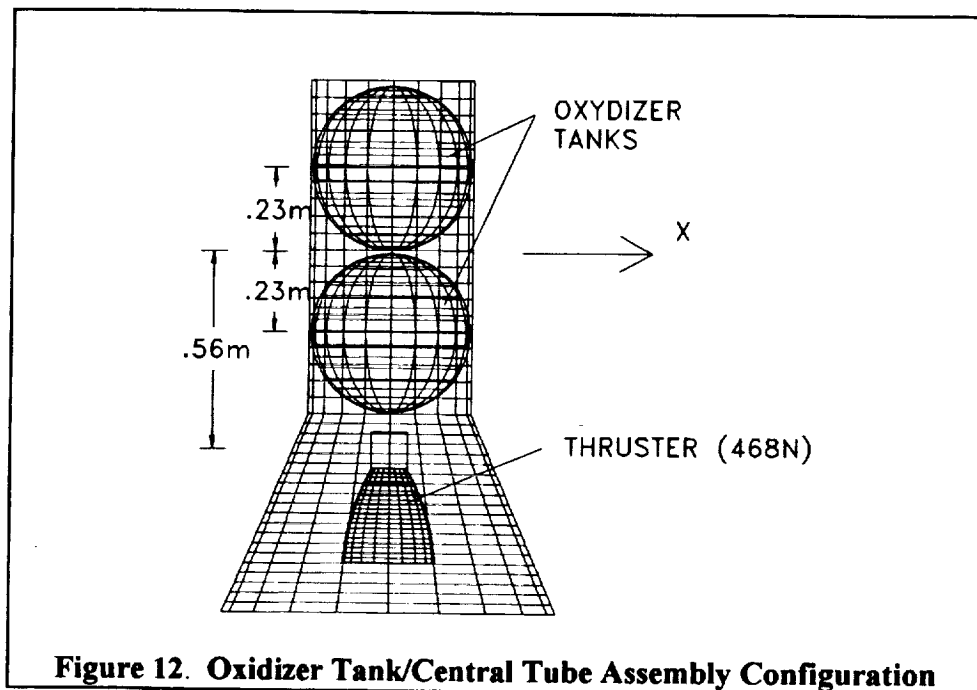
1. Oxidizer Tanks/Central Tube Assembly

In order to maximize packing efficiency and minimize moments of inertia, the oxidizer tanks were mounted inside the Central Tube Assembly, symmetrical about the X-Y plane. Mounting rings on the central tube provide lateral and axial support for the tanks. Additionally, the

468 N thruster is mounted below the oxidizer tanks inside the thrust cone. The general configuration and dimensions are shown below:

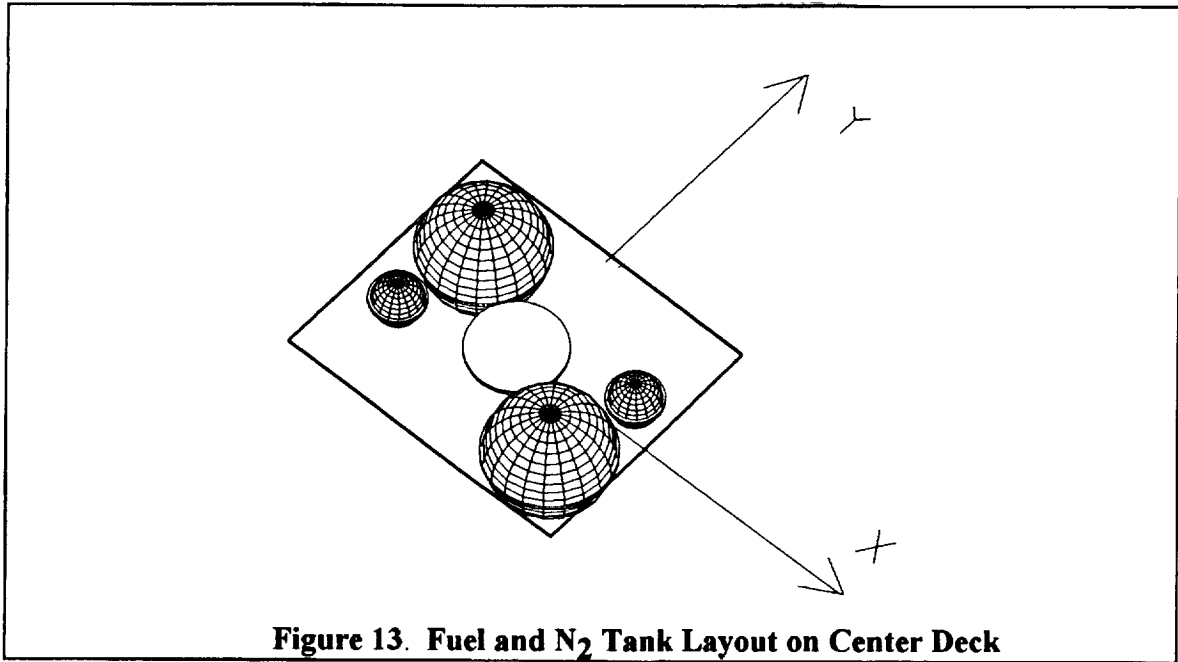
2. Fuel and N₂ Tank/Center Deck Configuration

The fuel tanks are situated on the X-Y plane in opposite corners of the spacecraft, symmetrical about the Z axis. Mounting and axial support is provided by two struts each, top and bottom. Lateral support is provided by the center deck. The two small N₂ tanks are also located on the X-Y plane and supported by the center deck. Layout of these tanks on the center deck is shown below in Figure 12.



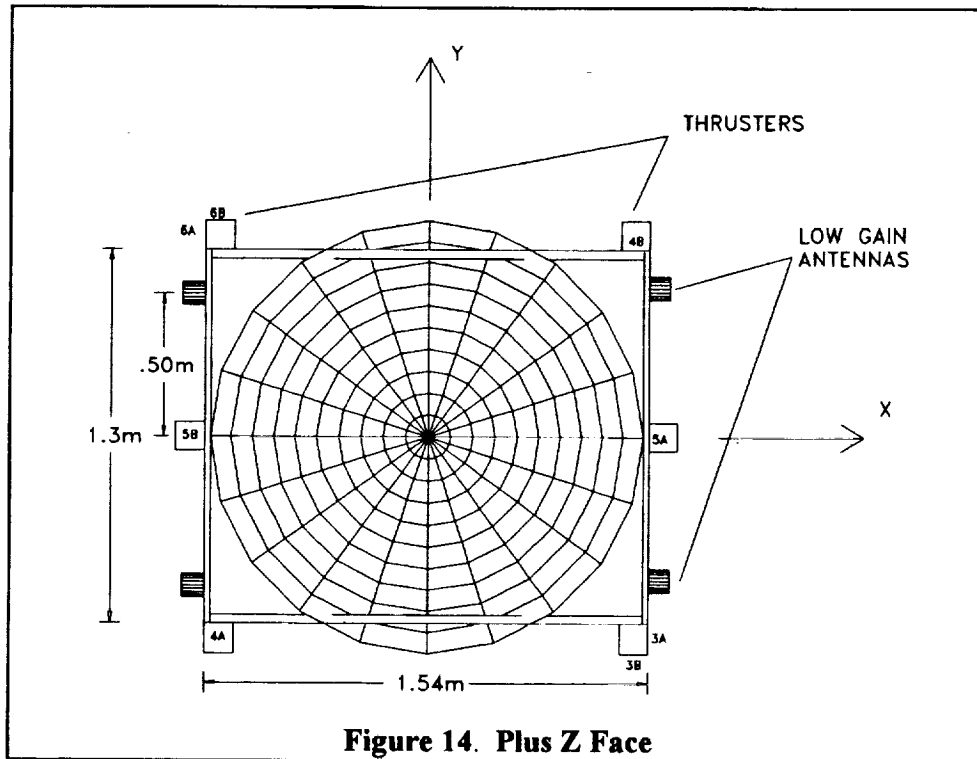
B. EQUIPMENT/INSTRUMENTATION CONFIGURATION

For thermal control reasons, most spacecraft equipment is mounted internally on the plus and minus Y faces. These equipment panels receive very little sunlight during all normal operating modes of the spacecraft and are also designed to carry extra loads. An exception to the above is the Reaction Wheel Assembly, which is mounted internally using struts. Payload instrumentation used for direct observation of the asteroid is mounted on the plus X face.



1. Plus Z Face

The Plus Z Face is dominated by the high gain parabolic antenna. The top deck completes this face by providing a seal and insulation mounting surface for thermal control.



2. Minus Z Face

The Minus Z Face (bottom) is dominated by the thrust cone, which extends below the bottom deck, and the 468 N thruster, which is mounted inside the thrust cone. The launch vehicle interface ring is also visible on this face. Like the top deck, the bottom deck serves to seal the spacecraft for thermal control.

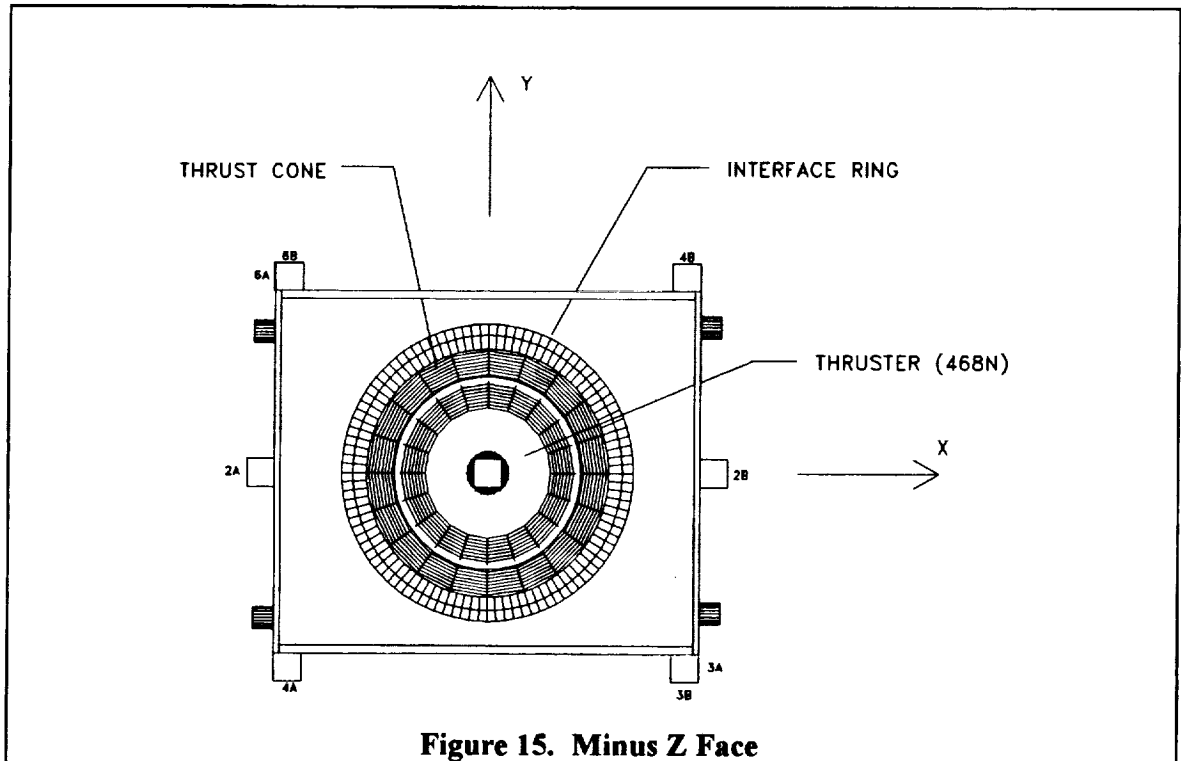


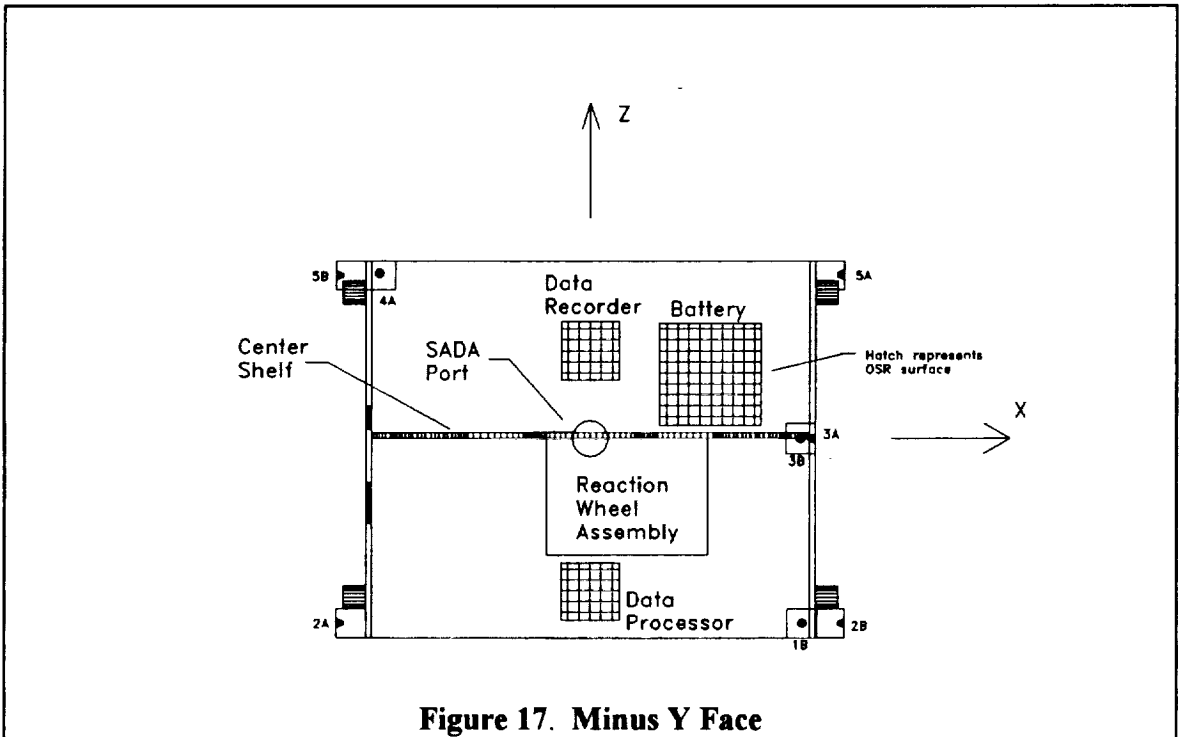
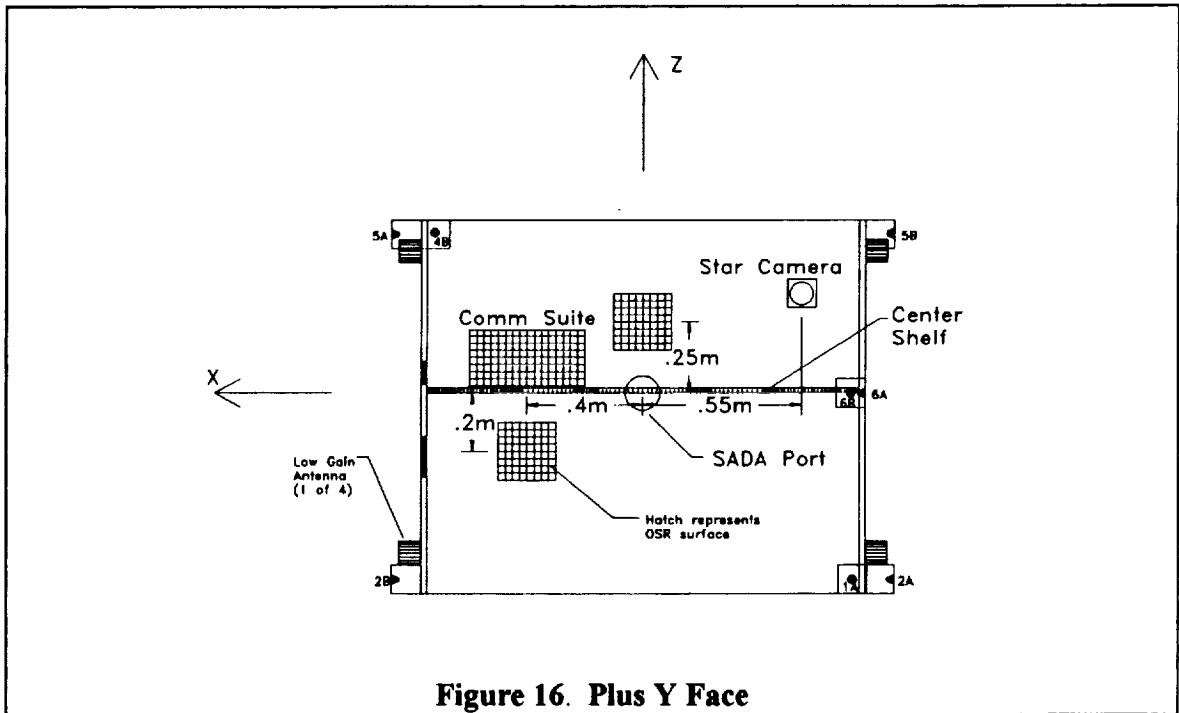
Figure 15. Minus Z Face

3. Plus Y Face

Equipment mounted on the Plus Y Face includes the comm suite, star camera, and one wing of the solar array. Thrusters 4B and 1A are mounted externally on this face.

4. Minus Y Face

Equipment mounted internally on the Minus Y Face includes the data recorder, battery, data processor and the other solar array wing. Thrusters 1B and 4A are mounted externally on this face.



5. Plus X Face

The Plus X Face is used to mount payload observational instruments. These include the IR spectrometer, laser altimeter and visible imager mounted internally each with a viewing port. Thrusters 2B and 5A and two of the low gain antennas are mounted externally on this face.

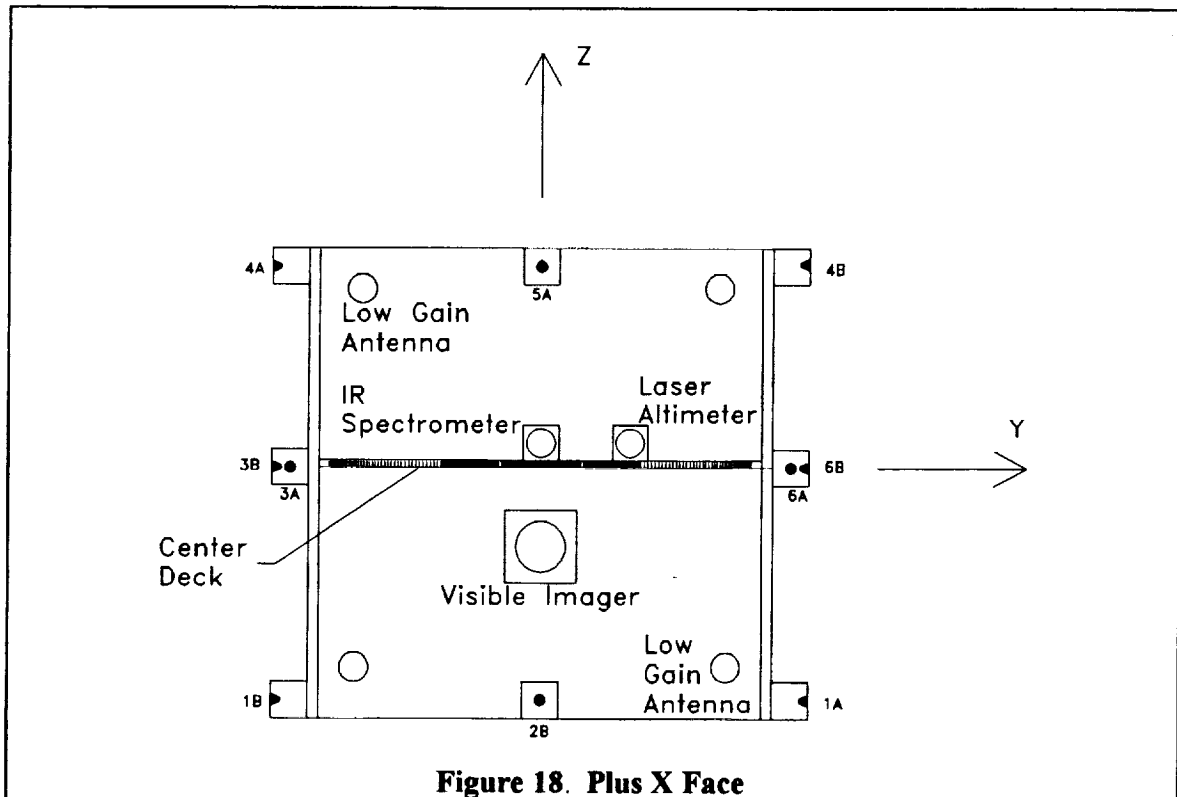


Figure 18. Plus X Face

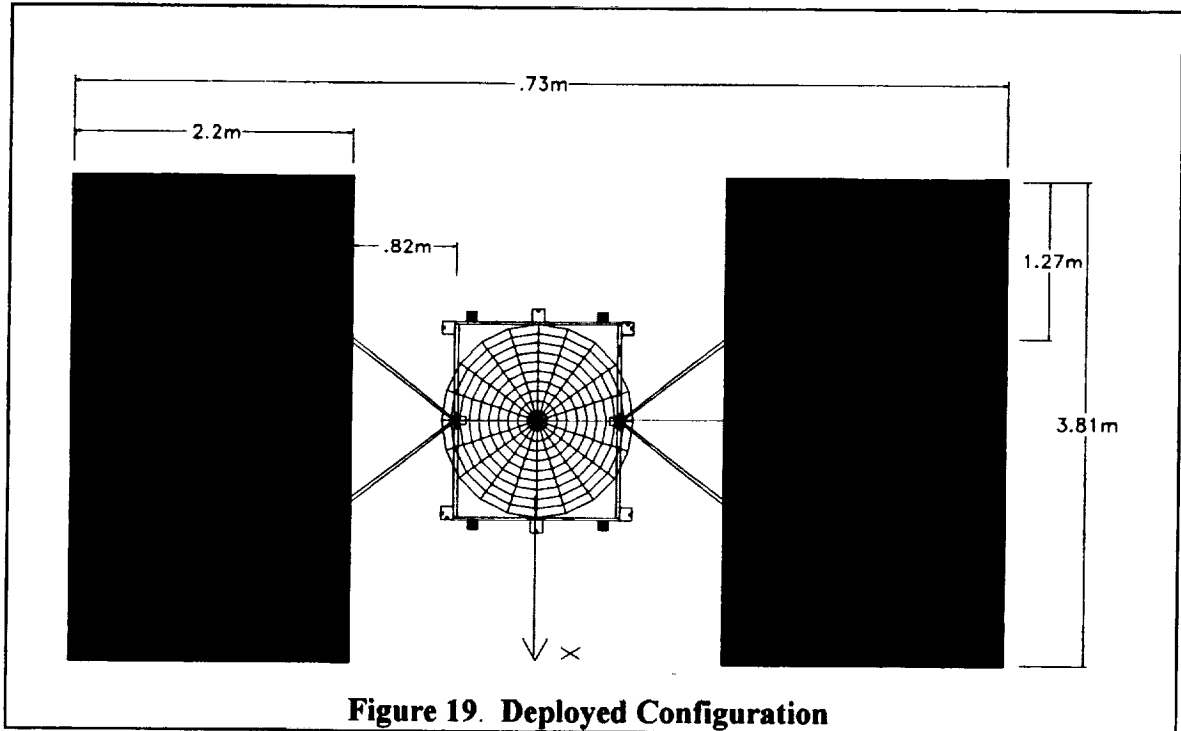
6. Minus X Face

Thrusters 2A and 5B and two low gain antennas are mounted externally on this face. No equipment is intended to be mounted internally here.

C. SOLAR ARRAY CONFIGURATION

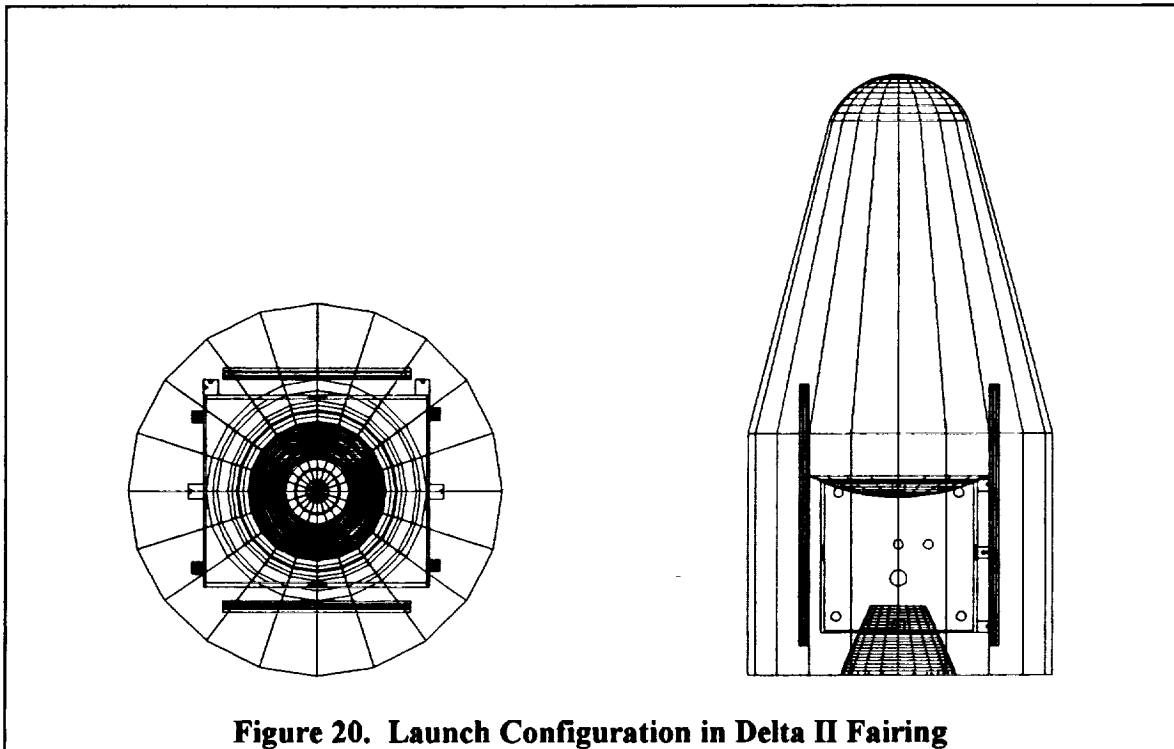
1. Deployed Configuration

The solar array consists of two three panel wings mounted on the plus and minus Y faces.



2. Launch Configuration

In the stowed configuration, one panel is folded under and one over the center panel of each wing. This allows one panel on each side of the spacecraft to be operational during the pre-deployed phase of flight. The yoke hinges down and the wing hinges up to be in a position parallel with the X-Z plane. The views below depict the spacecraft stowed in the Delta II 9.5 foot fairing.



D. INTERNAL PACKING

Internal packing was accomplished using the three dimensional functions in Autocad. Internal views with the side panels removed are shown on the next two pages.

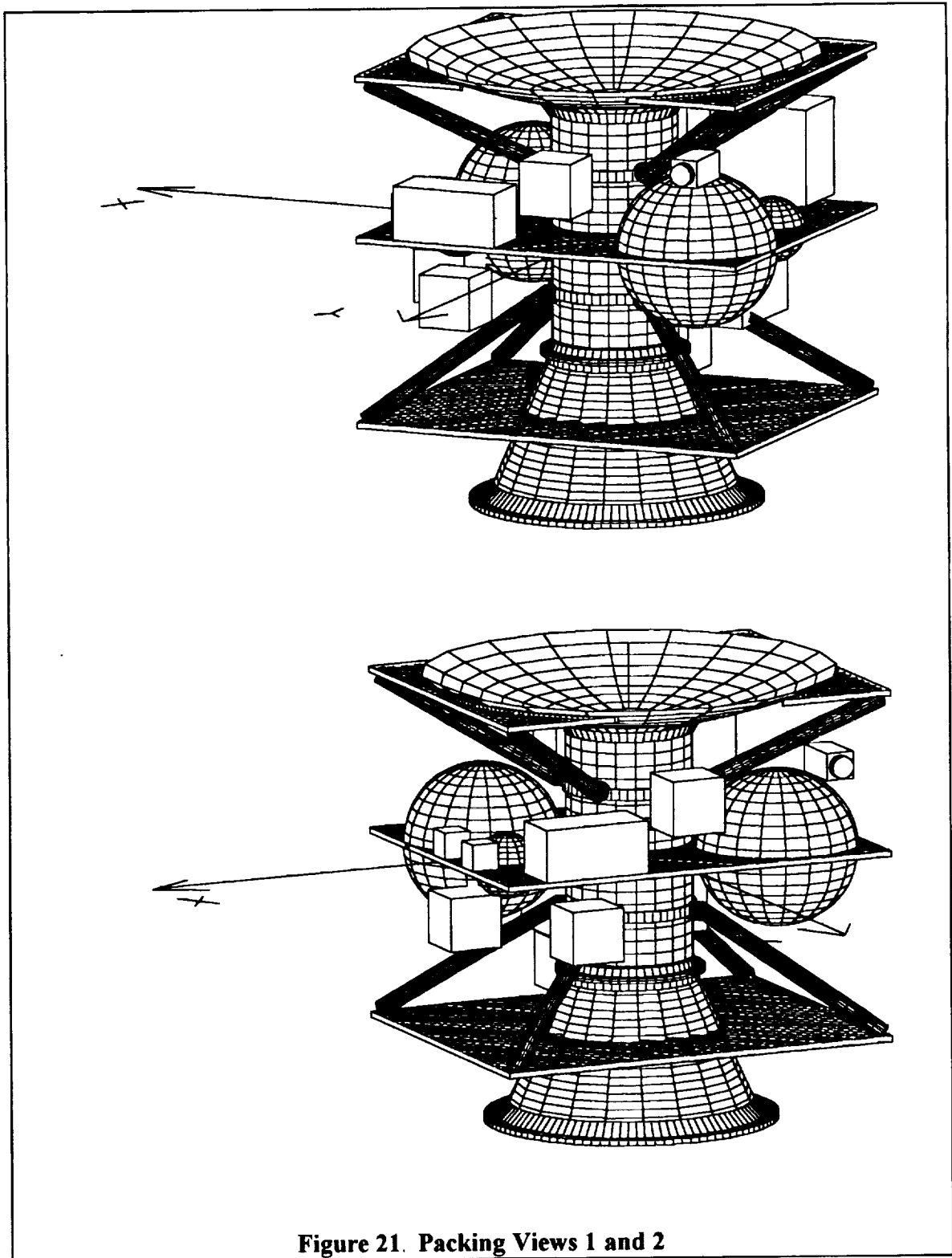


Figure 21. Packing Views 1 and 2

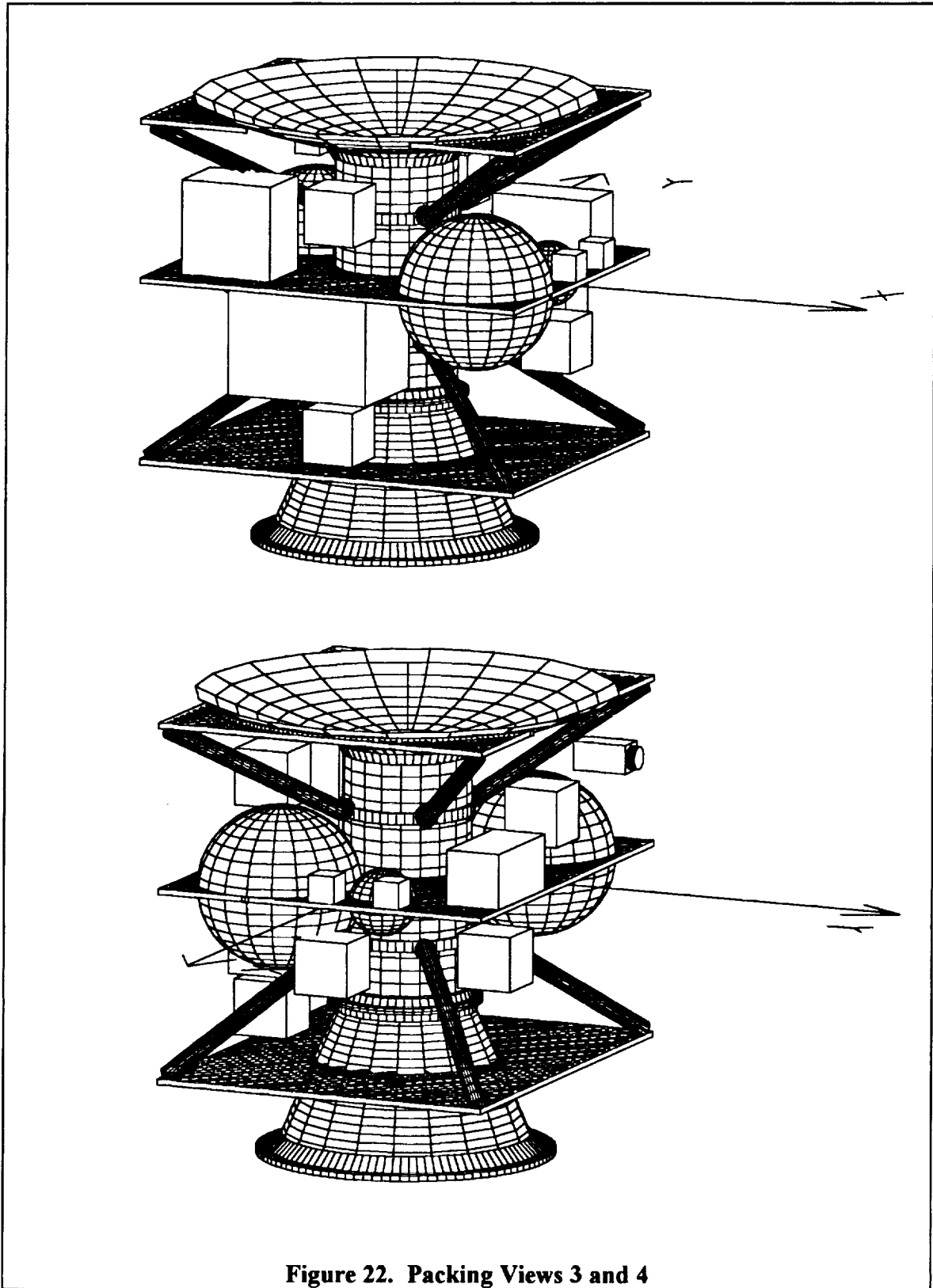


Figure 22. Packing Views 3 and 4

VI. PAYLOAD

A. FUNCTIONAL DESCRIPTION

1. Overview

The payload consists of the Science Payload subsystem, the RF Communications subsystem, and the Command and Data Handling (C&DH) Subsystem. The C&DH subsystem can be further broken into two functional groups: TT&C and data storage.

The mission of the payload is to obtain a variety of remote sensing data while in the vicinity of the asteroid, store the data and then transmit it to Earth via radio telemetry. The payload will also be responsible for all X-Band communication links. It will have the capability to maintain two-way X-Band Doppler through the end of mission as well as Doppler and Range-tracking capability simultaneously with command and telemetry. Furthermore, the RF Communications subsystem must be able to handle all command, ranging, and telemetry functions in either the uplink or downlink mode in conjunction with the 34-m high efficiency (HEF) subnet (Deep Space Station (DSS) 15, 45, and 65) of the Deep Space Network (DSN).

2. Science Payload Subsystem

The purpose of the Science Payload subsystem is to examine the diverse properties of the asteroid and infer, to the maximum extent possible, the chemical properties. The main science instrument is the Visible Imager. The imager is required to obtain six color images with resolution 6 m per pixel pair. Furthermore, the science mission must be scheduled to obtain low resolution images with two inbound and two outbound images exceeding 300 m per pair pixel resolution at thirty minute intervals for five hours preceding closest approach of full face.

3. RF Communications Subsystem

a. Frequency and Data Rate

The communication system will operate in X-band frequencies. The spacecraft will be capable of simultaneous X-band radiometric tracking, telemetry, and commanding. The communications system will operate with an uplink frequency range of 7145 MHz to 7190 MHz and downlink frequency range of 8400 MHz to 8450 MHz. The uplink command data rate will be 10 bps for the Low Gain Antennas (LGA) and 1000 bps for the High Gain Antenna (HGA) at 3 AU. The downlink command and telemetry data rate will be 5200 bps for the HGA. The downlink and uplink bit error rate (BER) should not exceed 1×10^{-6} .

b. Coding and Modulation

The downlink coding will be the concatenated Reed-Solomon and convolution coding required by the DSN. There will be three types of data systems modulated on the telemetry subcarrier. All data will be convolutionally encoded with a code rate $R=1/2$ bit/symbol and a code constraint length of $k=7$. The science and engineering data will be Reed-Solomon encoded (i.e., every 218 actual data bits from the science payload subsystem results in 250 Reed-Solomon encoded bits or "symbols"). The satellite health and status data is convolutionally encoded only. The downlink modulation will be pulse code modulation and phase modulation (PCM/PM). The uplink modulation will PCM (NRZ-L), phase shift keying (PSK), and phase modulation (PCM(NRZ-L)/PSK/PM).

c. Antennas

The satellite will have omnidirectional uplink capability using four low gain antennas, which will be used during emergencies, near-earth orbits, and during the periods when the directional antenna is not pointed towards earth. The satellite will have a high gain directional

antenna to achieve the high data rate downlink capability. These antennas will be supported by a redundant communication system that is capable of producing multiple downlink data rates.

4. Command and Data Handling Subsystem

The C&DH subsystem will act as the interface between the Science Payload subsystem and the RF Communication subsystem. It will collect the information relating to satellite health and status, monitor all system programming; receive, decode, process and distribute spacecraft commands and then it will gather, format, store and transmit all telemetry data. The command and data handling subsystem will be part of a main processor that will control all functions of the satellite. Because the spacecraft must point the science instruments directly at the asteroid to acquire data and then must point Earth to transmit, the command processor must work cooperatively with the other portions of the processing system in order to control the instruments, to properly direct the data streams, and to properly distribute communications signals. Furthermore, in the case of a disabling failure a fail-safe mode is planned to disengage the data streams, align the solar arrays with the sun, enable the LGAs and await instructions from Earth before continuing.

5. Summary of Payload Subsystem Operation

a. Normal Operations

Normal operations change with the mission phase. During Launch, Eclipse, and Post-Eclipse phases, the Main Processor is performing and monitoring housekeeping operations. The solid state recorder is on and storing telemetry information for later downlink. The command receivers are on and switched to the Low Gain Antennas (LGAs). All science instruments are off. During the Cruise phase, the transmitter power amplifier is turned on to provide a 5 W transmission signal. The antennas are switched to the High Gain Antenna (HGA) for transmission and all science instruments are still off.

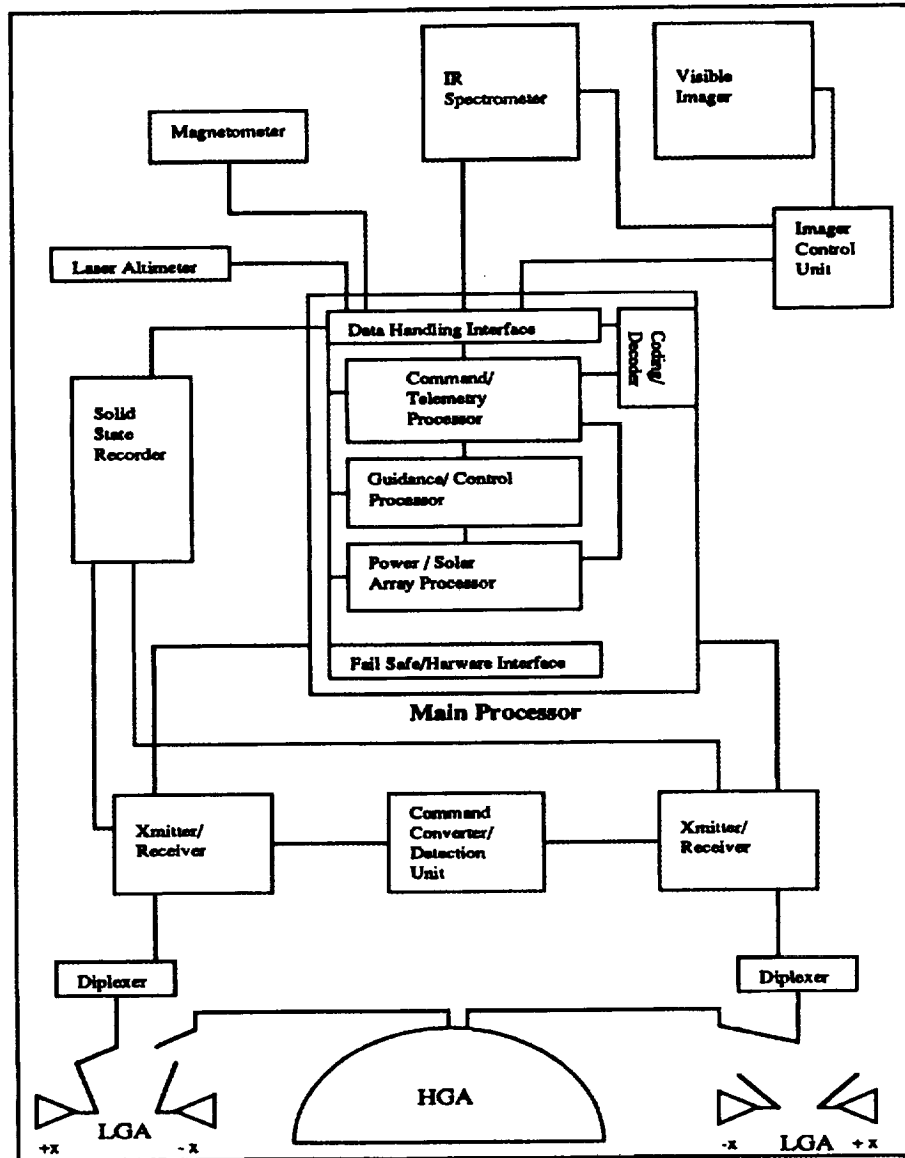


Figure 23. Functional Block Diagram of Payload System

The Acquisition phase consists of two sub-phases: science and transmission. During the science phase, the Visible Imager will be photographing the approaching asteroid target. The transmitter power amplifier will be off and the receiver will be switched back to the LGAs. All data from the Visible Imager is being stored in the solid state recorder. After accumulating enough data, data storage is stopped and the transmission phase is entered. During the transmission phase,

all science instruments will be off , the transmitter power amplifier will be on and set to produce a 10 W transmission signal, and the output will be switched to the HGA. The science data will be coded and multiplexed with the telemetry and ranging information and downlinked via the HGA to DSN 34m HEF on Earth.

The Mission phase also consists of two sub-phases: science and transmission. During the science phase, all science instruments will be on. All data will be stored in the solid state recorder. Once again, the power amplifier will be off and the LGAs will act as receivers. This continues until a command to transmit is received. During the transmission phase, all science instruments will be off and the HGA will be once again turned to earth to downlink science and telemetry information as in the Acquisition phase. These two phases will be cycled for one year: 14 hours of the science phases and 10 hours for transmission. It is assumed that this spacecraft will have to share the DSN 34 m HEF with other spacecraft and that 8 hours is all the downlink time that will be allotted for this mission.

b. Autonomous Operations

The spacecraft must have the capability to operate without ground contact for 7 days. To satisfy this requirement, the TT&C subsystem of the Main Processor will be capable of controlling all spacecraft operations for the duration. All telemetry will be stored in the solid state recorder for future transmission.

c. Emergency Operations

At some point during the mission, it is possible that there will be a software or hardware failure in the Main Processor. A fail-safe mode has been incorporated into the system. When the Main Processor fails, the system will switch to a hardware mode. The transponder will be left on and the antennas will be switch to the LGAs. This mode will stay in effect until the system failure is corrected by the ground station.

B. SUBSYSTEM DESIGN AND HARDWARE DESCRIPTION

1. Science Payload Subsystem

The Science Payload subsystem will consist of a CCD-based visible imager, an IR spectrometer, a laser altimeter, and a magnetometer. This subsystem is controlled by an processor embedded in the main processor architecture, which will operate the instruments and direct the data stream. A gamma ray spectrometer was not included because the mass was too great and the low altitude requirement of less than 1 km for one cumulative month was considered too large a constraint.

a. Equipment

1) Visible Imager. The Visible Imager will be a government furnished (GFP) camera. The GFP camera has been developed to support science and navigation requirements of the Near Earth Object Missions. The camera is compatible with both three axis controlled and spinning spacecraft. It has a 1024 x 1024 pixel CCD detector which can be

Characteristic	Description
Mass	3.5 kg
Power	8 W active, 1.5 W standby both at 28 Vdc
I FOV	12 x 12 mrad, Frame Mode 12 mrad x 12 rad, Scan Mode
Resolution	24 rad (2 x 2 pixels)
Detector	1024 x 1024 x 12 meter frame store CCD
Read Rate	1.6 Mbps
Read Noise	25 rms electrons
Operating Temperature	< 25o C
Encoding	12 bit ADC, 8 bit compressed
Effective Focal Length	1 meter
Focal Ratio	f / 10
Size / Configuration	cube, 18 cm
Optical Filters	6 (including 1 open hole)

operated in either a conventional image frame mode or in a Time Delay Integration (TDI) line scan mode. TDI operations will be achieved by synchronizing the clock rate of the CCD with the angular velocity of the spacecraft and the image in the camera's focal plane. The GFP camera has adequate sensitivity or integration to obtain: 1) a science image in a single exposure or scan and

2) navigation images of objects brighter than visual stellar magnitude nine in the same field of view as the target body.

The camera operates in two modes: Frame Mode and Scan Mode. The data acquisition timing sequences for the modes are:

i. Frame Mode Science Images (resolved body at 1.1 AU from Sun with albedo of 0.2).

Integration Time	2.2 msec
Readout Time	5 sec
Frame to Frame Cadence	6 sec

ii. Frame Mode Navigation Images

Integration Time	10 msec
Readout Time	5 sec

iii. Scan Mode Science Images.

Integration time (20 pixel TDI scan at 1 rpm)	2.2 sec
Scan Duration	6.9 sec
Readout Time	5 sec
Scan to Scan Cadence (at 1 rpm)	60 sec

2) IR Spectrometer. The IR Spectrometer is essentially a filter wheel camera. It has an object field-of-view (FOV) of approximately 4°, and a wavelength range of 0.9 μ m to 2.7 μ m.

There are 8 filters (probably 3-5 % FWHM).

The signal to noise ratio (SNR) will be greater than 15 dB at the poorest performance point with an integration time of greater than

Equipment	Heritage
Shutter	Craf / Cassini
Filter Wheel	Galileo
Sensor	HIRIS (128 x128 HgCdTe)
Telescope	many technologies available

or equal to 1.0 sec. The system size is 10 x 10 x 15 cm rectangle with a circular aperture. The mass of the system is 10 kg. The system power requirement is 5 W. Radiative plate cooling is possible, but temperatures will probably be no lower than 150 K. The IR spectrometer will be a match with the camera system with respect to data processing and data fusion. The IR

Spectrometer is connected to a control unit and processor, which serves as the interface between the instrument and the data handling interface in the main processor.

3) Laser Altimeter. The laser altimeter provides ranging information to the satellite with heritage from SDI instruments for the telescope and from the Mars Observer for the laser. This instrument will be used for topographical mapping and for attitude control during close orbits of the asteroid. The operational range of the laser altimeter is 20 km with a resolution accuracy of 50 cm. Global coverage at this accuracy would yield a volume determination with an accuracy of less than 0.2% for the asteroid McAuliffe.

4) Magnetometer. The purpose of the magnetometer is to study the intrinsic magnetic field of the asteroid. The range for operation is 10 asteroid body radii. The magnetometer will be attached to the body of the spacecraft. Cancellation circuitry will be built into the sensor to cancel out any residual spacecraft magnetic fields.

Parameter	Description
Heritage	Giotto Polar Bear
Manufacturer	JHU/APL and NASA/Goddard
Mass	1 kg
Power	1 W

b. System Integration

1) Science Data Interface. The science payload data will be downloaded to the solid state recorder via the data handling interface in the main processor. The visible imager and imaging spectrograph data stream will be processed in their joint control unit/processor and then will be read out on bursts up to 4 Mbps to the data interface. The magnetometer and laser altimeter can read out data at less than 1 kbps, so the buffer will enhance stream performance. The data interface will control and monitor all phases of storage and transmittal of data.

2. Communications and Data Handling Subsystems

a. Equipment

1) High Gain Antenna (HGA). The HGA is an X-Band parabolic dish antenna with a diameter of 1.5 m and a f/d ratio of 0.4. The antenna was designed to have a 1dB beam width of 0.95 degrees and a gain of 40 dBi. Parabolic dish antennas are easy to manufacture and have a known track record. The narrow beam width and the high gain will allow the high data rates required for uplink and downlink operations at 3 AU. The HGA will be a fixed antenna and must be pointed at Earth in order to transmit and receive data.

2) Low Gain Antenna (LGA). There are four Low Gain Antennas. Two LGAs will operate at one time with the other two acting as backups. The primary function of the LGAs is to act as receivers and as transmitting antennas if the HGA fails. During emergencies or system failure, two LGAs will be automatically switched on to act as receivers. They are located on the +x and -x sides of the spacecraft. Each is placed on opposing corners to achieve hemispherical coverage. Each LGA is an omnidirectional helical antenna, and is approximately 7.6 cm in diameter and 7.6 cm in height.

3) Support Electronics. The RF Communications subsystem is a fully redundant system with the exception of the HGA. There are two sets of transponders, power amplifiers, switches, diplexers, LGAs and other supporting electronics, one primary and one backup. The power amplifiers can be switched between a 10 W and 5 W transmission signal. Each set of equipment is connected to the Main Processor. The Main Processor continuously monitors, controls and processes all data received by the system. In case of system failure, the Main Processor will switch from the primary to the backup communication system.

b. System Integration

The RF Communications subsystem will receive the uplink X-band carrier transmitted from the Deep Space Network (DSN) to the spacecraft. The uplink is received by one of the two

transponders via the omnidirectional wide beam width Low Gain Antennas or by the narrow beam width High Gain Antenna. The command data and the phase modulated ranging signal is demodulated. The received command stream is submitted to the C&DH subsystem for decoding and processing.

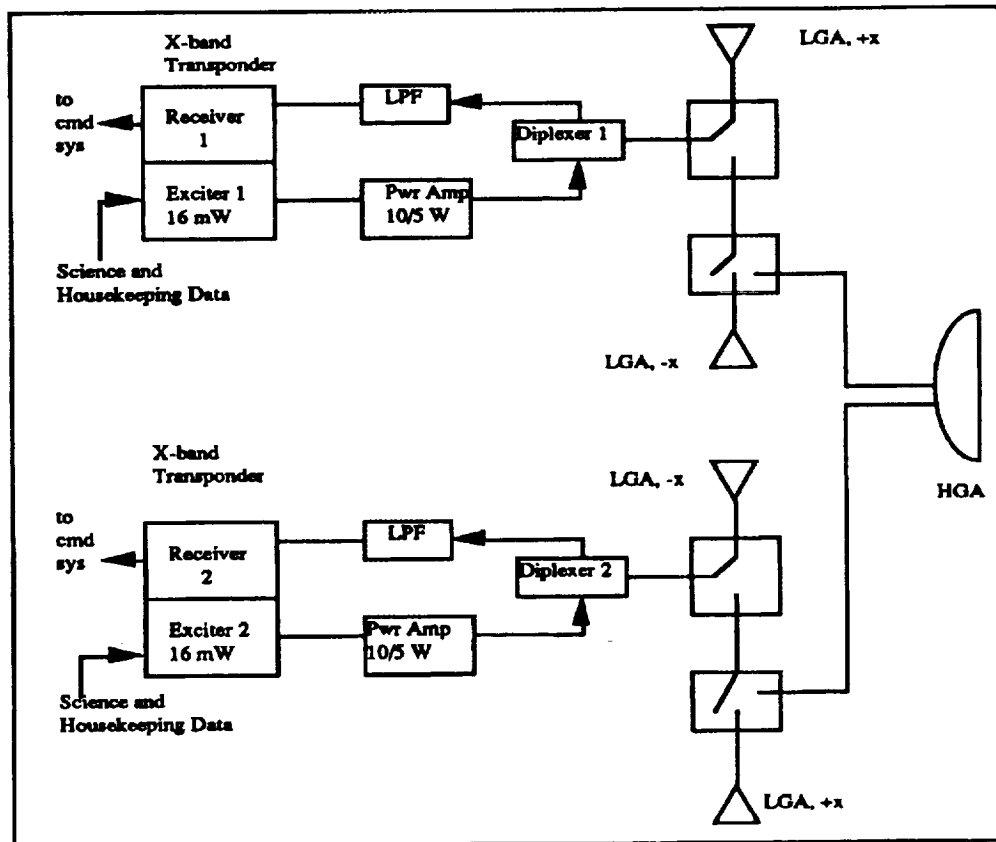


Figure 24. Functional Diagram of RF Communications

The X-band downlink carrier is generated in the exciter. The X-band coherent frequency is exactly 880/749 times the uplink frequency. The downlink carrier is phase modulated with a square-wave subcarrier on which the housekeeping telemetry and science data is PSK modulated by the C&DH subsystem. The science data is retrieved from the solid state recorder via the data handling interface. The housekeeping telemetry is utilized for monitoring the operating

conditions of the RF Communications subsystems as well as the status of the rest of the spacecraft. The two way ranging signal may also be used to phase modulate the downlink carrier. The downlink signal is amplified (10 W or 5 W depending on the mission phase) and then transmitted via either the LGA or the HGA. The RF Communications subsystem permits control of the subsystem by ground command to select proper signal routing and operation.

c. Link Budget

The RF communications system must be designed to support all prescribed NEAR missions. The ranges utilized in the link budget analysis will support all missions. Note also that the ranges used in the link budget analysis are the distance from earth to the spacecraft. For simplification in measurements for the link budgets, the range for the spacecraft will be set at the mean range for each phase: the Eclipse and Post Eclipse phases will be designated to take place at a range of 1 AU, the Cruise phase will be a range of 2 AU and the Acquisition phase and Mission Phase will be at a range of 3 AU. The range of 3.6 AU is assumed to be the worst case. The distance limits the data transmission rate.

1) Deep Space Network (DSN). All uplink communications will utilize the DSN 34m (HEF) antenna. This is the only type that supports X-band frequencies. Downlink communications will be split between the 70 m and the 34m (HEF) antennas. The 70m antenna will be required for the emergencies and when the spacecraft is outside the 3 AU range. The 34 m (HEF) antenna will be utilized for all normal downlink communications between the HGA and earth within the 3 AU range. The parameters for the 34 m (HEF) and 70 m antennas used in the link budget analysis are in Appendix C.

2) Losses. The losses normally associated with a communications link are atmospheric loss and free space propagation loss. Other significant losses associated with this spacecraft are polarization loss, pointing loss and remodulation loss. The pointing loss and

polarization loss are a function of the transmitting antenna . These losses are very significant in an X-band communications system. (See Appendix C for exact numbers).

3) Data Rates. The resulting bit rates are shown below:

a) DownLink

Range	Antenna		DSN		P _T		Data Rate (bps)
	LGA	HGA	70 m	34m	10 W	5W	
1 AU	X		X		X		48
		X				X	21,183
2AU	X				X		12.5
		X				X	5000
3AU	X		X		X		6.4
		X		X	X		5200
		X	X		X		19,400
3.6 AU	X		X		X		4
		X		X	X		3184
		X	X		X		11,700

b) Uplink

Range	Antenna		DSN	P _T	CMD Data Rate (bps)
	LGA	HGA	34m	20 kW	
1 AU	X		X	X	90
2AU	X		X	X	22.5
		X	X	X	2000
3AU	X		X	X	10
		X	X	X	1000
3.6 AU	X		X	X	6.65
		X	X	X	781

3. Command and Data Handling Subsystem

a. Main Processor

The Main Processor will control all activities aboard the spacecraft. It will be a single processor that will handle TT&C, Data Handling (C& DH), Guidance and Control, coding and decoding of communication, and other onboard functions discussed in other sections.

The internal electronics will conform to Military Specification 1553B. This standard establishes the requirements for digital, command/response, time division multiplexing (data bus)

techniques on aircraft. This standard encompasses the data bus line and its interfaces and also defines the concept of operation and information on the multiplex data bus and the electrical and functional formats to be employed.

1) Science Data. The data retrieved from the science instruments will enter the data handling interface (DHI) of the main processor. The DHI will store the information in the solid state recorder. When instructed by the Command/Telemetry Processor that the communications system is in the transmission phase, the DHI will retrieve the data from the solid state recorder and send the data to the encoder. The data will then be prepared for transmission (See RF communications system integration)

2) Command and Telemetry. The status (health) of all systems will be monitored by the main processor. Each piece of equipment will be attached to the command / telemetry processor. The telemetry data will be stored in the solid state recorder until it can be transmitted back to earth. All systems will be updated based upon the equipment status and spacecraft needs.

b. Solid State Recorder Equipment Specifications

Characteristic	Specification
Capacity	512 Megabits
Data Channels	Modular expansion from 1 to 8
Maximum Data Rate	< 140 Mbps
Data Read / Write	Instantaneous
Data Input (redundant)	NRZ-L or NRZ-M Differential Input Clock (0 to 10 Mbps)
Data Output (redundant)	NRZ-L, NRZ-M, or Bi-phase
Bit Error Rate	10^{-10} through EOL
Reliability	> 90 % over five years Mean time to failure = 10 yrs
Power	4 watts
Size	21 x 28 x 17 cm
Mass	13 kg
Heritage	Qualified for flight on Air Force P87-2
Model	SSR1-512/B

VII. ELECTRICAL POWER SUBSYSTEM (EPS)

A. FUNCTIONAL REQUIREMENTS

1. Overview

The electrical power subsystem of the NEAR satellite must be capable of providing adequate power to the satellite for all six phases of the mission. This will be accomplished using a sun-pointing array for the primary power source and a battery for the secondary/supplementary power source. The EPS must draw power from the solar array and the battery and condition this power in order to meet the specified power requirements for each of the satellite's subsystems. The EPS will also consist of components to provide bus voltage regulation, power distribution, telemetry data, and electronic power conditioning. The control of the EPS will be provided by the microprocessor-based Command and Data Handling (C&DH) processor.

2. Power Requirements

The EPS must provide a $28\pm 4\%$ VDC bus voltage through End-of-Life (EOL). The power requirement, in addition to the amount of load shared between the battery and the solar array, depends on the mission phase. The greatest power demand is a 221 W requirement for the asteroid acquisition phase. For example, during the launch phase and eclipse phase, the power is provided primarily by the battery, but during the post-eclipse and cruise phases power will be supplied primarily by the solar array. While in the asteroid-acquisition phase and mission phase, the base power will be provided by the solar array, with power peaks floated by the battery. Each earth-day of the mission phase is subdivided into 14 hours gathering science data and 10 hours transmitting data back to earth via the DSN. Additionally, should it become necessary for the satellite to reacquire the sun, the battery must be capable of providing power during reacquisition. The power budget and the power profile for the different mission phases are shown in the following tables.

Subsystem	Peak Power	Standby Power	Average Power
Receiver	24	24	24
Transmitter (Lo)	40	40	0
Transmitter (Hi)	80	80	0
Science	34	15	1
Thermal	20	21	23
Electrical	25	35	10
Attitude Control	60	42	19
Propulsion	54	36	1
C&DH Processor	24	24	24
Total	339	279	116

Table 14. Power Budget.

Subsystem	Phase					
	Eclipse	Post Eclipse	Cruise	Acquisition	Mission	
					Science	Xmit
Receiver	24	24	24	24	24	24
Transmitter (Lo)	0	0	40	0	0	0
Transmitter (Hi)	0	0	0	80	0	80
Science	0	0	0	0	34	0
Thermal	20	10	20	20	20	20
Electrical	23	21	25	25	21	25
Attitude Control	29	38	30	38	36	36
C&DH Processor	24	24	24	24	24	24
Margin	10	10	10	10	10	10
Total	130	127	173	221	169	219

Table 15. Power Profile for Mission Phases

Because of mass constraints, there is no redundancy in the power sources. Therefore, if the battery or a portion of the solar array is lost, the EPS will go into a degraded mode. In the degraded mode, the C&DH processor will autonomously prioritize power distribution to the spacecraft's subsystems based on a pre-programmed hierarchy and remove nonessential devices

from the bus via switching relays. The ground station will have the capability of overriding and/or changing the hierarchy depending on user requirements.

B. EPS DESCRIPTION

1. General

The power source of the EPS is furnished by a solar array supplemented by a single 25AH NiH₂ battery for peak load periods. The power is utilized by EPS regulatory circuitry to: charge the battery; discharge pyrotechnics for solar array release; and condition the power to meet the necessary power requirements for housekeeping, communication, control, thermal, and gathering science data. The block diagram of the EPS is shown in Figure 25.

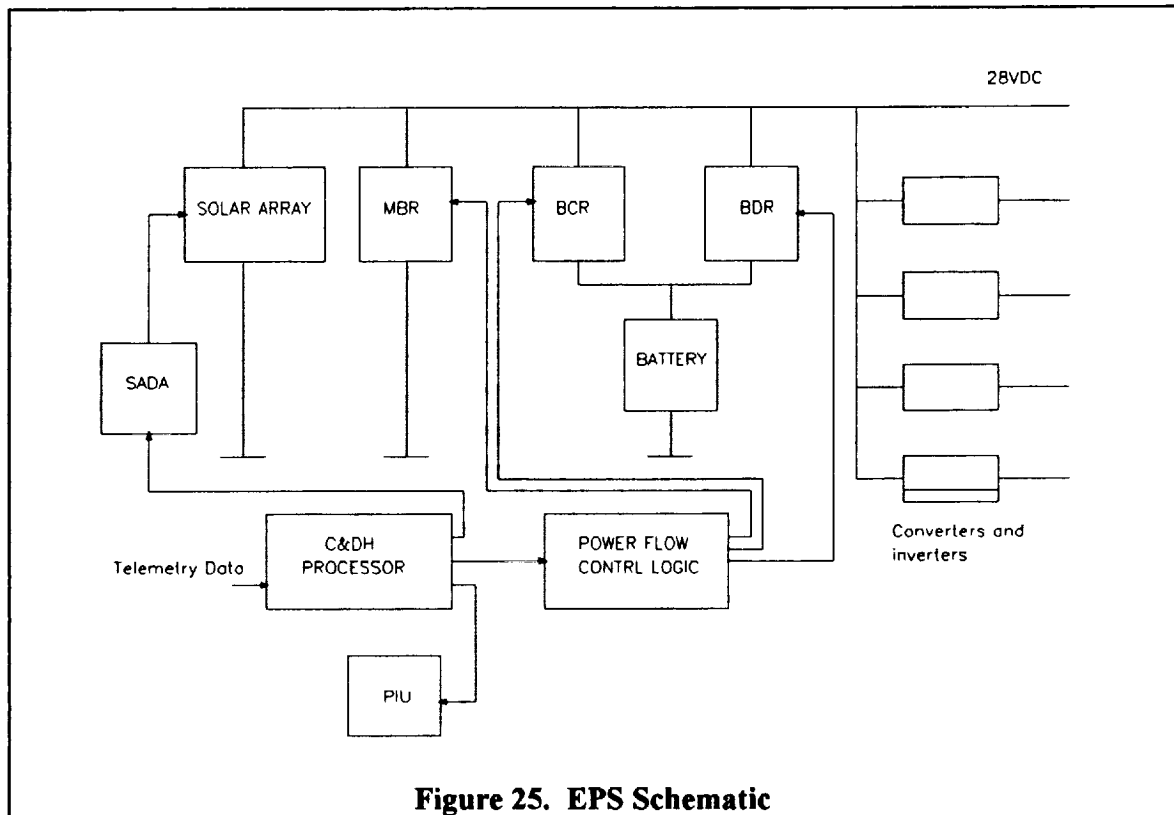


Figure 25. EPS Schematic

2. Solar Array

The solar array consists of two wings; each wing incorporates three panels to produce the power required by the spacecraft. The wings are mounted to the satellite with solar array drive assemblies (SADA), which allow full array rotation about one axis. The array was designed to provide 34.2VDC bus voltage at 192W maximum power at end of life.

When deployed, the solar array wings will have the configuration shown in Figure 19. This configuration was chosen to provide structural stability during acceleration of the spacecraft by raising the resonant frequencies. As a result, the center panel will be mounted to the yoke. In the stowed configuration, the panels will be folded so that a conditioned surface will be facing outward in order to supplement the battery prior to deploying the array.

3. Battery

The battery is intended to supply power to the satellite during launch, eclipse and reacquisition of the sun. In addition, it will supplement the solar array during peak power usage. The battery chosen to meet these requirements is a 28V, 25Ah NiH₂ battery constructed by Eagle-Picher Industries. The maximum load required by the spacecraft during the launch/eclipse phase and the post-eclipse phase is approximately 130W and 127W respectively. Assuming open-circuit failure of one cell, a 65% depth of discharge (DOD), and 0.5 hours in the launch/eclipse phase, the battery is capable of furnishing the load requirements of the post-eclipse phase for up to 2.5 hours without recharging. The battery will be recharged during the cruise phase, where the maximum load requirement is 173W. At a distance of 1AU, the solar arrays can provide up to 1975.7W of power at BOL. This is far in excess of the satellite power requirement, so the system will rotate the solar arrays to increase the angle of incidence while still providing adequate power for the spacecraft and for recharging the battery at any acceptable charge rate.

The battery was designed to float 27W of peak power during the entire 10 hour transmission portion of the mission phase at EOL (at 50% DOD). Under these conditions, it is

capable of completely recharging during the 14 hour science data gathering portion of the mission phase with a charge rate of C/38.

In the event that the battery is needed to furnish the entire 221W for sun reacquisition, it can do so for up to 1.77 hours at EOL for a 65% DOD. Assuming the satellite is placed into a receive only mode (with no transmitting or science data gathering) while recharging, it will take about 7.6 hours to recharge. Depending on user requirements, the ground station can shorten or lengthen the recharge time by selectively switching loads on or off.

4. Power Conditioning and Distribution

The EPS will employ a centralized, fully regulated scheme for supplying power to the individual subsystems. The solar array provides unregulated power to the main bus. The EPS must condition and distribute this power to meet the power requirements of each subsystem.

Power conditioning can be divided into three operation modes: shunt, charge, and discharge. Each mode is executed by either the main bus regulator (MBR), the battery charge regulator (BCR), and the battery discharge regulator (BDR), respectively. As implied, each regulator is capable of maintaining the bus voltage at its proper value.

Some devices will be able to use the 28VDC directly from the main bus. However, because of the variety of power needs for different subsystems, the bus voltage may require being stepped-up, stepped-down, or inverted. This is achieved by the appropriate use of DC-DC converters and inverters.

The monitoring and control of the power regulation and distribution is furnished by the C&DH processor. A system of switching relays will provide the C&DH processor with the ability to switch between redundant systems in the event of a device failure and to shed unnecessary loads in case the spacecraft enters a degraded mode of operation. In addition, the C&DH will be able to vary the solar array power output by altering the angle of incidence on the solar array panels via control of the SADA. This may become necessary when the satellite is at BOL and/or in close

vicinity to the sun in order to reduce the amount of power that must be dissipated through the shunt regulator; which will subsequently reduce the amount of heat generated within the spacecraft.

a. *Main Bus Regulator (MBR)*

The main bus regulator is a nondissipative shunt regulator used to maintain the bus voltage at the proper value. The MBR employs a power transistor to shunt power from the bus as needed. The current flow through the transistor is regulated by a PWM signal from the C&DH processor. By monitoring the difference between the actual bus voltage and the desired bus voltage, the C&DH processor applies the appropriate PWM signal to the transistor which corresponds to the current flow that gives the desired bus voltage.

b. *Battery Charge Regulator (BCR)*

The primary function of the battery charge regulator is to control the charging of the battery with a variable current while maintaining the bus voltage at $28\pm 4\%$ VDC. Secondary functions include control of the battery heaters and telemetry outputs such as battery voltages, cell temperatures, charge currents, and solar panel currents. The BCR will be monitored and controlled by the command and data handling (C&DH) processor.

The battery charge regulator is based on a pulse-width-modulated (PWM) buck regulator. A buck regulator is capable of providing an output voltage which is less than the input bus voltage. This topology accommodates the differences in the voltage furnished by the solar array which occur during the life of the spacecraft. In addition, the PWM feature allows the BCR to vary the charging current to accommodate a variety of charging modes. Each mode is associated with a different charging rate to provide either a rapid charge, a normal charge, a trickle charge, or no charge.

c. Battery Discharge Regulator (BDR)

The primary function of the battery discharge regulator is to maintain the bus voltage when the solar array is incapable of meeting the demand. The BDR is based on a boost-type switching regulator which is controlled by a PWM signal from the C&DH processor.

C. EPS COMPONENT DESIGN, ANALYSIS, AND SELECTION

1. Battery

The 25 AH battery selected for the NEAR mission is comprised of 22 NiH₂ cells in individually encapsulated, common pressure vessels (CPV). The battery meets or exceeds design requirements with the assumptions of an open-circuit failure of one cell and a 65% depth of discharge (DOD). The battery has a mass of approximately 21.3kg as per the design features provided by Eagle-Picher Industries. This includes the 22 cells, packaging, heater, and miscellaneous hardware. Eagle-Picher boasts an impressive heritage for their flight qualified hardware in several on-going missions.

The three primary candidates for the type of battery were: silver-zinc (Ag-Zn), nickel-cadmium (Ni-Cd), and nickel-hydrogen (NiH₂). Ag-Zn was not considered due to its low cycle (20 to 200 cycles) capability. NiH₂ was selected because it can operate at a higher DOD for the same lifetime as a Ni-Cd battery and has a longer life if used at the same DOD.

Many factors were taken into account while determining the necessary features of the battery. The most restrictive constraint was to minimize the capacity (and therefore the mass) of the battery while providing maximum supplementary power during peak power demand so that the dimensions and mass of the solar array could be minimized. It was determined that the battery could provide 27 W of power during the entire 10 hour transmission phase without a reduction in normal operations. Using a 50% depth of discharge, a battery with a 25AH capacity was selected. Details of this design are given in Appendix D.

2. Solar Array Design

The proposed configuration of the spacecraft and the size constraints of the shroud placed limitations on the maximum size of the solar array panels. As a result, the solar array had to provide 192W at EOL, the difference between the 219W required by the spacecraft during the transmission phase and the 27W provided by the battery. Designing a solar array that met this requirement and conformed to the size constraints of the shroud resulted in 2 wings, with each wing consisting of three 1.27 x 2.2 meter panels.

The solar array design consisted of two phases: the preliminary conceptual design and a detailed design. In each phase, the design was conducted with four different solar cells for comparison. All four cells were products of Spectrolab, Inc., and utilized design parameters from Spectrolab specification sheets. The designs looked at three different silicon cells with varying parameters and one GaAs cell.

a. Radiation Degradation

The NEAR satellite spends only a few days within the vicinity of the earth. Therefore the total equivalent 1-MeV electron fluence associated with this short period of time is considered negligible. The radiation degradation in free space is due almost entirely to protons generated by solar flare activity. The determination of the equivalent 1-MeV electron fluence for solar flare protons for this design is based entirely on historical data. The largest anomalously large (AL) solar flare event occurred during solar flare cycle number 20 in 1972, so measurements from this period are regarded as worst case values.

The annual equivalent 1-MeV electron fluence values used are for a distance of 1AU from the sun. The intensity of the flux is inversely proportional to the distance from the sun squared (i.e., flux intensity $\propto d^{-2}$). With the exception of Orpheus, the perihelion of each candidate asteroid is greater than 1AU and therefore the 1AU data is an adequate worst case assumption. In the case of Orpheus, although the greatest dosage of radiation generated by a solar flare occurs

within a one to three day period, it is assumed that the probability of this coinciding with Orpheus being within 1AU of the sun is small. The unlikelihood of this event does not justify designing to guard against its effects.

Using the annual equivalent 1-MeV electron fluence for solar flare protons corresponding to 1972, four different coverglass thicknesses were compared and the respective annual fluences for each thickness were multiplied by four to conform to the planned mission life. The results are in the table below (JPL, pg. 6-52).

Cell Parameter	Coverglass Thickness (mils)			
	3	6	20	60
V_{oc} and P_{max}	6.00e+14	3.64e+14	1.40e+14	5.20e+13
I_{sc}	3.00e+14	2.00e+14	9.60e+13	4.00e+13

Table 16. Equivalent 1 MeV Electron Fluence for Solar Flare Protons

b. Coverglass Selection

In order to compare the trade-off between protection and mass, four separate preliminary designs were performed. Each of the four designs kept all factors the same except for the coverglass thickness. Typical silicon cells with dual anti-reflection coating (DAR), back surface reflector (BSR), back surface field (BSF), 10 ohm resistivity, and 8 mil thickness, were used. The 6 mil coverglass was selected for both the preliminary conceptual design and the detailed design because it offered the best balance between thickness (i.e. mass) and protection.

c. Substrate

The selection of the substrate was based on heritage from the Tracking and Data Relay Satellite (TDRSS). The front facesheets are 0.075 mm thick Kapton; the rear facesheets are 0.13 mm thick Kapton and 51% of the surface area of the facesheets are perforated with circular holes spaced on an equilateral triangle pattern. The holes permit heat from the front facesheet to radiate through the back. A 75 µm thick layer of perforated Kapton is bonded to the facesheets in areas

where the substrates are attached to the frames. The honeycomb core of the substrate is 10 mm thick aluminum. The overall density is approximately 0.735 kg/m² (JPL, 1976, pg. 335).

d. Solar Cell Selection

Although the required bus voltage is 28±4%VDC, the solar arrays must provide 33.9V at EOL in order to meet the charging requirements of the battery. This, in conjunction with the 210W power requirement for the spacecraft were the driving factors in the array design. The design was carried out to completion for each of the four candidate cells for mass and weight comparisons. A basic description of the three Spectrolab silicon cells is given in Table 17.

SILICON CELL TYPE:	K6700A	K7700A	K7700B
Resistivity (p-type)	10 Ohm-cm	10 Ohm-cm	10 Ohm-cm
Metallization (Front)	TiPdAg	TiPdAg	TiPdAg
Metallization (Back)	AlTiPdAg	AlTiPdAg	AlTiPdAg
Anti-Reflective Coating	Multi-Layer	Multi-Layer	Multi-Layer
Back Surface Reflector	Aluminum	Aluminum	Aluminum
Back Surface Field	Aluminum	Aluminum	Boron
Thickness	200 Microns	200 Microns	62 Microns
Areal Density (mg/cm ²)	55	55	24

Table 17. Silicon Cells Considered for NEAR Missions

A basic description of Spectrolab's GaAs cell includes germanium substrate, multi-layer anti-reflective coating, aluminum BSR, 175 Micron thickness and an area density of 100 mg/cm². With the selected coverglass and substrate, the GaAs/Ge solar cell offered the most favorable results. However, because of the cost difference, a silicon solar cell was selected. The silicon solar cell which offered the best combination of mass and dimensions is the K6700A. It provided a panel dimension of 1.27 x 2.2 m². The total array required 19344 K6700A solar cells resulting in a total array area of 16.73 m² and mass of 26.0 kg. More extensive design analysis and the solar cell arrangement is given in Appendix D.

3. Frame Selection

Graphite fiber-reinforced plastic (GFRP) box beam frames were selected to support the substrate of the solar array panels. Adhesive bonding will be used to affix the frames to the rear facesheets of the panel substrates. The GFRP frames are lightweight yet offer the stability and durability required for acceleration. The heritage of the frame is based on the Tracking and Data Relay Satellite (TDRSS). The frame of each wing will have mass of approximately 9.4kg for a combined mass of 18.8kg (Rauschenbach, 1980, pg. 335).

4. Solar Array Drive Assembly (SADA) Selection

The SADA was selected from the heritage of the Nimbus II, and consists of a motor gearhead unit, a potentiometer unit, and a subassembly unit containing a clutch, output shaft, and gearing. It provides an overall gear ratio of 84,847:1 and a nominal output torque of 367 N·cm. The SADA is driven by a 26Vac, 400Hz servo motor. As a result, a DC-AC converter must be used to provide the appropriate power (Rauschenbach, 1980, pp. 361-362).

5. Power Conditioning and Distribution

The main bus regulator (MBR) is a shunt regulator that maintains the appropriate bus voltage by dissipating unused power when the power from the solar array exceeds the amount of power required. The battery charge regulator (BCR) and the battery discharge regulator (BDR) are nondissipative power regulating systems that operate in the switch mode which results in higher efficiencies. The nondissipative system provides a highly efficient conversion of DC-to-AC. The AC signal is then rectified back to DC using LC circuitry to provide the appropriate filtering.

Each of the three regulators has a transistor which is switched off and on at a set frequency. The duty cycle, or the length of time that the transistor is on, is controlled by a PWM signal provided by the C&DH processor. By varying the duty cycle, the C&DH processor can vary the amount of current passing through the appropriate transistor. This allows the C&DH to control the bus voltage, the charge rate of the battery, and amount of power the battery provides to the bus.

All three regulators can independently maintain the bus voltage and therefore only one regulator will be operating at any given instant of time. By monitoring telemetry information, such as battery voltage, battery temperature, charge and discharge rates, solar array voltage, etc., the C&DH processor determines which regulator must be on by utilizing algorithms based on the necessary battery parameters and telemetry. The power flow control logic then routes the PWM signal to the appropriate regulator.

For example, if the battery requires charging, the BCR is used to charge the battery and maintain the bus voltage. If the battery becomes fully charged, the battery is placed on trickle charge and the shunt regulator is turned on to maintain the bus voltage. When the battery is needed to supplement the solar array or provide all power requirements, the discharge voltage is turned on.

The inductor and the capacitor of the BCR and BDR can be selected so that they can be shared by the two regulators. As a result, all three regulators can be combined in the same circuit as shown in the diagram below (Chetty, 1986, pp.153-157).

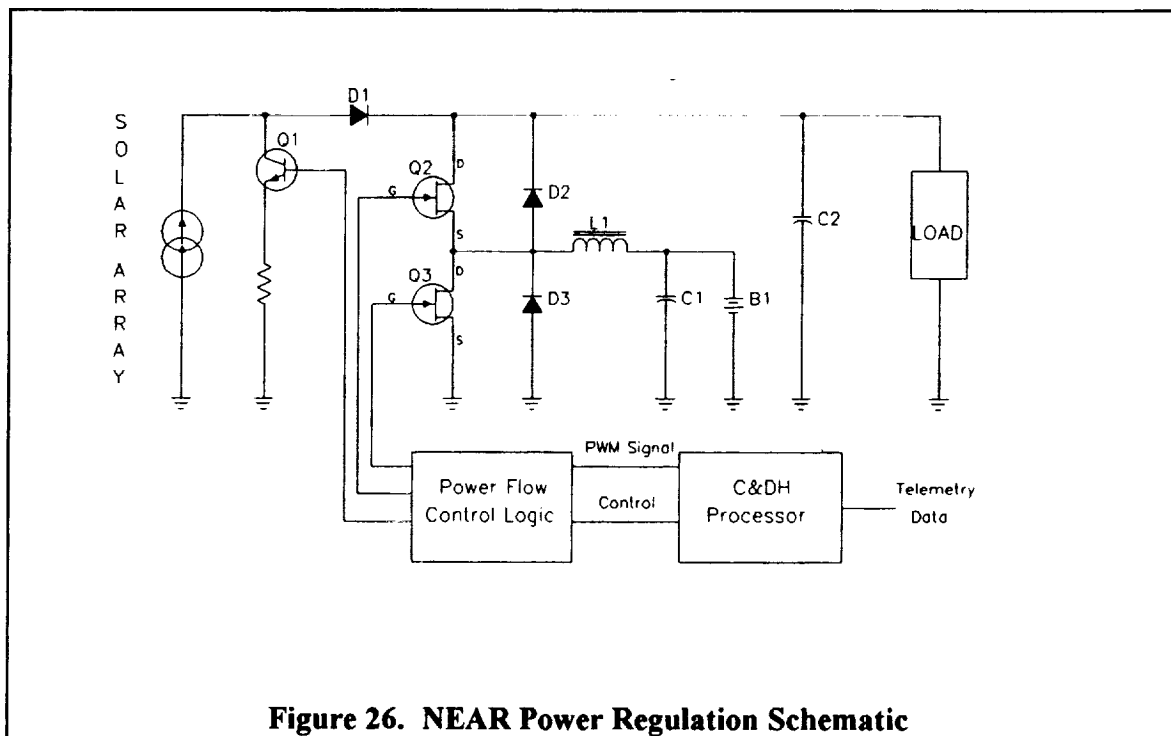


Figure 26. NEAR Power Regulation Schematic

VIII. ATTITUDE CONTROL

A. FUNCTIONAL REQUIREMENTS

The Guidance and Attitude Control System (GACS) maintains the correct spacecraft attitude from post-launch separation through the end of the mission. Initially, the satellite will be spin-stabilized after separation from the launcher. During this phase, twelve small thrusters will perform the required corrections both for free flight and for when the third stage fires for transfer orbit insertion. The spacecraft attitude control will then transition to three axis control for the remainder of the mission. The three-axis control will be maintained by three orthogonal reaction wheels, with twelve small thrusters available for large burn stability, momentum dumping, reaction wheel backup, and small orbital changes. A fourth wheel is skewed from each of the orthogonal axes to serve as a backup in case of any wheel failure. Once the solar arrays are fully deployed the reaction wheel assemblies will provide torque for all rotations during acquisition of the asteroid.

The attitude control system will be heavily tasked once the asteroid is acquired, since the spacecraft will routinely rotate through large angles. Payload instrumentation is fixed, so the spacecraft must be maneuvered for data acquisition. After data collection is complete, the attitude control system will reposition the spacecraft for transmission of data back to earth. This process will repeat throughout the mission. The attitude control system is designed to continuously stabilize the spacecraft while operating in standby, sensing and transmission modes. The attitude control computer will receive data from the gyros, sun sensors and star trackers. Once in orbit around the asteroid the laser altimeter will also provide input to the attitude control system for collision avoidance and precise orbital information.

The attitude control processor will continuously point the solar array assembly toward the sun for maximum power while the acquisition/transmission cycle continues. To facilitate concurrent

solar array pointing and earth pointing, the solar arrays may be rotated through 360° , such that the spacecraft has two degrees of freedom. This design does raise the complexity of the control system, but the solar array size is reduced by consistently maintaining a solar incidence angle of zero degrees.

Successful completion of the mission is dependent upon the satellite's ability to reorient itself between data acquisition and data transmission evolutions. Precise antenna pointing during both these modes is required. Antenna pointing accuracies and placement of our data collecting instruments provide the specifications around which the attitude control system is designed.

1. Operational Requirements

The design specifications determined by the design team as the minimum to meet the mission requirements are:

- a) Three axis stability with slew capability for sensing and transmission modes.
- b) Antenna specifications require pointing accuracies of $\pm 0.1^\circ$ about any axis.
- c) Sun tracking solar arrays.
- d) Minimum slew rate of $6^\circ/\text{min}$.

2. Designs Concept and Tradeoffs

Various attitude control systems were examined in order to select the system best able to meet the stated requirements. Skewed and biased momentum wheel systems were looked at before deciding on the three axis stabilized reaction wheel system. The desired system is asteroid-pointing during data collection and earth-pointing during data transmission. The configuration was also driven by the requirements to be able to slew about multiple axes in varying geometries and to maintain accurate three axis stability throughout. There are two types of three-axis stabilized systems commonly in use today, zero-momentum and bias-momentum. Zero-momentum systems use three reaction wheels that are initially at rest. Disturbance torques cause these wheels to gain speed which must then be dumped. Bias-momentum systems utilize a single momentum wheel

whose spin axis is aligned with the negative pitch axis. The momentum wheel spins continuously at a high speed providing gyroscopic stiffness which, in turn, provides coarse yaw control. Bias-momentum systems have the advantage of being simpler than zero-momentum systems and are less expensive, so they are commonly used in earth satellite systems. A reaction wheel system was chosen for slew capability. In system component selection, mass and power were kept to the minimum required within the constraints. Heritage was also a key factor and proven reliable systems were selected where possible.

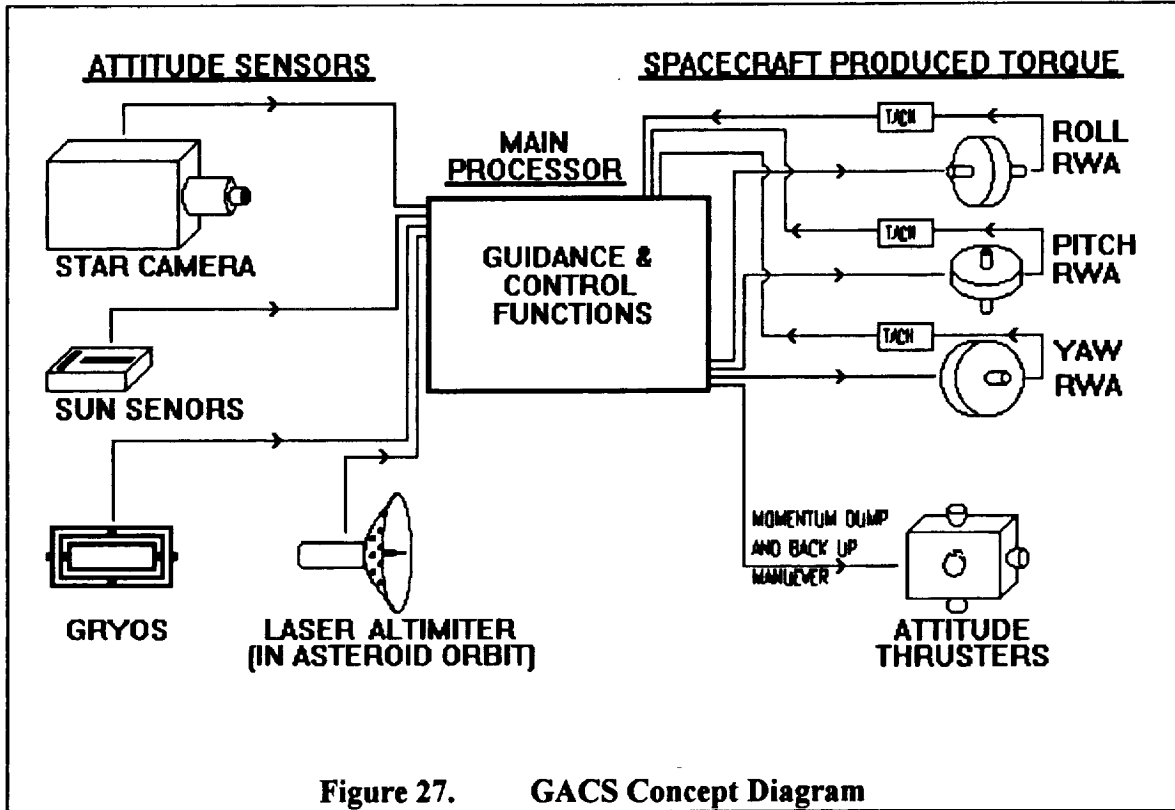
B. SYSTEM DESCRIPTION

Three orthogonal Reaction Wheel Assemblies (RWA's), one along each body axis, allow independent control of rotation about each axis. In the event of a RWA failure, the slewed fourth wheel will be used. Momentum dumping is accomplished by twelve orthogonal attitude control thrusters. Normal operations call for pairs to work simultaneously to rapidly desaturate the RWA's before slew maneuvers and to periodically activate to keep the RWA bias low, with automatic desaturation beginning at 210 rpm. This will minimize dynamic coupling in the Euler equations describing the spacecraft motion. The propulsion system will give limited three-axis stability in the event of multiple RWA failure. The algorithm will contain all described failure modes. The control system concept is depicted in Figure 27.

The GACS provides autonomous and commanded attitude control through the use of three zero-momentum reaction wheels. Thrusters are incorporated to provide the same control for back up or desaturation of the reaction wheels. The Fiber Optic Gyros (FOGS) are essentially an inertia measuring unit. They will be periodically calibrated using the star sensors and sun sensors and will provide a short term attitude reference.

Attitude errors are induced by solar disturbance torques, perturbations during desaturation and Δv maneuvers. Aerodynamic disturbances will be nonexistent and gravity gradient and magnetic

disturbance torques will effect the satellite to a very small degree, due to the relatively small asteroid mass.



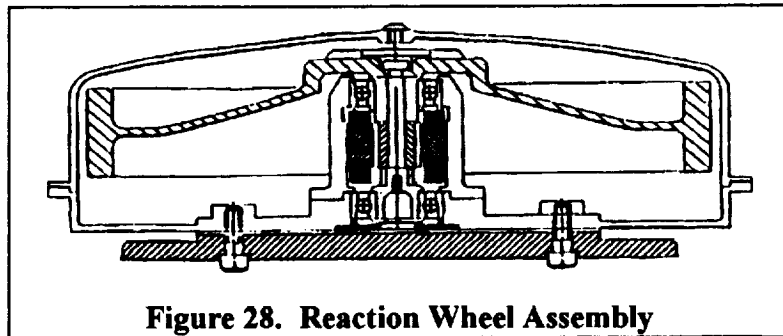
The Attitude Control Computer receives data from the gyros, the star camera and the two sun sensors to compute and store two sets of these errors: (1) the Euler angles with respect to the standard nadir pointing sensing coordinates, and (2) the Euler angles with respect to the coordinates which track the sun. From these, the computer can calculate the direction cosine matrix used in its duty slew direction. The first set of errors include the orbital rate while the second set are fixed with respect to the orbit normal coordinate system. Twelve independent transformations exist in each case (sign ambiguities are removed), and the computer defaults to the one which results in the minimum total correction path (or slew path) although any specific direction cosine matrix can be chosen. The computer then commands the RWA's to perform the chosen sequence of

single axis slews to reach the target axes (i.e. to zero the euler angles). From here, smaller slews can be commanded to accomplish offset nadir pointing or to correct a thermal problem. Single axis slew sequences are not the fastest method but they simplify constraint checking, allow separate orthogonal error computation, and minimize dynamic coupling.

C. COMPONENT DESCRIPTION

1. Reaction Wheel Assemblies (RWA's)

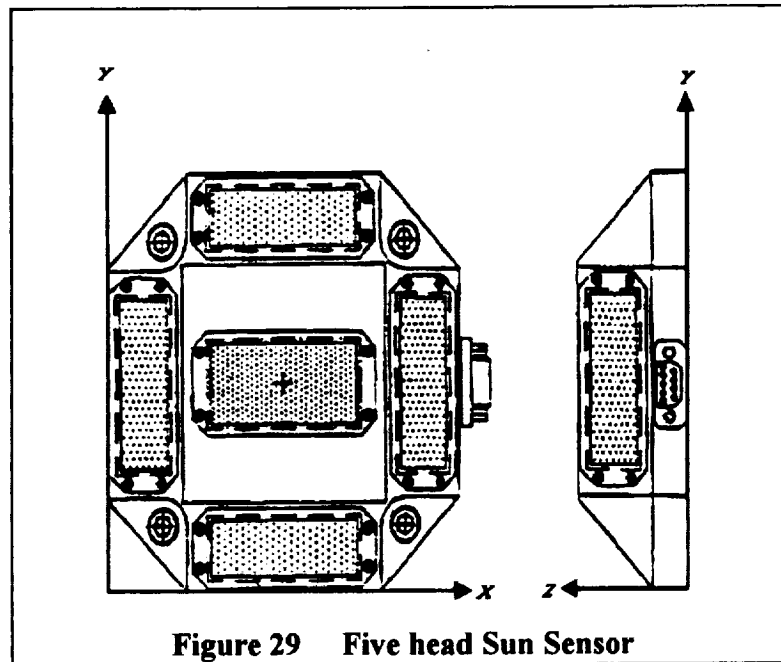
Three Space Science Corporation RWA's will be used and they will be located on orthogonal axes. To save weight only three main wheels will be included with back up provided by the thrusters. Available acceleration torque per wheel is ± 0.335 Nm and available brake torque is ± 0.365 Nm. Figure 28 shows a cross section of the model 3030 Momentum/Reaction wheel assembly that will be used. All three RWA's will be located close together to reduce wiring and simplify construction. Orientation maneuvering will be accomplished by single axis rotations using the individual RWA's.



2. Sun Sensors

Two of the five-head Space Science Corporation sun sensors provide an attitude reference relative to the sun. One will be mounted on each solar array panel. The sun sensors provide measurements in a field-of-view of $\pm 90^\circ$ by $\pm 90^\circ$ (hemispheric field of view). Instrument accuracies of 0.462° are typical and are 0.768° worst case. Typical power requirements are 0.25

Watts with a maximum of 0.5 Watts. Once the solar arrays are deployed the sun sensors will be used to ensure that the arrays continuously point toward the sun. Only one will actually be required to obtain an accurate fix.



3. Fiber Optic Gyros (FOGS)

Fiber optic gyros are small, have no moving parts and are light. Performance is the same in almost any environment. Out of all the guidance and control system equipment used in this design, these require the most amount of power at 19 Watts. Their accuracy is $0.01^\circ/\text{hr}$. In an inertial measurement unit, three gyroscopes are part of a system that steadies a platform to serve as a reference point for changes in the vehicle's attitude. The platform is usually mounted in a gimbal framework attached to the spacecraft. The gimbals transmit to the platform the slightest pitching, rolling and yawing rates and motions of the spacecraft, and a sensor passes the acceleration information to a computer, which can either send instructions to the reaction wheels or thrusters to return the spacecraft to its original orientation or to complete other navigational calculations.

4. Star Camera

One star camera will provide three axis attitude knowledge to about 1 arc second in conjunction with the gyros and the sun sensors. It will be able to detect fourth magnitude stars. Power consumption is a constant 10 Watts. The star camera will be oriented along the +Y axis. Once in orbit around the asteroid the + and - Y faces will rarely point at the sun, which is ideal for star tracking. The basic operation consists of the camera recording images through various filters. Light passes through a lens and shutter, then strikes an electrically charged plate at one end of a vidicon tube, causing an image to form on the back of the plate. Electrons will be present in dark areas, absent in light areas. From the other end, an electron beam scans the plate, replacing lost electrons in proportion to the intensity of light. A brightness value is assigned to each picture element on the plate and compared via the flight data computer to the known constellations.

D. SYSTEM INTEGRATION AND PERFORMANCE

The characteristics of the reaction wheel components are listed in Table 18.

Wheel Assembly Size	Storage Capacity (Nms)	Peak Torque (Nm)	Maximum Speed	Mass (kg)	Power (Watts)
11.40 x 34.32cm	10 Nms @ 6000 RPM	±0.350 Nm	6000 RPM	3.78 kg each	8 W

Table 18. Reaction Wheel Assembly Characteristics.

The storage capacity and peak torque specifications of the reaction wheels are important for satellite rotations since the storage capacity caps the maximum motor speed that can be used to turn the spacecraft, and the peak torque limits the rate of turn since the rate of motor acceleration is limited.

1. Moments of Inertia

The moments of inertia (MOI) of the spacecraft are

$$I_{xx} = 481 \text{ Nms}^2$$

$$I_{yy} = 310 \text{ Nms}^2$$

$$I_{zz} = 559 \text{ Nms}^2$$

The +z axis is the axis passing through the antenna center, the +x axis is the instrument panel, and the +y axis is in the direction of the solar array such that a right-hand orthogonal system is formed. Cross-terms do exist in the inertia matrix, but they are small compared to the principle axes, so they are ignored in the design.

The twelve 4.5N thrusters provide torques about the three principle axes and the angular momenta imparted for a desaturation firing of 20 milliseconds are

$$h_x = 0.1068 \text{ Nms} \quad h_y = 0.1068 \text{ Nms} \quad h_z = 0.1246 \text{ Nms}$$

2. Spin Stabilization

The spacecraft is spin stabilized when separated from the booster. Spin stabilization will continue until after the insertion into the transfer orbit. If the spacecraft is assumed to dissipate energy while spinning, which is a valid assumption since it will not be perfectly rigid, the energy sink approach dictates that a stable spin is possible only about the axis with the maximum MOI (Agrawal, pg. 118). This design has a maximum MOI about the z-axis, which is also the large thruster centerline and the intended spin axis, so the spin stabilization will be stable about this axis. Rigorous modeling of the spacecraft to fully design the operating characteristics of this control system has not been done, since it is a common attitude control mode that is well understood, and because the small thrusters are already in place (near the rim of the spinning spacecraft and oriented parallel to the spin axis) to satisfy the three-axis momentum desaturation requirements.

3. Acquisition Sequence

After the transfer orbit insertion, the 4.5N thrusters will be used to de-spin the craft and start the transition to three-axis control. The solar arrays are folded so that one-third of the cell area is exposed for power collection while spinning, with a sun sensor mounted on the array on each side of the spacecraft. When the spin is removed, it will be convenient to align one array such that the sun line is perpendicular to the folded array. This allows an accurate attitude determination by using the sun line and the line of bearing from the star tracker. With the power available, the reaction wheel system should be enabled to take over the attitude control. The spacecraft is then turned on the z axis 45° and the arrays deployed. This will allow the array to receive 71% ($\cos 45^\circ$) of the incident light while preparing to deploy the array. After the array is deployed, the remaining 45° turn is made, so that the unfolded array is perpendicular to the sun line. The next step is to rotate the body so that the high-gain antenna points earth for system checks and validation.

4. Three-axis Stabilization

Adequate control must be maintained for three cases: 1) while firing the small thrusters for wheel desaturation, 2) while repositioning the spacecraft with the reaction wheels, and 3) while performing large Δv burns with the large thruster. The references to axes assume that the x-axis is roll, y is pitch, and z is yaw, much like the typical earth orbit assignments. The only external torques of any significance for the NEAR missions are solar radiation torques. Because most of the spacecraft lifetime is spent at distances greater than 1 AU from the sun, 1 AU is chosen as the worst case for solar radiation disturbance torques. The solar torque is the product of the solar pressure, the exposed area, and the offset between the center of pressure (CP) and the center of mass (CM). The exposed area of this spacecraft is symmetrical about all axes, so the center of pressure is the origin of the spacecraft coordinate system. The spacecraft center of mass is

$$CM_x = 0.020\text{m} \quad CM_y = -0.010\text{m} \quad CM_z = 0.010\text{m}.$$

At 1 AU the solar pressure is essentially a constant at $4.644 \times 10^{-6} \text{ N/m}^2$. Assume a coefficient of specular reflection of 0.2 and no diffuse reflection. When the solar array normal is parallel to the z axis, the exposed area is 18.77 m^2 , and the solar disturbance torques are

$$M_{sx} = 1.046 \times 10^{-6} \text{ Nms.} \quad M_{sy} = 2.092 \times 10^{-6} \text{ Nms} \quad M_{sz} = 0 \text{ Nms.}$$

When the solar array normal is parallel to the x axis, the exposed area is 18.45 m^2 , so the solar disturbance torques are

$$M_{sx} = 0 \text{ Nms.} \quad M_{sy} = 1.028 \times 10^{-6} \text{ Nms} \quad M_{sz} = 1.028 \times 10^{-6} \text{ Nms.}$$

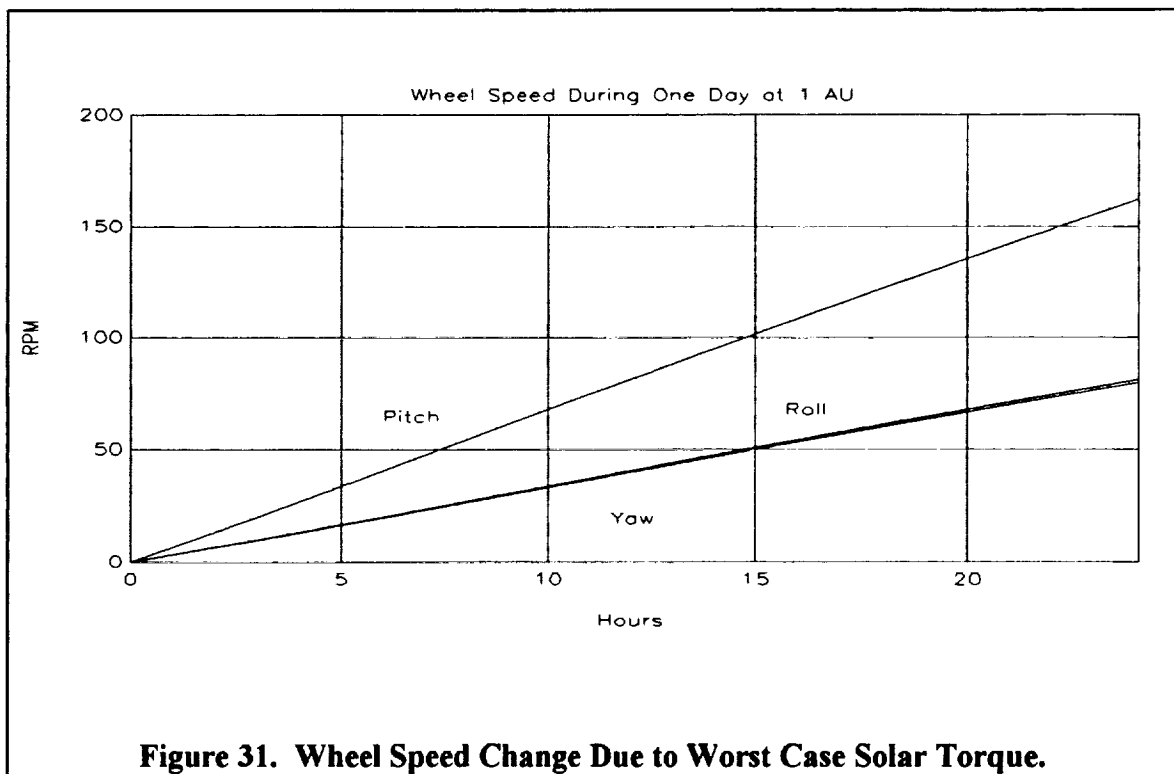
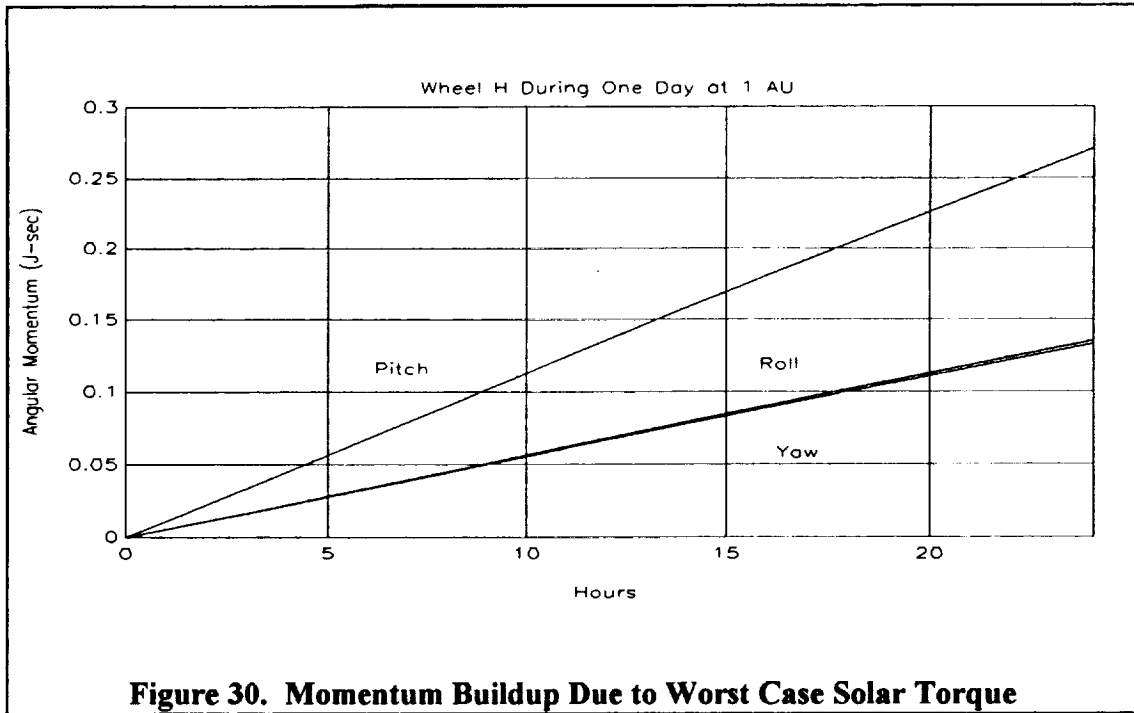
The worst case solar torques about the body axes are then, with a 50% error margin,

$$M_{sx} = 1.569 \times 10^{-6} \text{ Nms.} \quad M_{sy} = 3.137 \times 10^{-6} \text{ Nms} \quad M_{sz} = 1.542 \times 10^{-6} \text{ Nms.}$$

If the wheels are allowed to build momentum until one thruster firing is required to zero the wheel speed, the time between desaturation thruster firings is the time required for one wheel to build up to the amount of momentum removed by one desaturation firing. The minimum time to desaturate is 9.5 hours for the pitch (y) axis wheel in worst case conditions. In reality, the spacecraft attitude will be arbitrary with respect to the sun with only the arrays perpendicular to the sunlight, so that the time between desaturation should be larger as the wheels share the burden. Figures 30 and 31 show the buildup of momentum in the reaction wheels due to the worst case.

Because the momentum wheels retain an angular momentum that is nominally zero and the rotation rate of the spacecraft pointing the asteroid to earth is small, the linearized equations of motion for the spacecraft orientation are uncoupled and yield Equation 1 (Agrawal, 149).

$$\begin{aligned} M_x &= I_{xx} \phi'' + 4\omega_o^2 (I_{yy} - I_{zz}) \phi + h'_x \\ M_y &= I_{yy} \theta'' + 3\omega_o^2 (I_{xx} - I_{zz}) \theta + h'_y \\ M_z &= I_{zz} \psi'' + \omega_o^2 (I_{zz} - I_{xx}) \psi + h'_z \end{aligned} \quad (1)$$



System inputs are available for angular error and error rate using the star trackers, the sun sensors and the FOGS. For this reason, the wheel angular momenta are changed according to Equation 2.

$$\begin{aligned} \mathbf{h}'_x &= K_\phi (\tau_\phi \phi' + \phi) \\ \mathbf{h}'_y &= K_\theta (\tau_\theta \theta' + \theta) \\ \mathbf{h}'_z &= K_\psi (\tau_\psi \psi' + \psi) \end{aligned} \quad (2)$$

The pitch axis control constants are derived as an example of the method (Agrawal, pp. 136-139). If Equation 2 is inserted into Equation 1, the pitch equation becomes

$$M_y = I_{yy} \theta'' + K_\theta \tau_\theta \theta' + K_\theta \theta \quad (3)$$

If a transfer function for the angle as a function of the moment is derived, and critical damping is assumed,

$$\tau = \frac{\tau_\theta}{2} = \sqrt{\frac{I_{yy}}{K_\theta}} \quad (4)$$

and

$$\frac{\theta(s)}{M_y(s)} = \frac{1}{I_{yy} (s + \sqrt{K_\theta / I_{yy}})^2} \quad (5)$$

If M_y is assumed to be an impulse, the maximum pitch error occurs at time $t=\tau$ and has the value

$$\theta_{\max} = \frac{M\tau}{I_{yy}e} \quad (6)$$

The maximum allowable pointing errors are assumed to be 0.2° for ϕ and θ ; 0.4° is the allowable error for ψ , since the high gain antenna needs to point earth very accurately, but is symmetrical in ψ . With the thruster momenta and MOI already specified, and using these maximum angle assumptions, the control system constants are

$\tau_\phi = 86.88 \text{ sec}$	$K_\phi = 0.2631 \text{ Nm / rad}$
$\tau_\theta = 55.78 \text{ sec}$	$K_\theta = 0.4035 \text{ Nm / rad}$
$\tau_\psi = 173.32 \text{ sec}$	$K_\psi = 0.07576 \text{ Nm / rad}$

Figure 32 shows the attitude stability of the system for one day.

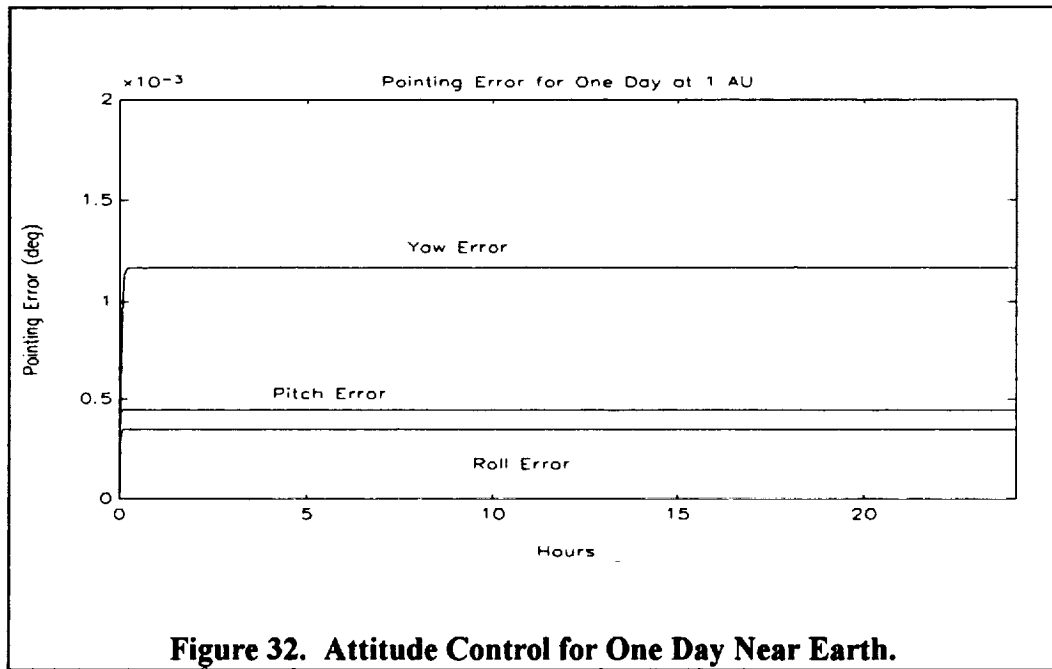


Figure 32. Attitude Control for One Day Near Earth.

The control system should also keep the error within the design limits when the thruster is fired to desaturate the wheel. Figure 33 is a plot of pointing error after a desaturation event on any single axis. Figure 34 is a plot of the wheel speed change as a result of the desaturation firing.

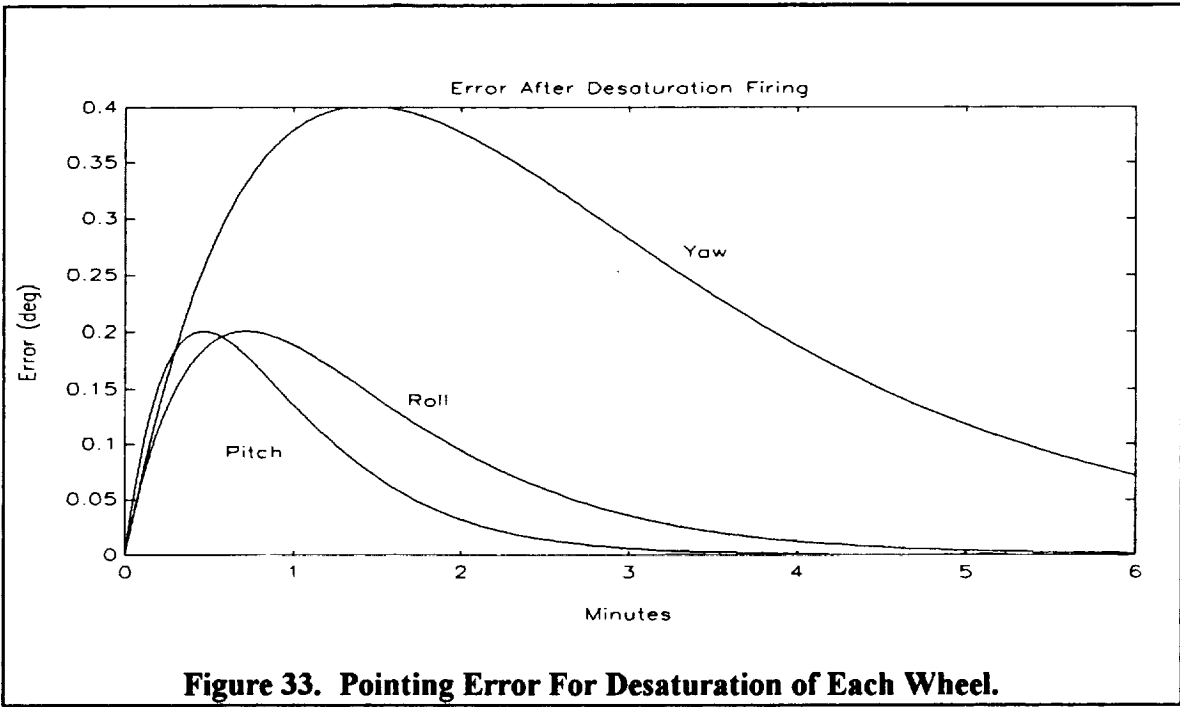


Figure 33. Pointing Error For Desaturation of Each Wheel.

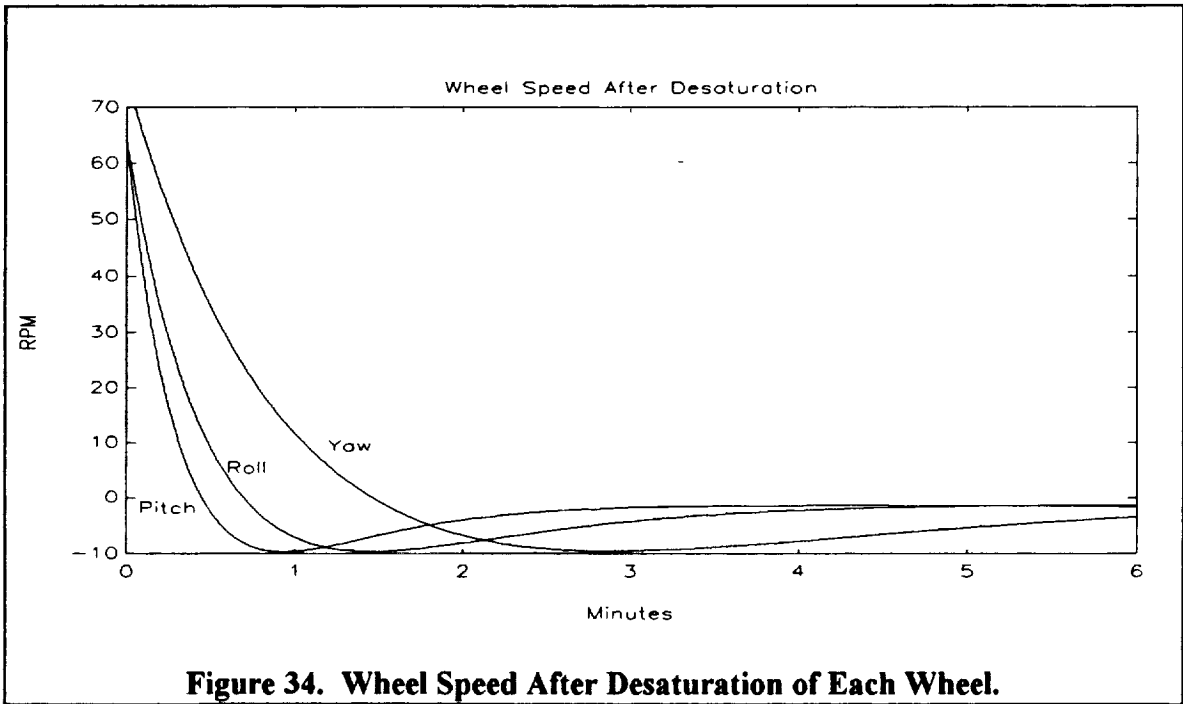


Figure 34. Wheel Speed After Desaturation of Each Wheel.

a. Spacecraft Reorientation

If the spacecraft is rotated one-axis at a time, the equations of motion remain uncoupled, so a simple model of rotational behavior has already been established. The preceding section demonstrated the control system performance during desaturation maneuvers. To reorient the spacecraft, the same control system can be used. To do this, the system is commanded to a new orientation, so that the system then detects an angular error. If the system is constrained to one axis maneuvers, the wheel responsible for controlling the appropriate axis will accelerate to turn the spacecraft. When the error is diminished, the wheel will slow down, and when the error is within the assumed maximum error the wheel will return to its initial zero-momentum state.

It is also important for the control system to not exceed any of the wheel peak torque specifications or maximum RPM. Furthermore, the solar array can rotate at only 19.2° per minute, so the slew rate should be slow enough to let the solar array continue to track the sun. Commanded errors of 30° meet all of these requirements and allow the spacecraft to be turned to new orientations rather quickly. Figure 35 is a plot of system response to 30° error.

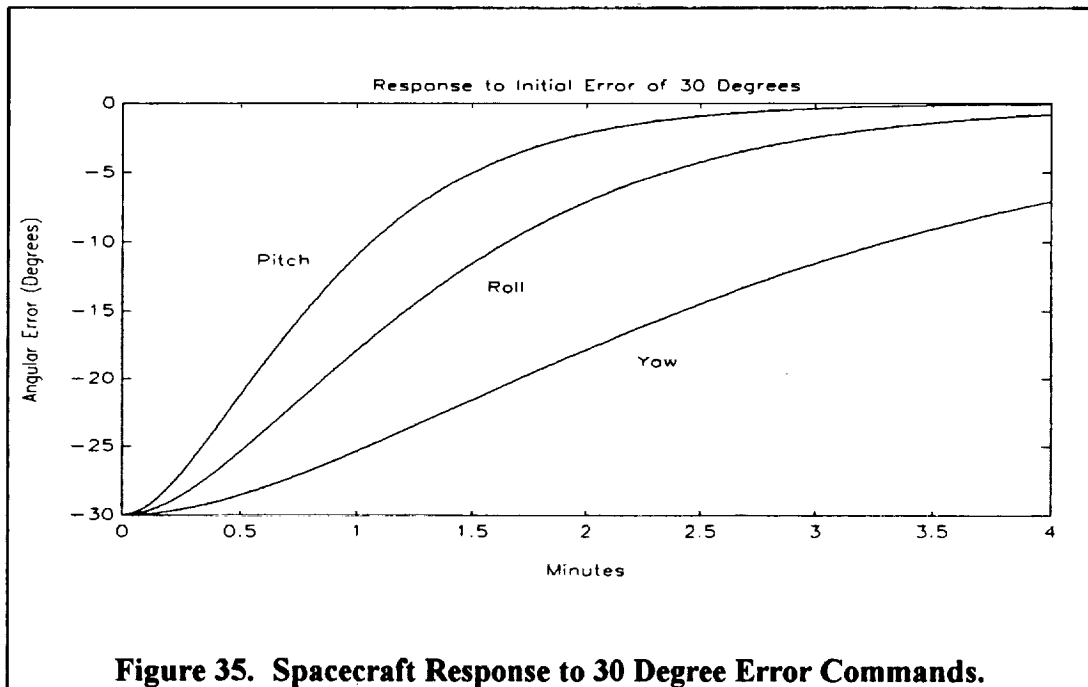


Figure 35. Spacecraft Response to 30 Degree Error Commands.

b. Large Thruster Burns

During large thruster burns during three-axis stabilization, the reaction wheels may not be able to maintain adequate attitude control. The attitude control system should use the twelve thrusters during this period to maintain correct orientation so that the large thruster pushes the spacecraft in the proper direction. This control method was not simulated for the preliminary design.

IX. PROPULSION SUBSYSTEM

A. FUNCTIONAL REQUIREMENTS

The propulsion subsystem must be capable of executing a mid-course trajectory correction maneuver and a rendezvous/capture maneuver with a total delta-V of 1.85 km/sec. The spacecraft must also be able to maneuver in the vicinity of the asteroid for a minimum of one year. The propulsion system will serve as a backup for the attitude control momentum wheels, and will provide attitude control during large Δv maneuvers.

B. DESIGN AND HARDWARE

The propulsion system consists of one 468-N (105 lbf) thruster used for large Δv maneuvers and twelve 4.5-N (1 lbf) thrusters for attitude control and small Δv maneuvers. The large thruster will be used whenever possible for delta-V maneuvers to maximize efficiency using its higher specific impulse. The 468-N thruster utilizes bi-propellant fuel while the 4.5-N thrusters are monopropellant. Propellant consists of Nitrogen-Tetroxide (N_2O_4) and Hydrazine (N_2H_4). There are four propellant tanks (two for each propellant) made of titanium alloy, associated fill and drain valves, isolation valves, filters, pressure regulators, pressure transducers, and fuel lines. See Figure 36 for the schematic diagram.

1. 468-N Thruster

Delta-V maneuvers will be accomplished using the Royal Ordnance Leros 1 dual mode engine. See Figure 12 for location and Table 19 for design and performance characteristics. A bi-propellant thruster is required to achieve the high Δv required while minimizing propellant weight. Achieving the same Δv with a monopropellant thruster would require 26% more propellant by weight (assuming a specific impulse of 225 sec).

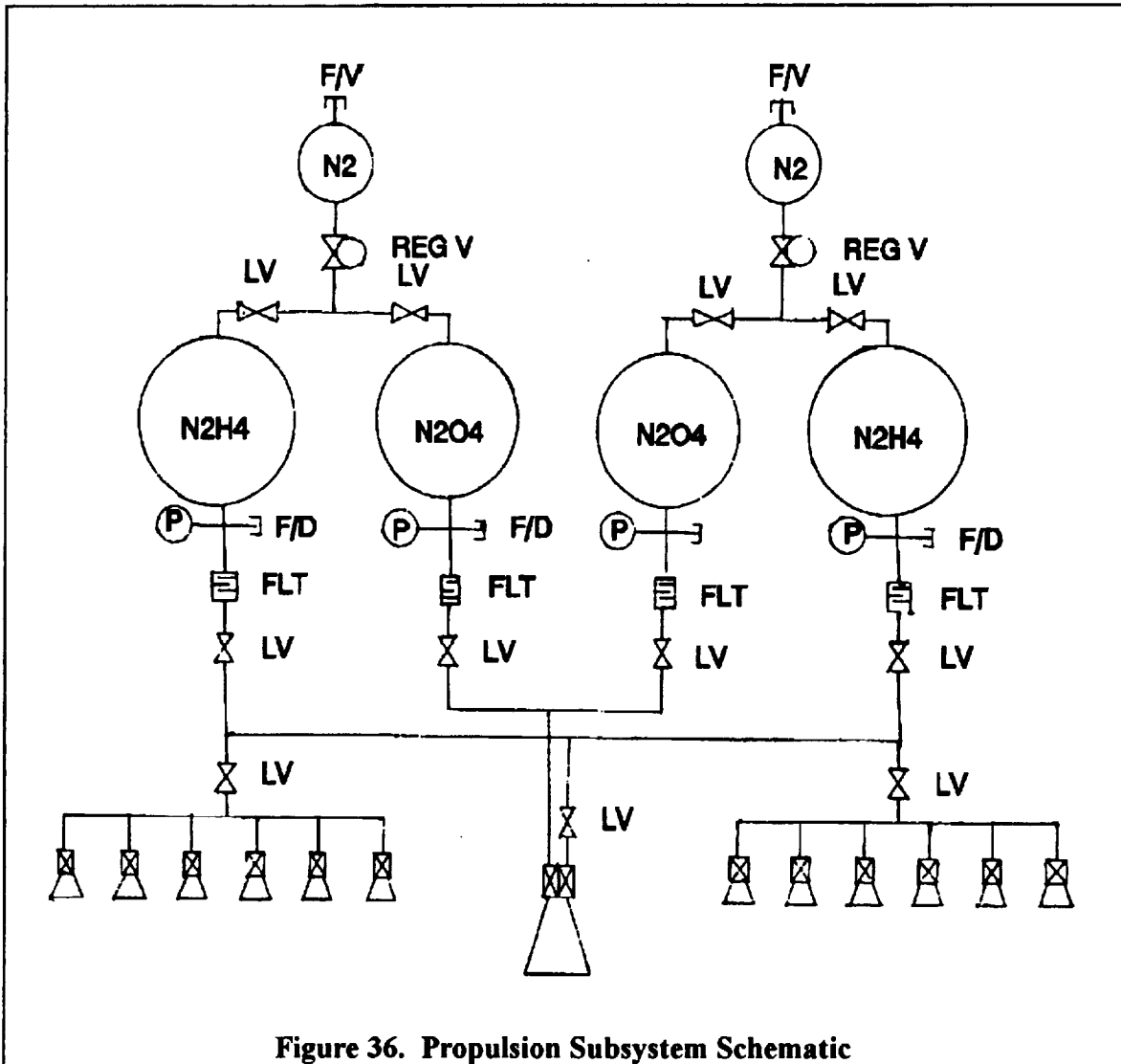


Figure 36. Propulsion Subsystem Schematic

Propellant	Nitrogen Tetroxide/Hydrazine
Thrust	468-N (105 lbf)
Feed Pressure	1.44479 MPa (210psia)
Chamber Pressure	.5516-.7584 MPa(80-110 psia)
Expansion Ratio	150:1
Mass	4.173 kg
Specific Impulse	314 sec

Table 19. Characteristics of LEROS 1 thruster

2. 4.5-N Thrusters

Attitude control and small maneuvers will be accomplished with twelve Rocket Research MR-111C 4.5-N (1 lbf) thrusters, which have been previously used on numerous missions. These thrusters were chosen for their size, weight, and simplicity. Monopropellant thrusters allow the use of smaller torques than with bi-propellant systems, and thus allow a finer degree of attitude control. They are lighter in weight than the smallest bipropellant thruster, and have a simpler control design. Table 20 gives the design and performance characteristics of the thruster, and Table 21 shows thruster operations. Because of the high reliability of these thrusters, no redundancy is incorporated. Figures 14 through 18 show the location of the thrusters. Thruster locations were chosen to minimize piping, minimize impingement on solar arrays and payload, and provide redundancy. Five kilograms of hydrazine were allocated for attitude control, plus any excess hydrazine from the Δv maneuvers. The use of these thrusters results in a minimum weight savings of 7 kg over bipropellant thrusters which weigh 0.848 kg/thruster and which require more piping for their fuel supply.

Propellant	Hydrazine
Catalyst	Shell 405
Steady State Thrust	5.338-1.334 N (1.2-.3 lbf)
Feed Pressure	2.7579-.5516 MPa (400-80lbf)
Chamber Pressure	1.2066-.3447 MPa (175-50lbf)
Expansion Ratio	74:1
Flow Rate	2.404-.635 g/s
Mass	0.33113 kg
Specific Impulse	229-226 sec
Minimum Impulse Bit	0.0845N/s@2.4132 MPa&20ms ON

Table 20. Characteristics of the MR-111C Thruster

Operation	Thruster Pair
Positive Roll (+X)	1B,4B
Negative Roll (-X)	1A,4A
Positive Pitch (+Y)	5B,2B
Negative Pitch (-Y)	5A,2A
Positive Yaw (+Z)	3B,6B
Negative Yaw (-Z)	3A,6A

Table 21. Thruster Operations

3. Propellant Tanks

Four propellant tanks made of titanium alloy TI-6AL-4V are required. Two tanks for each propellant are utilized to hold the required amount of propellant, fit into the spacecraft, and provide some ability to isolate faults while maintaining reduced capabilities. A capillary/surface tension propellant management system will be used similar to that used in Viking and Intelsat (expulsion diaphragms or bladders are not compatible with N_2O_4). Tank sizes are calculated in Appendix F. Based on these calculations and the tanks available off the shelf, new tanks will be required. Although the tank sizes will be new, the technology has been proven in the Viking and Intelsat programs. Two 0.59m diameter tanks are required for the N_2H_4 . This will adequately hold the required 190.0 kg of N_2H_4 , with a 10% volume margin for the propellant management system and ullage. The dry weight of each tank is estimated to be 7 kg. Two 0.47m diameter tanks are required for the N_2O_4 . This will adequately hold the required 142.4 kg of propellant with a 10% volume margin for the propellant management system and ullage. The dry weight of each tank is estimated to be 5 kg.

Two pressurant tanks for N_2 are required, one for each set of propellant tanks. Volumes of tanks are calculated in Appendix F. Two tanks of 0.24m diameter are needed similar in construction to those on Intelsat made of graphite or TRW titanium alloy used on numerous missions. Estimated dry weight is 1.5 kg per tank. Tank size is based on operating pressure of 4000 psi. This will allow continuous pressurization of the propellant tanks to 200 psi for steady, predictable thruster operation.

4. Miscellaneous

Each propulsion tank has an associated fill/drain valve, filter, pressure transducer, and latching isolation valve. The pressurant tanks are connected to the propellant tanks via pressure regulators and latching isolation valves with each pressurant tank having a fill/vent valve.

C. PERFORMANCE

The system as designed will produce a 1.85 km/sec Δv using the Leros 1 thruster with a specific impulse of 314 sec., at a feed pressure of 210 psia, and a mixture ratio of 0.77/1 N_2O_4/N_2H_4 by weight. The attitude control thrusters could be used for small Δv corrections, however their specific impulse of 225 sec. would be inefficient. The mass budget for the propulsion system is shown in Appendix G. The power requirements of the system are minimal and short-term.

X. THERMAL CONTROL SUBSYSTEM

A. FUNCTIONAL REQUIREMENT

The purpose of the Thermal Control Subsystem is to ensure that the spacecraft and its internal components are maintained at the temperatures required for proper operation. Locations of components in relation to the boundaries of the spacecraft and to each other will affect the ability of the system to maintain the required temperatures. Normal operating temperatures for some of the major components are given below:

COMPONENT	OPERATING RANGE(°C)
Battery	0 to 60
Fuel Tanks	5 to 60
General Electronics	-29 to 66
Communications:	
Receiver	-20 to 50
Transmitter	-15 to 45
TWTA	-30 to 55
Instruments:	
Camera/Imager	-35 to 5
Laser Altimeter	0 to 10
IR Spectrometer	-35 to 5

Table 22. Component Temperature Limitations

B. DESIGN

The NEAR spacecraft will use a passive thermal control system with heater augmentation for those components that need it. The preliminary design is based on the expected mission of the spacecraft and the thermal environment it is expected to encounter during that mission. In this case, the analysis must look at the great variation in the spacecraft's distance to the sun. Unlike standard Earth orbiting satellites, which are subject to a relatively constant solar flux as well as the Earth's own heating effects, the NEAR spacecraft will be between one and two AU's from the sun during the course of the asteroid's elliptical orbit and will not be subject to Earth's heating effects.

During the initial phases of the mission, the spacecraft will be traveling away from the Earth, but it will not be generating much power. During the communications portions of the mission phase at the asteroid however, the internal power generation will be at its maximum, but the spacecraft will also be at a much greater distance from the sun for long periods of time. These two situations actually help to minimize the need for a complex thermal control system that would be required to either reject or produce significant amounts of heat to maintain normal operating temperatures.

Preliminary thermal design involves the use of a heat balance equation to measure the heat input from external and internal sources, balanced against the heat rejection to space. Prior to a detailed analysis, a heat balance equation for an isothermal spacecraft the size of the NEAR craft was used to get an estimate of the temperature ranges for varying conditions. Solar intensity for the two extreme distances were taken to be 1353 W/m² (the average at Earth) and 179 W/m² at 2.75 AU. The analysis further assumes a maximum internal power generation equal to the spacecraft's rated maximum power, 250 watts. This maximum is only applicable when the high gain transmitters are used to relay data to Earth. The majority of the time is spent at much lower power.

A rough estimate of spacecraft temperature is obtained by

$$T_e = \sqrt[4]{\frac{P + \alpha_s S \mu_i a}{\epsilon A \sigma}} \quad (1)$$

where:

- P = Internal power dissipated
- α_s = Solar absorptance of MLI (0.35)
- S = Solar intensity (W/m²)
- μ_i = Solar aspect coefficient (1)
- a = area exposed to sun (1.5x1.33)
- ϵ = Emissivity of OSR (0.8)
- A = OSR area for heat rejection (1 m²)
- σ = Stefan-Boltzmann constant, 5.67 x 10⁻⁸ W/m²K⁴

If the power dissipated by the spacecraft is a minimum of 127 Watts and a maximum of 250 Watts, Equation 1 yields the equilibrium temperatures listed in Table 23. These temperatures are only a rough estimate of the average temperature. Component temperature prediction requires a much more rigorous model.

CONDITION	TEMPERATURE (C)
Maximum power and distance	17
Minimum power, maximum distance	-15
Maximum power, minimum distance	91
Minimum power and distance	76

Table 23. Temperatures for the Four Extreme Cases

C. COMPONENTS

1. Multi-layer Insulation (MLI)

The spacecraft's exterior surfaces will be covered with MLI to minimize heat transfer across the surface panels. The entire exterior surface will be covered except for areas required for the instruments and the thermal radiator. It will also be used to insulate fuel and oxidizer tanks and lines to prevent freezing. The insulation for this spacecraft will consist of twenty layers of aluminized kapton on the exterior surface and mylar insulation between the kapton and the surface of the spacecraft. Exact thicknesses in certain areas can be adjusted to control the heat conductance from the internal equipment to the spacecraft's surface..

2. Optical Solar Reflectors (OSR)

Heat is rejected to space via the OSR, located on the same faces as the solar array drive motors to avoid direct sunlight. Their size and location depends upon the location and amount of heat dissipation of the spacecraft components. They are thermally coupled to the equipment attached to the interior surface of the structure at the OSR panel. This includes but is not limited to the TWTA's, the communications equipment and the battery. Based on computer modeling, an

area of 1 m² is required, 400 cm² for each communications suite and TWTA; and 200 cm² for the battery.

3. Heaters

Electric heaters will be used when and where necessary to maintain temperatures of key spacecraft components above the minimums required for proper operation. These components include the fuel tanks and lines, thruster valves, momentum wheels, and the battery. The heaters can work either based on thermistors or thermocouples for automatic cycling or on command enable/disable. Each fuel tank, oxidizer tank, and battery require one five watt heater, for a total of five heaters. It is also anticipated that smaller heaters are required for the fuel lines and valves to prevent freezing.

D. THERMAL ANALYSIS AND PERFORMANCE

The thermal analysis for the NEAR spacecraft was performed using the software program, PC-ITAS, developed for personal computers by the ANALYTIX Corporation. PC-ITAS is a menu driven, graphics capable program that allows the designer to build a geometric model of the spacecraft and then model all or some of it for subsequent thermal analysis based on internal heat generation, orbital characteristics, optical and physical properties of spacecraft material, and view and shadowing factors. This is done by designating (or allowing the computer to designate) up to 240 surfaces as "nodes" for calculations of temperatures throughout the spacecraft.

For this project, a complete geometric structural representation of the NEAR spacecraft and its major internal components was constructed. This resulted in over 800 surfaces, so a thermal model was built using surfaces in which heat is generated, surfaces thermally coupled to the heaters, structural members like the panels and central tube, and the OSR. The exterior was assumed to consist either of MLI or OSR and the interior surfaces were assumed to be painted black to help effectively radiate heat away from the components but keep it within the spacecraft.

Thermal dissipation values were assigned to various surfaces to simulate either equipment heat dissipation values or heater values if there were heaters in the vicinity. Using this information, the computer calculated estimated temperatures for each of these locations that can be used to evaluate the performance of the thermal control system. If necessary, further models of the spacecraft as a whole, as well as specific portions can be built for further analysis and design changes.

E. PC-ITAS NODE ANALYSIS INITIAL CONDITIONS AND ASSUMPTIONS

For thermal node modeling purposes, 88 surfaces or nodes were used, consisting of electronic equipment, fuel and oxidizer tanks, exterior structural faces, and instruments. Since each piece of equipment is encased in a box, consisting of six surfaces, the surfaces were all interconnected to simulate a point source for heat dissipation and temperature and to reduce the number of nodes, thus simplifying the calculations (surfaces that are flush with the payload shelf were not included in the thermal model). The computer used one of two methods in determining thermal conductances. For radiative heat transfers, the conductances were entered as surface areas in watts per square centimeter. For heat transfers by conduction, the conductance is a function of material and could be expressed in terms of watts per degree C. The component temperatures could then be controlled by

NODES	COMPONENT
1-10	Spacecraft skin surfaces (internal and external)
11,15	Heater/Tank combination
13,17	"
19,23	"
21,25	"
12,14,16,18 20,22,24	Tank/Cylinder structural connections
26-34	Cylinder to Bottom structure
35-38	Momentum Wheels
39-43	Communications Suite
44-48	TWTA #1
49-53	TWTA #2
54-58	IR Spectrometer
59-63	Laser Altimeter
64-68	Camera/Imager
69-73	Processors
74-78	Magnetometer
79-83	Recorder
84-88	Battery

Table 24. Thermal Model Nodes

controlling the radiative or conductive paths and values, either by creating a path to the spacecraft's exterior or by sufficiently insulating the equipment box within the spacecraft. The nodes were broken down as shown in Table 24. Thermal dissipation, in watts, can be used in the

ITAS model at various nodes to produce temperature changes in components. The heat load assumptions are shown in Table 25. The model used two distances (1 and 2.75 AU) and two solar intensities (1353 and 179 W/m²) to simulate the varying thermal environments expected for this spacecraft. The spacecraft was also given an arbitrary spin rate of 10 revolutions per orbit to simulate the motion of the spacecraft about the asteroid as it conducts its scientific data gathering and turns to transmit the results to Earth. The program calculated steady state temperatures from a baseline of 0°C over a two hour period, as recommended by the software documentation. The four cases for thermal analysis discussed earlier were each modeled using PC-ITAS. The results appear in Tables 26 through 29.

Components	Heat Dissipation (W)
Momentum Wheels	5
Communications	12
IR Spectrometer	2
Laser Altimeter	2
Camera/Imager	4
Processors	5
Magnetometer	1
Recorder	4
Battery	5 (heater only) 10 (when operating)
TWTA	20 (when transmitting)

Table 25. Heat Loads Assumed for Spacecraft Equipment

COMPONENTS	TEMPERATURE (°C)
Fuel and Oxidizer Tanks	34.2
Momentum Wheels	31.8
Communications Suite	-3.3
TWTA	-144.7
IR Spectrometer	-11.1
Laser Altimeter	2.3
Camera/Imager	-9.2
Processors	29.5
Magnetometer	12.0
Recorder	12.8
Battery	-20.1

Table 26. Minimum Power/Maximum Distance (Cold Case)

COMPONENTS	TEMPERATURE (°C)
Fuel and Oxidizer Tanks	34.2
Momentum Wheels	31.8
Communication Suite	-3.3
TWTA	91.3
IR Spectrometer	-9.4
Laser Altimeter	-3.4
Camera/Imager	-11.0
Processors	32.3
Magnetometer	30.6
Recorder	16.5
Battery	30.5

Table 27. Maximum Power/Minimum Distance (Hot Case)

COMPONENTS	TEMPERATURE (°C)
Fuel and Oxidizer Tanks	34.2
Momentum Wheels	33.2
Communication Suite	-3.3
TWTA	-117.8
IR Spectrometer	-9.7
Laser Altimeter	3.3
Camera/Imager	-11.0
Processors	33.2
Magnetometer	26.6
Recorder	16.2
Battery	-14.2

Table 28. Minimum Power/Minimum Distance

COMPONENTS	TEMPERATURE (°C)
Fuel and Oxidizer Tanks	34.1
Momentum Wheels	33.2
Communication Suite	-3.3
TWTA	91.1
IR Spectrometer	-11.0
Laser Altimeter	2.7
Camera/Imager	-10.4
Processors	31.8
Magnetometer	17.8
Recorder	14.8
Battery	30.6

Table 29. Maximum Power/Maximum Distance

F. CONCLUSIONS

Since the conductances for individual components could be adjusted, the components could be almost essentially isolated from the skin of the spacecraft to help maintain its temperature. As a result of this, the small conductances used for these components result in relatively similar temperatures throughout the spacecraft's voyage. In the case of the TWTAs, the conductance paths to the optical solar reflector radiators are much greater and the temperatures show this; extremely cold when the transmitter is not operating and hot when it is.

The fuel and oxidizer temperatures, as well as the temperature for the idle battery, are based upon continuous 5 watt heater operation, which explains the relative inelasticity of these temperatures. Without the heaters, these temperatures would drop to the low points of the surrounding structure.

The instruments and electronic equipment are all maintained within the allowed operating ranges. The expected ranges are limited by a lack of specific manufacture's data, which would be necessary prior to any final design development and modeling. If the instruments were to require special temperature ranges, then special precautions would be required to keep them in that range. Additionally, each component could be modeled in much greater detail using ITAS to determine its own thermal characteristics. The four conditions analyzed will cover all phases of the mission, as the maximum power cases are only encountered when transmitting data to Earth during the communications portion of the mission phase, which could happen at any distance to the sun during the asteroid's orbit, and the minimum power cases are based on the lowest power budgeted, which will cover all other mission phases requiring less than full power.

XI. CONCLUSION

This spacecraft design was completed in less than three months using a very straightforward approach to mission analysis and component selection/design. All systems were designed using proven methods. The structure is a fairly standard configuration and constructed of low-cost materials. The electrical system uses existing technology and low-cost solar cells to accomplish its mission with little compromise. Thermal control is accomplished relatively easily by standard means such as the use of heaters and OCRs. The use of off-the-shelf components keeps the cost of the payload, communications, and propulsion systems down. The attitude control system is used to accomplish all required pointing tasks for communications and data acquisition and also assists in solar array pointing. This reduces the complexity of those systems. Redundancy is designed into the attitude control system to minimize the chance of a failure in this system causing a mission abort. Discipline in keeping the spacecraft separation mass down makes possible relatively low-cost launch by the Delta II.

It is concluded that careful determination of mission and performance requirements, close attention to target asteroid and orbit selection and the use of off-the-shelf components and existing technology, results in a flexible, capable and low-cost spacecraft able to complete the NEAR mission.

APPENDIX A - STRUCTURAL CALCULATIONS

A. CALCULATIONS

Structural calculations were performed for two basic types of components; cylindrical shells and flat, honeycomb plates. The formulas were placed in Microsoft Excel spreadsheets and calculations carried out for specific components by changing user-defined variables. Generic formulas and methods are laid out here, followed by tables with component specific results from spreadsheet calculations.

1. Central Tube/Struts

Axial load:

$$P = (\text{mass})(\text{design factor})(\text{launch load})(g)$$

Bending moment:

$$M = (\text{mass})(\text{design factor})(\text{lateral launch load})(\text{moment arm})(g)$$

Axial compression:

$$\phi = \frac{1}{16} \sqrt{\frac{r}{t}}$$

where: t = thickness of the shell

r = radius of the shell

$$\gamma = 1 - 0.9(1 - e^{-\phi})$$

critical buckling stress:

$$\sigma_c = \gamma \frac{E}{\sqrt{3(1-\nu^2)}} \frac{t}{r} = .6\gamma E \frac{t}{r} \quad (\text{for } \nu = 0.3)$$

where: E = modulus of elasticity of the material

Critical buckling load:

$$P_c = \sigma_c 2\pi r t$$

Bending:

$$\gamma = 1 - 0.731(1 - e^{-\phi})$$

Critical bending stress:

$$\sigma_b = 0.6\gamma E \frac{t}{r}$$

Critical bending moment:

$$M_c = \sigma_b \pi r^2 t = 0.6\gamma \pi E r t^2$$

Combined load:

Critical load ratios:

$$R_c = P/P_c$$

$$R_b = M/M_c$$

Margin of Safety:

$$M.S. = \frac{1}{(R_c + R_b) - 1}$$

Natural Frequency:

$$\omega_n = K \sqrt{\frac{EI}{\mu l^4}}$$

where: K = boundary condition coefficient

E = modulus of elasticity

I = area moment of inertia

l = beam length

μ = mass per unit length

2. Thrust Cone

Axial load:

$$P = (\text{mass})(\text{design factor})(\text{launch load})(g)$$

Bending moment: $M = (\text{mass})(\text{design factor})(\text{lateral launch load})(\text{moment arm})(g)$

Axial compression:

Critical buckling load:

$$P_c = 0.3994\pi Et^2 \cos^2 \alpha$$

where: α = deviation from vertical at the base

Bending:

Critical bending moment:

$$M_c = 0.24814E\pi r_1 t^2 \cos^2 \alpha$$

Combined load:

Critical load ratios:

$$R_c = P/P_c$$

$$R_b = M/M_c$$

Margin of Safety:

$$M.S. = \frac{1}{(R_c + R_b) - 1}$$

3. Equipment Panels, Sides and Decks:

Panel Stiffness:

$$D = .549Eth^2 \text{ (for } \nu=.3\text{)}$$

where: t = face skin thickness

h = honeycomb core thickness

Fundamental Frequency:

$$f = \frac{1}{2\pi} \beta \sqrt{\frac{D}{\gamma a^4}}$$

where: a = length of short edge

β = coefficient as the function of panel edge

conditions and aspect ratio

γ = mass per unit area

Stress:

$$\sigma_{\max} = \beta \frac{wa^2c}{6th} \text{ (assuming a uniformly loaded panel)}$$

where: w = uniform load/unit area

c = distance from center of cross section to top

B. SPREADSHEET RESULTS

The following spreadsheet tables contain calculation results for the central tube, struts, thrust cone, central deck, equipment panels and side panels. Each spreadsheet is self-contained with all relevant formulas embedded in it. User defined variables are denoted by ***. Calculations are based on 6061-T6 aluminum. Mass for honeycomb sections is calculated assuming that the core mass is 30 percent of the face skin mass.

initial spacecraft mass (kg) ***	7.250E+02
design factor ***	1.500E+00
axial load (g) *** (a)	7.000E+00
lateral load (g) *** (l)	2.500E+00
moment arm (m) *** (ma)	5.500E-01
g (m/s ²) ***	9.806E+00
modulus ***	6.700E+10
Axial Load (N)	7.465E+04
Bending Moment (Nm)	1.466E+04
thickness (m) ***	2.888E-03
Base diameter (m) ***	9.398E-01
Top diameter (m) ***	4.600E-01
Height (m) ***	5.500E-01
alpha (rad)	4.113E-01
Critical buckling load	2.872E+05
Critical bending moment	4.035E+04
Load Ratio Rc	2.645E-01
Load Ratio Rb	3.634E-01
Margin of Safety	5.974E-01
material volume (m ³)	2.419E-03
material density (kg/m ³) ***	2.710E+03
structural mass (kg)	6.555E+00

Thrust Cone Calculations

Total Shelf Mass (including equipment) ***	1.000E+01
Shelf Length (m) ***	1.500E+00
Shelf Width (m) ***	1.300E+00
Shelf Area (m ²)	1.950E+00
Mass per unit area (kg/m ²)	5.128E+00
Beta (from table 4.9)	3.322E+01
E = modulus of elasticity	6.700E+10
h = honeycomb core thickness (m)	2.000E-02
t = face skin thickness	5.888E-04
D = panel stiffness	7.363E+03
f = fundamental frequency of panel (Hz)	1.185E+02
margin	
face skin volume	9.750E-04
material density (kg/m ³)	2.710E+03
face skin mass	2.642E+00
core mass	7.977E-01
shelf mass	3.435E+00

Center Deck Calculations

Total Panel Mass (including equipment) ***	1.000E+01
Length (m) ***	1.300E+00
Width (m) ***	1.300E+00
Area (m ²)	1.729E+00
Mass per unit area (kg/m ²)	5.784E+00
Beta (from table 4.9)	1.949E+01
E = modulus of elasticity	6.700E+10
h = honeycomb core thickness (m)	2.888E-02
t = face skin thickness	5.888E-04
D = panel stiffness	3.146E+03
f = fundamental frequency of panel (Hz)	4.288E+01
margin	
uniform dynamic acceleration ***	3.000E+01
w = uniform load/unit area (N/m ²)	1.735E+02
Beta (from table 4.10)	2.970E-01
maximum stress	1.452E+06
allowable yield stress ***	2.410E+08
margin	9.948E-01
face skin volume	8.645E-04
material density (kg/m ³)	2.710E+03
face skin mass	2.343E+00
core mass	7.028E-01
panel mass	3.046E+00

Equipment Panel Calculations

Total Panel Mass (including equipment) ***	9.000E+01
Length (m) ***	1.500E+00
Width (m) ***	1.300E+00
Area (m ²)	1.950E+00
Mass per unit area (kg/m ²)	4.615E+01
Beta (from table 4.9)	3.322E+01
E = modulus of elasticity	6.700E+10
h = honeycomb core thickness (m)	3.888E-02
t = face skin thickness	5.888E-04
D = panel stiffness	1.657E+04
f = fundamental frequency of panel (Hz)	5.927E+01
margin	
uniform dynamic acceleration ***	3.000E+01
w = uniform load/unit area (N/m ²)	1.385E+03
Beta (from table 4.10)	3.400E-01
maximum stress	8.840E+06
allowable yield stress ***	2.410E+08
margin	9.433E-01
face skin volume	9.750E-04
material density (kg/m ³)	2.710E+03
face skin mass	2.642E+00
core mass	7.977E-01
Panel mass	3.435E+00

Side Panel Calculations

strut supported mass (kg) ***	2.000E+01
design factor ***	1.500E+00
axial load (g's) ***	7.000E+00
lateral load (g's) ***	2.500E+00
moment arm (m) ***	1.650E+00
g (m/s^2)***	9.806E+00
alpha (angle from horizontal)	2.499E+01
P = Axial Load (N)	1.537E+03
M = Bending Moment (Nm)	2.395E+03
r = strut radius(m) ***	3.000E-02
t = strut thickness (m) ***	3.000E-03
l = strut length (m) ***	1.095E+00
phi	1.976E-01
gamma	8.386E-01
nu ***	3.000E-01
modulus ***	6.700E+10
critical buckling stress	3.401E+09
critical buckling load	1.923E+06
gamma	8.689E-01
critical bending stress	3.523E+09
critical bending moment	2.989E+04
critical load ratio Rc	7.991E-04
" " " Rb	8.014E-02
Margin of Safety	1.136E+01
material volume (m^3)	6.192E-04
material density (kg/m^3) ***	2.710E+03
strut mass (kg)	1.678E+00
I = area moment of inertia of beam cross section (m^4)	5.064E-05
K = first mode coefficient	3.520E+00
K = second mode coefficient	2.204E+01
mu = mass per unit length (kg/m)	1.532E+00
natural frequency (Hz)	6.982E+02
second mode (Hz)	4.353E+03

Strut Calculations

initial spacecraft mass (kg) ***	7.250E+02
design factor ***	1.500E+00
axial load (g's) ***	7.000E+00
lateral load (g's) ***	2.500E+00
moment arm (m) ***	1.650E+00
g (m/s^2)***	9.806E+00
P = Axial Load (N)	7.465E+04
M = Bending Moment (Nm)	4.399E+04
r = central tube radius(m) ***	2.300E-01
t = tube thickness (m) ***	2.000E-03
l = tube length (m) ***	9.300E-01
phi	6.702E-01
gamma	5.604E-01
nu ***	3.000E-01
modulus ***	6.700E+10
critical buckling stress	1.976E+08
critical buckling load	5.712E+05
gamma	6.430E-01
critical bending stress	2.267E+08
critical bending moment	7.536E+04
critical load ratio Rc	1.307E-01
" " " Rb	5.837E-01
Margin of Safety	3.997E-01
material volume (m^3)	2.688E-03
material density (kg/m^3) ***	2.710E+03
central tube mass (kg)	7.284E+00
I = area moment of inertia of beam cross section (m^4)	5.064E-05
K = first mode coefficient	3.520E+00
K = second mode coefficient	2.204E+01
mu = mass per unit length (kg/m)	7.833E+00
natural frequency (Hz)	4.263E+02
second mode (Hz)	2.669E+03

Central Tube Calculations

APPENDIX B - ORBITAL MECHANICS CALCULATIONS

This appendix presents the MathCAD worksheet used to develop the graphs in the Orbital Mechanics chapter. The spreadsheet in its entirety is included for one example asteroid - McAuliffe.

Constants

AU = 1.4959965 · 10⁸ km Astronomical Unit ρ McAniff = 3. $\frac{\text{g}}{\text{cm}^3}$ Assumed Density of Asteroid
 G = 6.67 · 10⁻¹¹ newton $\frac{\text{m}^2}{\text{kg}^2}$ Gravitational Constant ε = 23.5-deg Ecliptic Angle
 δ₁ = 28.5-deg Declination of Cape Kennedy

Sun Characteristics

μ_{sun} = 1.3271544 · 10¹¹ $\frac{\text{km}^3}{\text{sec}^2}$ Mass_{sun} = 1.9891 · 10³⁰ · kg

Earth Orbital Characteristics

a_{earth} = 0.99979947 · AU e_{earth} = 0.017 i_{earth} = 0.0-deg
 Q_{earth} = 0.0-deg ω_{earth} = 101.2499-deg P_{earth} = a_{earth} · (1 - e_{earth})²
 T_{earth} = 365.2422-day v_{earth} = 29.78 $\frac{\text{km}}{\text{sec}}$
 r_{earthp} = a_{earth} · (1 - e_{earth}) r_{earthp} = 0.983 · AU
 r_{eartha} = a_{earth} · (1 + e_{earth}) r_{eartha} = 1.017 · AU
 Mass_{earth} = 5.9758 · 10²⁴ · kg r_{earth} = 6378.145-km μ_{earth} = G · Mass_{earth} μ_{earth} = 3.986 · 10⁵ $\frac{\text{km}^3}{\text{sec}^2}$
 r₀ = 200-km + r_{earth} v_{200km} = $\sqrt{\frac{\mu_{\text{earth}}}{r_0}}$ v_{200km} = 7.784 $\frac{\text{km}}{\text{sec}}$ Velocity of a 200 km Circular Injection Orbit

C = $\begin{pmatrix} \cos(\omega_{\text{earth}}) & -1 \cdot \sin(\omega_{\text{earth}}) & 0 \\ \sin(\omega_{\text{earth}}) & \cos(\omega_{\text{earth}}) & 0 \\ 0 & 0 & 1 \end{pmatrix}$ C = $\begin{pmatrix} -0.195 & -0.981 & 0 \\ 0.981 & -0.195 & 0 \\ 0 & 0 & 1 \end{pmatrix}$ Conversion Matrix from Perifocal to Heliocentric Ecliptic DK Coord for Earth

v_{earth} (v_{earth}) = $\sqrt{\frac{\mu_{\text{sun}}}{P_{\text{earth}}}} \begin{pmatrix} -\sin(v_{\text{earth}}) \\ e_{\text{earth}} + \cos(v_{\text{earth}}) \\ 0 \end{pmatrix}$ Perifocal Velocity Components of Earth's Velocity About the Sun

Asteroid Orbital Characteristics

McAniff
 a_{McAniff} = 1.8787307 · AU e_{McAniff} = 0.3694649 i_{McAniff} = 4.77743-deg
 Q_{McAniff} = 106.90142-deg ω_{McAniff} = 15.59117-deg M_{McAniff} = 283.00658-deg radius_{McAniff} = 1.2-km
 r_{McAniffp} = a_{McAniff} · (1 - e_{McAniff}) r_{McAniffp} = 1.185 · AU
 r_{McAniffa} = a_{McAniff} · (1 + e_{McAniff}) r_{McAniffa} = 2.573 · AU
 T_{McAniff} = 2 · π · $\sqrt{\frac{a_{\text{McAniff}}^3}{\mu_{\text{sun}}}}$ T_{McAniff} = 940.5850349583479 · day
 Mass_{McAniff} = ρ_{McAniff} · $\frac{4}{3} \cdot \pi \cdot \text{radius}_{\text{McAniff}}^3$ Mass_{McAniff} = 2.171 · 10¹³ · kg
 μ_{McAniff} = G · Mass_{McAniff} μ_{McAniff} = 1.448 · 10⁻⁶ $\frac{\text{km}^3}{\text{sec}^2}$

Transfer Orbit Characteristics

Launch

C3_{McAniff} = 38.746 $\left(\frac{\text{km}}{\text{sec}}\right)^2$ Δv_{injMcAniff} = 4.862 $\frac{\text{km}}{\text{sec}}$
 DLA_{McAniff} = 6.607-deg RLA_{McAniff} = 210.995-deg Declination and Right Ascension of Launch Asymptote Earth Equator and Equinox of 1950 Coordinates

$$\delta_{McAniffc} = \sin(-\sin(\tau) \cdot \cos(DLA_{McAniffc}) \cdot \sin(RLA_{McAniffc}) + \cos(\tau) \cdot \sin(DLA_{McAniffc}))$$

$$RA_{McAniffc} = \arctan\left(\frac{\cos(\tau) \cdot \sin(RLA_{McAniffc}) \cdot \cos(DLA_{McAniffc}) + \sin(\tau) \cdot \sin(DLA_{McAniffc})}{\cos(DLA_{McAniffc}) \cdot \cos(RLA_{McAniffc})}\right)$$

$$\delta_{McAniffc} = 18.029^\circ \text{deg} \quad RA_{McAniffc} = 26.429^\circ \text{deg} \quad \text{Declination and Right Ascension of Launch Asymptote Ecliptic and Equinox of 1950 Coordinates}$$

$$E_{\text{Inch earth}} = 15.037421 \text{deg} \quad E_{\text{Inch McAniffc}} = 341.975 \text{deg} \quad \text{Eccentric and True Anomaly of Earth and Asteroid at Launch}$$

$$v_{\text{earth}} = 15.292243 \text{deg} \quad v_{McAniffc} = 333.686 \text{deg}$$

$$v_{\text{earth}}(v_{\text{earth}}) = \begin{pmatrix} -7.857 \\ 29.244 \\ 0 \end{pmatrix} \cdot \frac{\text{km}}{\text{sec}} \quad \text{Earth Orbital Velocity at Launch in Perifocal Coordinates}$$

$$v_{\text{earthijk}} = C \cdot v_{\text{earth}}(v_{\text{earth}}) \quad v_{\text{earthijk}} = \begin{pmatrix} -27.149 \\ -13.412 \\ 0 \end{pmatrix} \cdot \frac{\text{km}}{\text{sec}} \quad \text{Earth Orbital Velocity at Launch in Heliocentric Ecliptic IJK Coordinates}$$

$$RA_{McAniffc} = 180 \text{deg} + RA_{McAniffc} \quad v_{\text{hMcAniffc}} = \sqrt{C^3} \cdot \begin{bmatrix} \cos(\delta_{McAniffc}) \cdot \cos(RA_{McAniffc}) \\ \cos(\delta_{McAniffc}) \cdot \sin(RA_{McAniffc}) \\ \sin(\delta_{McAniffc}) \end{bmatrix}$$

$$v_{\text{hMcAniffc}} = \begin{pmatrix} -5.3 \\ -2.634 \\ 1.926 \end{pmatrix} \cdot \frac{\text{km}}{\text{sec}} \quad \text{Velocity at Infinity in Heliocentric Ecliptic IJK Coordinates}$$

$$v_{\text{inch McAniffc}} = v_{\text{hMcAniffc}} + v_{\text{earthijk}} \quad v_{\text{inch McAniffc}} = \begin{pmatrix} -32.449 \\ -16.046 \\ 1.926 \end{pmatrix} \cdot \frac{\text{km}}{\text{sec}} \quad \text{Velocity of Spacecraft at Launch in Heliocentric Ecliptic IJK Coordinates}$$

$$v_{\text{inchmag McAniffc}} = |v_{\text{inch McAniffc}}| \quad v_{\text{inchmag McAniffc}} = 36.251 \cdot \frac{\text{km}}{\text{sec}} \\ \text{incl McAniffc} = \arcsin\left(\frac{v_{\text{inch McAniffc}2}}{v_{\text{inchmag McAniffc}}}\right) \quad \text{incl McAniffc} = 3.046^\circ \text{deg} \quad \text{Inclination of Launch to the Ecliptic}$$

Transfer

$$r_{\text{Inch}} = a_{\text{earth}} \cdot (1 - e_{\text{earth}} \cdot \cos(E_{\text{Inch earth}})) \quad r_{\text{Inch}} = 0.983 \text{AU}$$

$$\text{Energy transfer1} = \frac{v_{\text{inchmag McAniffc}}^2}{2} - \frac{\mu_{\text{sun}}}{r_{\text{Inch}}} \quad \text{Energy transfer1} = -245.032 \cdot \frac{\text{km}^2}{\text{sec}^2}$$

$$e_{\text{transfer1}} = \frac{\mu_{\text{sun}}}{2 \cdot \text{Energy transfer1}} \quad e_{\text{transfer1}} = 1.81 \text{AU} \quad e_{\text{transfer1}} = 1 - \frac{r_{\text{Inch}}}{a_{\text{transfer1}}} \quad e_{\text{transfer1}} = 0.457$$

$$\Omega_{\text{transfer1}} = \theta_{\text{earth}} + v_{\text{earth}} \quad \Omega_{\text{transfer1}} = 116.542^\circ \text{deg} \quad \omega_{\text{transfer1}} = 0^\circ \text{deg} \quad i_{\text{transfer1}} = \text{incl McAniffc}$$

$$r_{\text{atransfer1}} = a_{\text{transfer1}} \cdot (1 + e_{\text{transfer1}}) \quad r_{\text{atransfer1}} = 2.637 \text{AU}$$

$$t_{\text{transfer1}} = 2 \cdot \pi \cdot \sqrt{\frac{a_{\text{transfer1}}^3}{\mu_{\text{sun}}}} \quad t_{\text{transfer1}} = 889.5200078433566 \text{day} \quad M_{\text{transfer1}} = 0^\circ \text{deg}$$

$$E_{\text{arr earth}} = 235.750236 \text{deg} \quad v_{\text{earth}} = 234.9489 \text{deg} \quad \text{Eccentric and True Anomaly of Earth and Asteroid at Arrival}$$

$$E_{\text{arr McAniffc}} = 350.266 \text{deg} \quad v_{McAniffc} = 345.694 \text{deg}$$

Conversion from Perifocal to Heliocentric Ecliptic IJK Coordinates

$$I_1(\Omega, \omega, \text{inc}) = \cos(\Omega) \cdot \cos(\omega) - \sin(\Omega) \cdot \sin(\omega) \cdot \cos(\text{inc})$$

$$I_2(\Omega, \omega, \text{inc}) = -\cos(\Omega) \cdot \sin(\omega) - \sin(\Omega) \cdot \cos(\omega) \cdot \cos(\text{inc})$$

$$e_1(\omega, \text{inc}) = \sin(\omega) \cdot \sin(\text{inc})$$

$$n \chi(\theta, inc) := \cos(\theta) \cdot \sin(inc)$$

$$m \chi(\Omega, \theta, inc) := \sin(\Omega) \cdot \cos(\theta) + \cos(\Omega) \cdot \sin(\theta) \cdot \cos(inc)$$

$$m \chi'(\Omega, \theta, inc) := -\sin(\Omega) \cdot \sin(\theta) + \cos(\Omega) \cdot \cos(\theta) \cdot \cos(inc)$$

$$a(a) := \sqrt{\frac{\mu_{sun}}{a^3}} \quad b(a, \theta) := a \sqrt{1 - e^2}$$

Calculation of Asteroid Ephemerides Based off November 5, 1990 Epoch Ephemerides

$$E := 80 \text{ deg} \quad T_{00} = \frac{M \cdot McAnliff_0^3 \cdot McAnliff_0}{2 \cdot \pi} \quad T_{00} = 739.422 \text{ day}$$

Given

$$\frac{2 \cdot \pi}{\tau} \cdot (t + T_0) \equiv (E - e \cdot \sin(E)) \quad Efcn(t, T_0, \tau, e) := Fnd(E) \quad \text{Function to find E}$$

$$i := 0..10 \quad t_i := i \cdot \tau \quad T_0 := T_{00}$$

$$\Omega := \Omega_{McAnliff_0} \quad \theta := \theta_{McAnliff_0} \quad inc := i_{McAnliff_0} \quad a := a_{McAnliff_0} \quad e := e_{McAnliff_0} \quad \tau := \tau_{McAnliff_0}$$

$$EMcAnliff_i := Efcn(t_i, T_0, \tau, e) \quad \nu McAnliff_i := \arccos\left(\frac{\cos(EMcAnliff_i) - e}{1 - e \cdot \cos(EMcAnliff_i)}\right)$$

$$rMcAnliff_i := a \cdot (1 - e \cdot \cos(EMcAnliff_i))$$

$$zxomy_i := a \cdot l_1(\Omega, \theta, inc) \cdot \cos(EMcAnliff_i) + b(a, \theta) \cdot l_2(\Omega, \theta, inc) \cdot \sin(EMcAnliff_i) - e \cdot l_1(\Omega, \theta, inc)$$

$$yomy_i := a \cdot m_1(\Omega, \theta, inc) \cdot \cos(EMcAnliff_i) + b(a, \theta) \cdot m_2(\Omega, \theta, inc) \cdot \sin(EMcAnliff_i) - e \cdot m_1(\Omega, \theta, inc)$$

$$zomy_i := a \cdot n_1(\Omega, \theta, inc) \cdot \cos(EMcAnliff_i) + b(a, \theta) \cdot n_2(\Omega, \theta, inc) \cdot \sin(EMcAnliff_i) - e \cdot n_1(\Omega, \theta, inc)$$

Yearly Asteroid Ephemerides from Nov 5, 1990 to Nov 5, 2000 $i := 0..10$

t_i yr	$EMcAnliff_i$ deg	$\nu McAnliff_i$ deg	$rMcAnliff_i$ AU	$zxomy_i$ AU	$yomy_i$ AU	$zomy_i$ AU
0	262.042	118.895	1.975	1.965	0.122	-0.16
1	443.846	105.848	1.804	-1.194	-1.346	0.128
2	556.559	168.721	2.544	1.796	-1.838	-0.096
3	692.665	39.433	1.262	0.151	1.252	-0.042
4	856.697	149.849	2.384	0.099	-2.381	0.05
5	963.094	134.769	2.193	2.136	-0.468	-0.159
6	$1.14 \cdot 10^3$	80.922	1.533	-1.402	-0.608	0.127
7	$1.261 \cdot 10^3$	179.228	2.573	1.409	-2.152	-0.06
8	$1.384 \cdot 10^3$	76.458	1.493	1.032	1.073	-0.109
9	$1.56 \cdot 10^3$	136.866	2.221	-0.407	-2.182	0.086
10	$1.666 \cdot 10^3$	148.036	2.363	2.126	-1.021	-0.145

$$E := 80 \text{ deg}$$

$$M8 \cdot McAnliff_8 := EMcAnliff_8 - e \cdot McAnliff_8 \cdot \sin(EMcAnliff_8)$$

$$T8_{00} = \frac{M8 \cdot McAnliff_8^3 \cdot McAnliff_8}{2 \cdot \pi}$$

$$M10 \cdot McAnliff_{10} := EMcAnliff_{10} - e \cdot McAnliff_{10} \cdot \sin(EMcAnliff_{10})$$

$$T10_{00} = \frac{M10 \cdot McAnliff_{10}^3 \cdot McAnliff_{10}}{2 \cdot \pi}$$

$$T8_{00} = 3.661 \cdot 10^3 \text{ day} \quad T10_{00} = 4.392 \cdot 10^3 \text{ day}$$

$$i := 0..87 \quad t_i := i \cdot \text{day} \quad T_0 := T8_{00} \quad \tau := \tau_{McAnliff_8}$$

$$\Omega := \Omega_{McAnliff_8} \quad \theta := \theta_{McAnliff_8} \quad inc := i_{McAnliff_8} \quad a := a_{McAnliff_8} \quad e := e_{McAnliff_8} \quad \tau := \tau_{McAnliff_8}$$

$$EMcAnliff_i := Efcn(t_i, T_0, \tau, e) \quad \nu McAnliff_i := \arccos\left(\frac{\cos(EMcAnliff_i) - e}{1 - e \cdot \cos(EMcAnliff_i)}\right)$$

$$r_{McAniff_i} = a_{McAniff_i} (1 - e_{McAniff_i} \cos(EMcAniff_i))$$

$$x_{sml_i} = a_{McAniff_i} \cos(\Omega, \theta, inc) \cos(EMcAniff_i) + b(a, e) \chi(\Omega, \theta, inc) \sin(EMcAniff_i) - a_{McAniff_i} \cos(\Omega, \theta, inc)$$

$$y_{sml_i} = a_{McAniff_i} \sin(\Omega, \theta, inc) \cos(EMcAniff_i) + b(a, e) \chi(\Omega, \theta, inc) \sin(EMcAniff_i) - a_{McAniff_i} \sin(\Omega, \theta, inc)$$

$$z_{sml_i} = a_{McAniff_i} \sin(\theta, inc) \cos(EMcAniff_i) + b(a, e) \chi(\theta, inc) \sin(EMcAniff_i) - a_{McAniff_i} \sin(\theta, inc)$$

Asteroid Ephemerides at date of launch, plus one day. Time in days past Nov 5, 1998

i = 71..72

t_i day	$EMcAniff_i - 6\pi$ deg	$v_{McAniff_i}$ deg	$r_{McAniff_i}$ AU	x_{sml_i} AU	y_{sml_i} AU	z_{sml_i} AU
71	341.975	26.314	1.219	-0.132	1.211	-0.019
72	342.565	25.467	1.216	-0.149	1.207	-0.017

Calculate Asteroid Ephemerides at time of spacecraft arrival

$$E = 90 \text{ deg} \quad i = 0.300 \quad t_i = i \text{ day} \quad T_{\theta} = T10 \text{ sec} \quad \tau = \tau_{McAniff}$$

$$\Omega = \Omega_{McAniff} \quad \theta = \theta_{McAniff} \quad inc = i_{McAniff} \quad a = a_{McAniff} \quad e = e_{McAniff} \quad \tau = \tau_{McAniff}$$

$$EMcAniff_i = Efcn(t_i, T_{\theta}, \tau, \theta)$$

$$v_{McAniff_i} = a_{McAniff_i} \frac{\cos(EMcAniff_i) - e}{1 - e \cos(EMcAniff_i)}$$

$$r_{McAniff_i} = a_{McAniff_i} (1 - e \cos(EMcAniff_i))$$

$$x_{smls_i} = a_{McAniff_i} \cos(\Omega, \theta, inc) \cos(EMcAniff_i) + b(a, e) \chi(\Omega, \theta, inc) \sin(EMcAniff_i) - a_{McAniff_i} \cos(\Omega, \theta, inc)$$

$$y_{smls_i} = a_{McAniff_i} \sin(\Omega, \theta, inc) \cos(EMcAniff_i) + b(a, e) \chi(\Omega, \theta, inc) \sin(EMcAniff_i) - a_{McAniff_i} \sin(\Omega, \theta, inc)$$

$$z_{smls_i} = a_{McAniff_i} \sin(\theta, inc) \cos(EMcAniff_i) + b(a, e) \chi(\theta, inc) \sin(EMcAniff_i) - a_{McAniff_i} \sin(\theta, inc)$$

$$v_{x_i} = \frac{v(a) \cdot a}{r_{McAniff_i}} (b(a, e) \chi(\Omega, \theta, inc) \cos(EMcAniff_i) - a_{McAniff_i} \cos(\Omega, \theta, inc) \sin(EMcAniff_i))$$

$$v_{y_i} = \frac{v(a) \cdot a}{r_{McAniff_i}} (b(a, e) \chi(\Omega, \theta, inc) \cos(EMcAniff_i) - a_{McAniff_i} \sin(\Omega, \theta, inc) \sin(EMcAniff_i))$$

$$v_{z_i} = \frac{v(a) \cdot a}{r_{McAniff_i}} (b(a, e) \chi(\theta, inc) \cos(EMcAniff_i) - a_{McAniff_i} \sin(\theta, inc) \sin(EMcAniff_i))$$

Asteroid Ephemerides for Date of Arrival, plus 10 days leading up to. Time in days past Nov 5, 2000

i = 285..295

t_i day	$EMcAniff_i - 8\pi$ deg	$v_{McAniff_i}$ deg	$r_{McAniff_i}$ AU	x_{smls_i} AU	y_{smls_i} AU	z_{smls_i} AU
285	344.283	22.995	1.211	-0.2	1.194	-0.013
286	344.878	22.137	1.209	-0.218	1.189	-0.011
287	345.473	21.276	1.207	-0.239	1.184	-0.01
288	346.069	20.413	1.205	-0.253	1.178	-0.008
289	346.667	19.547	1.203	-0.27	1.173	-0.007
289	347.265	18.679	1.202	-0.287	1.167	-0.005
290	347.863	17.809	1.2	-0.304	1.161	-0.004
291	348.463	16.936	1.199	-0.322	1.155	-0.002
292	349.063	16.061	1.197	-0.339	1.148	-8.18 · 10 ⁻⁴
293	349.664	15.184	1.196	-0.356	1.142	7.071 · 10 ⁻⁴
294	350.266	14.306	1.193	-0.373	1.135	0.002

Arrival t = 295 days

$$v_{arr} \text{ McAniff} = \begin{pmatrix} v_{x_{295}} \\ v_{y_{295}} \\ v_{z_{295}} \end{pmatrix}$$

$$v_{arr} \text{ McAniff} = \begin{pmatrix} -29.399 \\ -11.908 \\ 2.64 \end{pmatrix} \frac{\text{km}}{\text{sec}}$$

$$r_{arr} \text{ McAniff} = \begin{pmatrix} x_{smls_{295}} \\ y_{smls_{295}} \\ z_{smls_{295}} \end{pmatrix}$$

Transfer Orbit Ephemerides and Earth Position During Transfer Calculations (Phase 1)

$$E = 0 \text{ deg}$$

$$T_{oc} = \frac{\tau_{earth}}{2\pi} (E_{inck_{earth}} - e_{earth} \sin(E_{inck_{earth}}))$$

$$T_{oa} = 15 \text{ day}$$

$$T_{oa} = \frac{M_{transfer} \tau_{transfer}}{2\pi}$$

$$T_{oa} = 0 \text{ day}$$

$$i := 0..61 \quad t_i := i \cdot 5 \text{-day} \quad T_o := T_{oo} \quad \Omega := \Omega_{transfer} \quad e := e_{transfer} \quad inc := i_{transfer} \quad a := a_{transfer} \quad e := e_{transfer} \quad i := i_{transfer}$$

$$E_{transfer}_i := Efcn(t_i, T_o, i, e) \quad v_{transfer}_i := a \cdot \frac{\cos(E_{transfer}_i) - e}{1 - e \cdot \cos(E_{transfer}_i)}$$

$$r_{transfer}_i := a \cdot (1 - e \cdot \cos(E_{transfer}_i))$$

$$x1_i := a \cdot l_1(\Omega, e, inc) \cdot \cos(E_{transfer}_i) + b(a, e) \cdot l_2(\Omega, e, inc) \cdot \sin(E_{transfer}_i) - a \cdot e \cdot l_1(\Omega, e, inc)$$

$$y1_i := a \cdot m_1(\Omega, e, inc) \cdot \cos(E_{transfer}_i) + b(a, e) \cdot m_2(\Omega, e, inc) \cdot \sin(E_{transfer}_i) - a \cdot e \cdot m_1(\Omega, e, inc)$$

$$z1_i := a \cdot n_1(\Omega, e, inc) \cdot \cos(E_{transfer}_i) + b(a, e) \cdot n_2(\Omega, e, inc) \cdot \sin(E_{transfer}_i) - a \cdot e \cdot n_1(\Omega, e, inc)$$

$$\Omega := \Omega_{earth} \quad e := e_{earth} \quad inc := i_{earth} \quad a := a_{earth} \quad e := e_{earth} \quad i := i_{earth}$$

$$T_o := T_{oo} \quad i := 0..61 \quad t_i := i \cdot 5 \text{-day}$$

$$E_{earth}_i := Efcn(t_i, T_o, i, e) \quad v_{earth}_i := a \cdot \frac{\cos(E_{earth}_i) - e}{1 - e \cdot \cos(E_{earth}_i)}$$

$$r_{earth}_i := a \cdot (1 - e \cdot \cos(E_{earth}_i))$$

$$x1e_i := a \cdot l_1(\Omega, e, inc) \cdot \cos(E_{earth}_i) + b(a, e) \cdot l_2(\Omega, e, inc) \cdot \sin(E_{earth}_i) - a \cdot e \cdot l_1(\Omega, e, inc)$$

$$y1e_i := a \cdot m_1(\Omega, e, inc) \cdot \cos(E_{earth}_i) + b(a, e) \cdot m_2(\Omega, e, inc) \cdot \sin(E_{earth}_i) - a \cdot e \cdot m_1(\Omega, e, inc)$$

$$z1e_i := a \cdot n_1(\Omega, e, inc) \cdot \cos(E_{earth}_i) + b(a, e) \cdot n_2(\Omega, e, inc) \cdot \sin(E_{earth}_i) - a \cdot e \cdot n_1(\Omega, e, inc)$$

$$dist1_i := \sqrt{(x1_i)^2 + (x1_i - x1e_i)^2 + (y1_i - y1e_i)^2} \quad \text{Spacecraft-Earth Distance Inplane}$$

$$\Psi1_i := \arccos\left(\frac{(dist1_i)^2 - (r_{earth}_i)^2 - (r_{transfer}_i)^2}{-2 \cdot r_{earth}_i \cdot r_{transfer}_i}\right) \quad \text{Spacecraft-Sun-Earth Angle Inplane} \quad dist_{transfer}_i = dist1_i$$

$$\Omega1_i := \arcsin\left(\frac{r_{earth}_i \cdot \sin(\Psi1_i)}{dist1_i}\right) \quad \text{Sun-Spacecraft-Earth Angle} \quad \theta1_i := \arcsin\left(\frac{z1_i}{dist1_i}\right) \quad \text{Declination Angle of Earth from the Spacecraft}$$

$$\max(r_{transfer}) = 2.445 \text{ AU} \quad \text{Max and Min Sun-Spacecraft Ranges}$$

$$\min(r_{transfer}) = 0.983 \text{ AU}$$

$$\max(dist1) = 3.293 \text{ AU} \quad \text{Max and Min Earth-Spacecraft Ranges}$$

$$\min(dist1) = 1.211 \cdot 10^{-8} \text{ AU}$$

$$\max(\Omega1) = 90 \text{ deg} \quad \text{Max and Min Sun-Spacecraft-Earth Angle}$$

$$\min(\Omega1) = 10.174 - 64.851i \text{ deg}$$

$$\max(\theta1) = 18.002 \text{ deg} \quad \text{Max and Min Declination Angle of Earth from Spacecraft}$$

$$\min(\theta1) = 0 \text{ deg}$$

Transfer Orbit (Phase 1) and Earth Orbit Ephemerides at Mid-Course Delta-V $i := 60..61$

t_i day	$v_{transfer}_i$ deg	$r_{transfer}_i$ AU	$x1_i$ AU	$y1_i$ AU	$z1_i$ AU	v_{earth}_i deg	r_{earth}_i AU	$dist1_i$ AU	$\Omega1_i$ deg	$\theta1_i$ deg
300	154.07	2.431	0.027	-2.43	0.056	51.023	0.989	3.248	11.391	0.997
305	155.063	2.445	0.07	-2.444	0.053	45.981	0.988	3.293	10.251	0.953

Transfer Orbit Characteristics for Phase 2

$$\mathbf{vrel_McAuliffe} = \begin{pmatrix} -0.20 \\ -0.08 \\ 0.02 \end{pmatrix} \frac{\text{km}}{\text{sec}}$$
 Relative Velocity Cartesian Components with respect to asteroid/body-centered ecliptic and equinox of 1950

$$vrelmag = |\mathbf{vrel_McAuliffe}| \quad vrelmag = 0.216 \frac{\text{km}}{\text{sec}}$$

$$\mathbf{vtransfer2_arr} = \mathbf{vrel_McAuliffe} + \mathbf{vrel_McAuliffe} \quad \mathbf{vtransfer2_arr} = \begin{pmatrix} -29.599 \\ -11.968 \\ 2.62 \end{pmatrix} \frac{\text{km}}{\text{sec}}$$

$$vtransfer2mag = |\mathbf{vtransfer2_arr}| \quad vtransfer2mag = 32.041 \frac{\text{km}}{\text{sec}}$$
 Spacecraft Arrival Velocity in Heliocentric Ecliptic Coordinates

$$rarrmag = |\mathbf{rarr_McAuliffe}| \quad \text{Radius of Arrival from the Sun}$$

$$\mathbf{h_transfer2} = \mathbf{rarr_McAuliffe} \times \mathbf{vtransfer2_arr} \quad \mathbf{K} = \begin{pmatrix} 0 \\ 0 \\ 1 \end{pmatrix} \quad \mathbf{h_transfer2} = \mathbf{K} \times \mathbf{h_transfer2}$$

$$\mathbf{h_transfer2} = \begin{pmatrix} 4.489 \cdot 10^8 \\ 1.362 \cdot 10^8 \\ 5.694 \cdot 10^9 \end{pmatrix} \frac{\text{km}^2}{\text{sec}} \quad \mathbf{h_transfer2} = \begin{pmatrix} -1.362 \cdot 10^8 \\ 4.489 \cdot 10^8 \\ 0 \end{pmatrix} \frac{\text{km}^2}{\text{sec}}$$

$$e_transfer2 = \frac{1}{\mu_{sun}} \left[\left(vtransfer2mag^2 - \frac{\mu_{sun}}{rarrmag} \right) \cdot \mathbf{rarr_McAuliffe} - (\mathbf{rarr_McAuliffe} \cdot \mathbf{vtransfer2_arr}) \cdot \mathbf{vtransfer2_arr} \right]$$

$$e_transfer2 = \begin{pmatrix} -0.205 \\ 0.329 \\ 0.008 \end{pmatrix} \quad e_transfer2 = |e_transfer2| \quad e_transfer2 = 0.387 \quad P_transfer2 = \frac{(\mathbf{h_transfer2})^2}{\mu_{sun}} \quad P_transfer2 = 1.644 \text{ AU}$$

$$i_transfer2 = \arccos\left(\frac{h_transfer2_2}{|\mathbf{h_transfer2}|}\right) \quad i_transfer2 = 4.71 \text{ deg} \quad \Omega_transfer2 = \arccos\left(\frac{h_transfer2_0}{|\mathbf{h_transfer2}|}\right) \quad \Omega_transfer2 = 106.883 \text{ deg}$$

$$a_transfer2 = \arccos\left(\frac{h_transfer2_0 \cdot e_transfer2}{|\mathbf{h_transfer2}| \cdot |e_transfer2|}\right) \quad a_transfer2 = 15.115 \text{ deg} \quad \text{Energy_transfer2} = \frac{(\mathbf{vtransfer2_arr})^2}{2} - \frac{\mu_{sun}}{|\mathbf{rarr_McAuliffe}|}$$

$$\text{Energy_transfer2} = -229.297 \frac{\text{km}^2}{\text{sec}^2} \quad a_transfer2 = -\frac{\mu_{sun}}{2 \cdot \text{Energy_transfer2}} \quad a_transfer2 = 1.934 \text{ AU}$$

$$\tau_transfer2 = 2 \cdot \pi \cdot \sqrt{\frac{a_transfer2^3}{\mu_{sun}}} \quad \tau_transfer2 = 982.7528672040291 \text{ day} \quad Etransfer2 = 135 \text{ deg}$$

Transfer Orbit Ephemerides and Earth Position During Transfer Calculations (Phase 2)

$$E = 0 \text{ deg}$$

$$T_{ee} = \frac{\tau_{earth}}{2 \cdot \pi} \cdot (E_{earth}|_{\phi_1} - e_{earth} \sin(E_{earth}|_{\phi_1})) \quad T_{ee} = 320 \text{ day}$$

$$T_{ee} = \frac{\tau_{transfer2}}{2 \cdot \pi} \cdot (E_{transfer2} - e_{transfer2} \sin(E_{transfer2})) \quad T_{ee} = 325.641 \text{ day}$$

$$i = 0.130 \quad t_1 = 1.5 \text{ day} \quad T_o = T_{ee}$$

$$\Omega = \Omega_{transfer2} \quad \omega = \omega_{transfer2} \quad inc = i_{transfer2} \quad a = a_{transfer2} \quad e = e_{transfer2} \quad \tau = \tau_{transfer2}$$

$$Etransfer2_1 = Efcn(t_1, T_o, \tau, e) \quad vtransfer2_1 = \arccos\left(\frac{\cos(Etransfer2_1) - e}{1 - e \cos(Etransfer2_1)}\right)$$

$$rtransfer2_1 = a \cdot (1 - e \cos(Etransfer2_1))$$

$$\begin{aligned}
 x1_2 &= a_1 \gamma(\Omega, \theta, inc) \cos(Etransfer_2) + b(a, e) \gamma(\Omega, \theta, inc) \sin(Etransfer_2) - a \cos \gamma(\Omega, \theta, inc) \\
 y1_2 &= a m_1(\Omega, \theta, inc) \cos(Etransfer_2) + b(a, e) m_2(\Omega, \theta, inc) \sin(Etransfer_2) - a \sin \gamma(\Omega, \theta, inc) \\
 z1_2 &= a n_1(\theta, inc) \cos(Etransfer_2) + b(a, e) n_2(\theta, inc) \sin(Etransfer_2) - a \sin \gamma(\theta, inc) \\
 \Omega &= \Omega_{earth} \quad \theta = \theta_{earth} \quad inc = i_{earth} \quad a = a_{earth} \quad e = e_{earth} \quad \gamma = \gamma_{earth} \quad T_0 = T_{oc}
 \end{aligned}$$

$$\begin{aligned}
 Eearth2_i &= Efcn(i_1, T_0, \gamma, \theta) & vearth2_i &= \frac{\cos(Eearth2_i) - e}{1 - e \cos(Eearth2_i)} & rearth2_i &= a(1 - e \cos(Eearth2_i))
 \end{aligned}$$

$$\begin{aligned}
 x2e_i &= a_1 \gamma(\Omega, \theta, inc) \cos(Eearth2_i) + b(a, e) \gamma(\Omega, \theta, inc) \sin(Eearth2_i) - a \cos \gamma(\Omega, \theta, inc) \\
 y2e_i &= a m_1(\Omega, \theta, inc) \cos(Eearth2_i) + b(a, e) m_2(\Omega, \theta, inc) \sin(Eearth2_i) - a \sin \gamma(\Omega, \theta, inc) \\
 z2e_i &= a n_1(\theta, inc) \cos(Eearth2_i) + b(a, e) n_2(\theta, inc) \sin(Eearth2_i) - a \sin \gamma(\theta, inc)
 \end{aligned}$$

$$dist2_i = \sqrt{(x1_2 - x2e_i)^2 + (y1_2 - y2e_i)^2} \quad \text{Spacecraft-Earth Distance Inplane}$$

$$\Psi2_i = \arccos \left[\frac{(dist2_i)^2 - (rearth2_i)^2 - (rtransfer2_i)^2}{-2 rearth2_i rtransfer2_i} \right] \quad \text{Spacecraft-Sun-Earth Angle Inplane} \quad dist_{transfer2_i} = dist2_i$$

$$\Omega2_i = \arcsin \left(\frac{rearth2_i \sin(\Psi2_i)}{dist2_i} \right) \quad \text{Sun-Spacecraft-Earth Angle} \quad \theta2_i = \arcsin \left(\frac{z1_2}{dist2_i} \right) \quad \text{Declination Angle of Earth from the Spacecraft}$$

max(rtransfer2) = 2.684 AU Max and Min Sun-Spacecraft Range

min(rtransfer2) = 1.187 AU

max(dist2) = 3.56 AU Max and Min Earth-Spacecraft Range

min(dist2) = 1.585 AU

max(Ω) = 24.41 deg Max and Min Sun-Spacecraft-Earth Angle

min(Ω) = 0.267 deg

max(θ) = 0.944 deg Max and Min Declination Angle of Earth from Spacecraft

min(θ) = -4.553 deg

Transfer Orbit (Phase 2) and Earth Orbit Ephemerides at and after Mid-course Delta-V i = 0.2

i ₁ day	rtransfer2 _i deg	rtransfer2 _i AU	x1 ₂ AU	y1 ₂ AU	z1 ₂ AU	vearth2 _i deg	rearth2 _i AU	dist2 _i AU	Ω ₂ deg	θ ₂ deg
0	149.224	2.464	0.053	-2.463	0.053	45.981	0.988	3.315	10.094	0.944
5	150.259	2.478	0.1	-2.475	0.051	40.929	0.987	3.355	8.967	0.877
10	151.283	2.49	0.144	-2.486	0.048	35.866	0.986	3.393	7.831	0.812

Transfer Orbit Phase 2) and Earth Orbit Ephemerides for 10 days up to and including the arrival at the asteroid i = 127.129

i ₁ day	rtransfer2 _i deg	rtransfer2 _i AU	x1 ₂ AU	y1 ₂ AU	z1 ₂ AU	vearth2 _i deg	rearth2 _i AU	dist2 _i AU	Ω ₂ deg	θ ₂ deg
635	19.649	1.205	-0.258	1.177	-0.008	139.972	1.013	2.092	17.707	-0.214
640	15.264	1.197	-0.343	1.146	-2.563·10 ⁻⁴	135.163	1.012	2.08	17.96	-0.007
645	10.829	1.191	-0.43	1.111	0.007	130.347	1.011	2.071	18.18	0.202

Orbital Operations position, distances and angle calculations E = 0 deg

$$T_{oc} = \frac{r_{earth}}{2 \cdot \pi} (E_{arr_{earth}} - e_{earth} \sin(E_{arr_{earth}})) \quad T_{oc} = 240 \text{ day} \quad T_{oa} = \frac{r_{McAuliffe}}{2 \cdot \pi} (E_{arr_{McAuliffe}} - e_{McAuliffe} \sin(E_{arr_{McAuliffe}}))$$

T_{oa} = 924.504 day

i = 0..53 t_i = i-7 day T₀ = T_{0c}
 Q = Q_{earth} e = e_{earth} inc = i_{earth} s = s_{earth} e = e_{earth} t = t_{earth}

$$E_{earth_i} = E_{fn}(t_i, T_0, t, e)$$

$$v_{earth_i} = v_{oc} \left(\frac{\cos(E_{earth_i}) - e}{1 - e \cos(E_{earth_i})} \right)$$

$$r_{earth_i} = a(1 - e \cos(E_{earth_i}))$$

$$x_{oc_i} = a[1 - \chi(\Omega, \theta, inc) \cos(E_{earth_i}) + b(a, e) \chi(\Omega, \theta, inc) \sin(E_{earth_i}) - s \phi 1 \chi(\Omega, \theta, inc)]$$

$$y_{oc_i} = a \chi(\Omega, \theta, inc) \cos(E_{earth_i}) + b(a, e) \chi(\Omega, \theta, inc) \sin(E_{earth_i}) - s \phi m \chi(\Omega, \theta, inc)$$

$$z_{oc_i} = a \chi(\theta, inc) \cos(E_{earth_i}) + b(a, e) \chi(\theta, inc) \sin(E_{earth_i}) - s \phi n \chi(\theta, inc)$$

Q = Q_{McAniff} e = e_{McAniff} inc = i_{McAniff} s = s_{McAniff} e = e_{McAniff} t = t_{McAniff} T₀ = T_{0c}

$$E_{McAniff_i} = E_{fn}(t_i, T_0, t, e)$$

$$v_{McAniff_i} = v_{oc} \left(\frac{\cos(E_{McAniff_i}) - e}{1 - e \cos(E_{McAniff_i})} \right)$$

$$r_{McAniff_i} = a(1 - e \cos(E_{McAniff_i}))$$

$$x_{oc_i} = a[1 - \chi(\Omega, \theta, inc) \cos(E_{McAniff_i}) + b(a, e) \chi(\Omega, \theta, inc) \sin(E_{McAniff_i}) - s \phi 1 \chi(\Omega, \theta, inc)]$$

$$y_{oc_i} = a \chi(\Omega, \theta, inc) \cos(E_{McAniff_i}) + b(a, e) \chi(\Omega, \theta, inc) \sin(E_{McAniff_i}) - s \phi m \chi(\Omega, \theta, inc)$$

$$z_{oc_i} = a \chi(\theta, inc) \cos(E_{McAniff_i}) + b(a, e) \chi(\theta, inc) \sin(E_{McAniff_i}) - s \phi n \chi(\theta, inc)$$

$$d_{oc_i} = \sqrt{(x_{oc_i})^2 + (z_{oc_i} - r_{earth_i})^2 + (y_{oc_i} - r_{McAniff_i})^2}$$

Spacecraft-Earth Distance Inplane

$$\psi_{oc_i} = \cos^{-1} \left[\frac{(d_{oc_i})^2 - (r_{earth_i})^2 - (r_{McAniff_i})^2}{-2 r_{earth_i} r_{McAniff_i}} \right]$$

Spacecraft-Sun-Earth Angle Inplane

$$\Omega_{oc_i} = \sin^{-1} \left(\frac{r_{earth_i} \sin(\psi_{oc_i})}{d_{oc_i}} \right)$$

Sun-Spacecraft-Earth Angle $\theta_{oc_i} = \sin^{-1} \left(\frac{z_{oc_i}}{d_{oc_i}} \right)$ Declination Angle of Earth from the Spacecraft

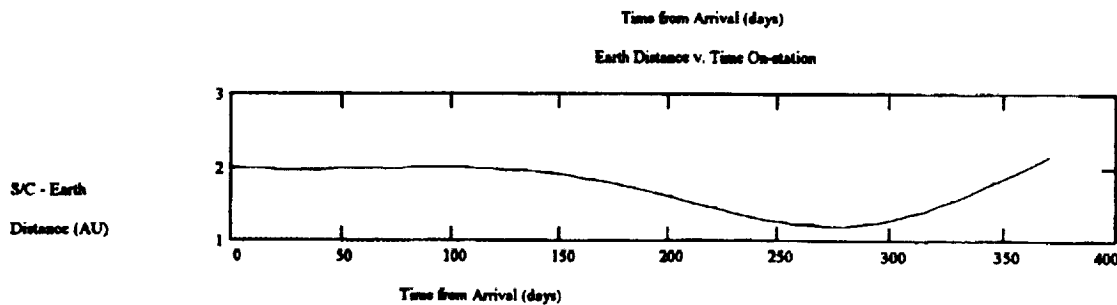
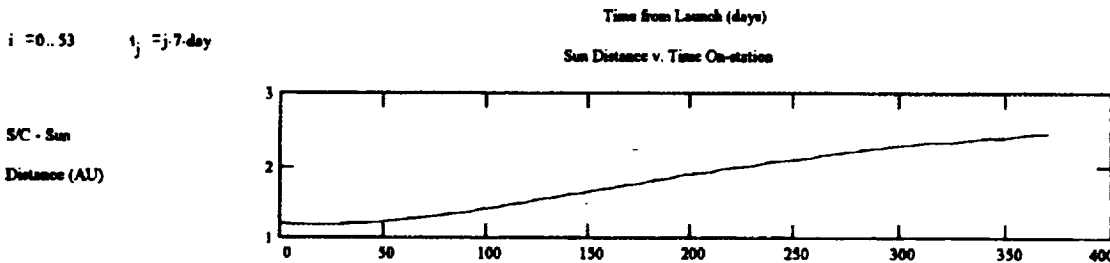
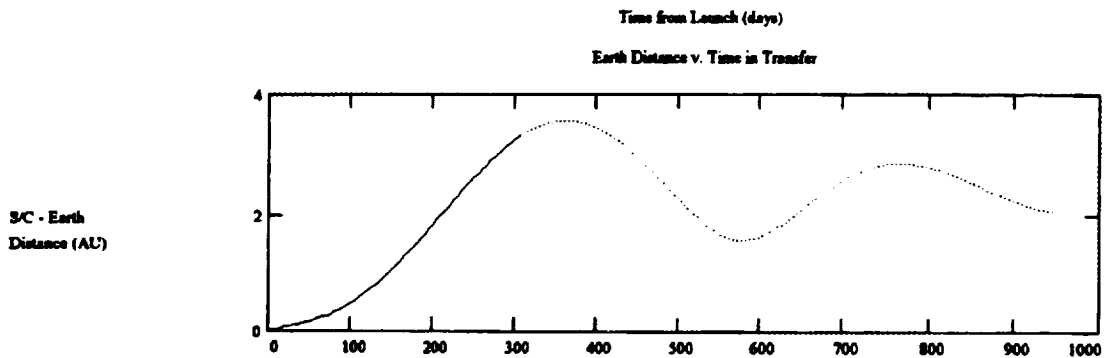
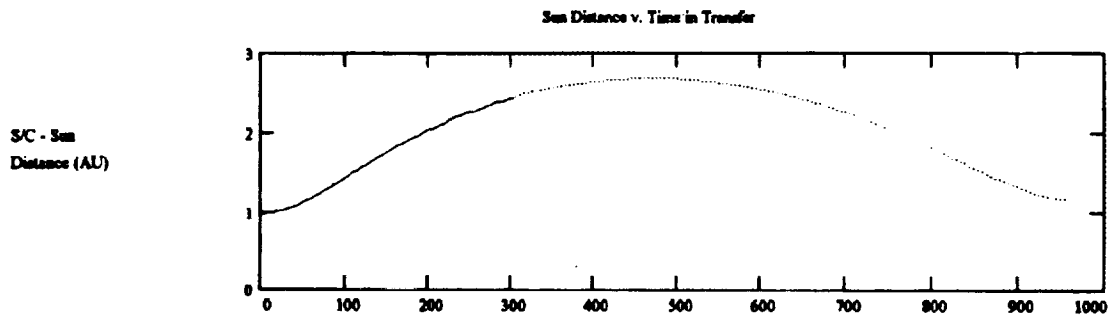
max(r_{McAniff}) = 2.463 AU Max and Min Sun-Spacecraft Ranges
 min(r_{McAniff}) = 1.185 AU
 max(d_{oc}) = 2.176 AU Max and Min Earth-Spacecraft Ranges
 min(d_{oc}) = 1.209 AU Max and Min Declination Angle of Earth from Spacecraft
 max(θ_{oc}) = 4.615 deg
 max(Ω_{oc}) = 32.219 deg Max and Min Sun-Spacecraft-Earth Angle
 min(Ω_{oc}) = 1.733 deg min(θ_{oc}) = 0.063 deg

Asteroid and Earth Orbit Ephemerides during On-Station Operations including Sun Angle i = 0..53

t _i day	v _{McAniff_i} deg	r _{McAniff_i} AU	x _{oc_i} AU	y _{oc_i} AU	z _{oc_i} AU	v _{earth_i} deg	r _{earth_i} AU	d _{oc_i} AU	Ω _{oc_i} deg	θ _{oc_i} deg
0	148.036	1.195	-0.373	1.135	0.002	125.051	1.009	2.015	21.864	0.063
56	146.22	1.244	-1.142	0.486	0.08	70.072	0.994	1.994	23.878	2.283
112	144.371	1.469	-1.407	-0.405	0.122	13.501	0.983	2.007	27.732	3.494
168	142.483	1.745	-1.261	-1.2	0.13	43.472	0.987	1.832	31.925	4.068
224	140.535	2.004	-0.889	-1.793	0.115	99.267	1.002	1.447	28.318	4.544
280	138.584	2.22	-0.41	-2.18	0.086	153.418	1.015	1.213	4.334	4.055
336	136.565	2.386	0.106	-2.383	0.049	153.157	1.015	1.648	20.726	1.698

i = 0..61 j = 0..130 time_i = i-5 day t_j = j-5 day

ORIGINAL PAGE IS
 OF POOR QUALITY

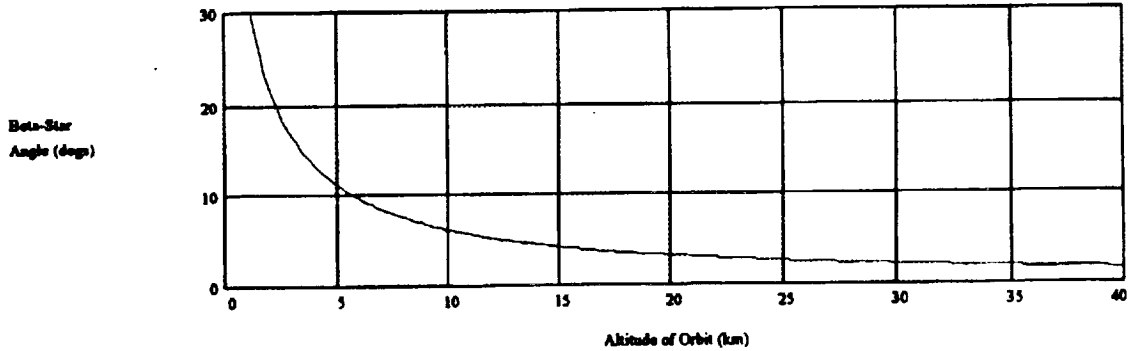


Eclipse Periods

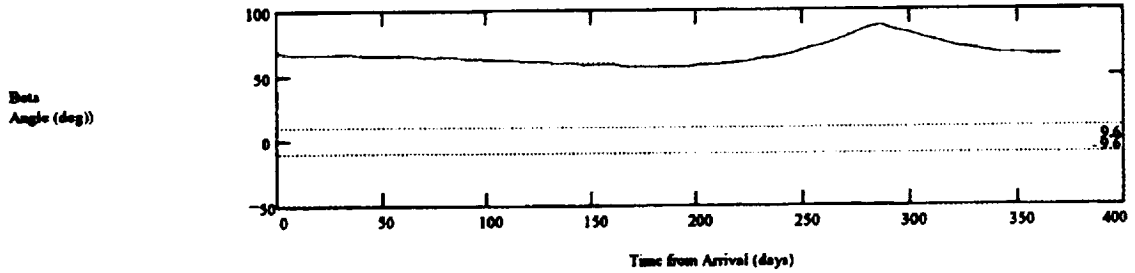
$$\beta_{star}(alt) = \arcsin\left(\frac{radius\ McAniffc}{radius\ McAniffc + alt}\right)$$

$$alt = radius\ McAniffc \cdot (radius\ McAniffc + .2\ km) \cdot 40\ km$$

Beta-Star Angle v. Altitude of Orbit



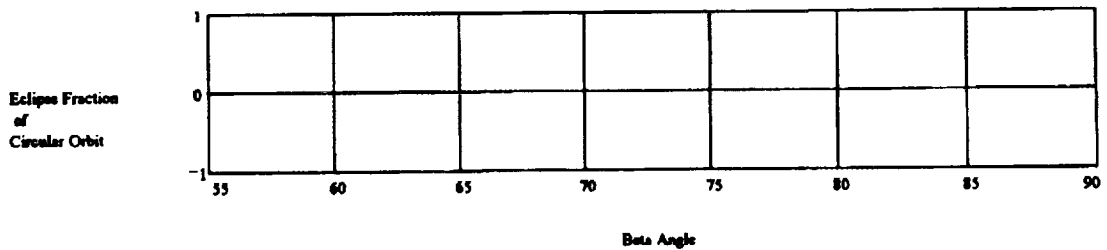
Magnitude of Beta Angle (deg)



Eclipse Time as a function of Beta Angle

$$alt = 6\ km \quad i = 0.53 \quad Period = \frac{2\pi}{\sqrt{\mu\ McAniffc}} \cdot (alt + radius\ McAniffc)^{1.5} \quad t_{eq} = \frac{Period}{\pi} \cdot \arccos\left[\frac{\sqrt{alt^2 + 2 \cdot radius\ McAniffc \cdot alt}}{(radius\ McAniffc + alt) \cdot \cos(90\ deg - Obs_v)}\right]$$

Eclipse Time v. Beta-Angle Magnitude (6 km orbit) for Duration of Operations



$E = 90\text{-deg}$ $T_{\text{os}} = 0\text{-day}$
 $i = 0..189$ $t_j = i/5\text{-day}$ $T_{\text{os}} = T_{\text{os}}$
 $\Omega = \Omega_{\text{McAniffc}}$ $e = e_{\text{McAniffc}}$ $\text{inc} = i_{\text{McAniffc}}$ $a = a_{\text{McAniffc}}$ $e = e_{\text{McAniffc}}$ $t = t_{\text{McAniffc}}$

$\text{EMcAniffc}_i = \text{Efcn}(t_j, T_{\text{os}}, t, e)$ $\text{vMcAniffc}_i = a \cos\left(\frac{\cos(\text{EMcAniffc}_i) - e}{1 - e \cos(\text{EMcAniffc}_i)}\right)$

$r\text{McAniffc}_i = a (1 - e \cos(\text{EMcAniffc}_i))$

$x\text{osm}_i = a \cdot 1 \cdot 1(\Omega, e, \text{inc}) \cos(\text{EMcAniffc}_i) + b(a, e) \cdot 1 \cdot 2(\Omega, e, \text{inc}) \sin(\text{EMcAniffc}_i) - a \cdot e \cdot 1 \cdot 1(\Omega, e, \text{inc})$
 $y\text{osm}_i = a \cdot m \cdot 1(\Omega, e, \text{inc}) \cos(\text{EMcAniffc}_i) + b(a, e) \cdot m \cdot 2(\Omega, e, \text{inc}) \sin(\text{EMcAniffc}_i) - a \cdot e \cdot m \cdot 1(\Omega, e, \text{inc})$
 $z\text{osm}_i = a \cdot n \cdot 1(e, \text{inc}) \cos(\text{EMcAniffc}_i) + b(a, e) \cdot n \cdot 2(e, \text{inc}) \sin(\text{EMcAniffc}_i) - a \cdot e \cdot n \cdot 1(e, \text{inc})$

$\Omega = \Omega_{\text{earth}}$ $e = e_{\text{earth}}$ $\text{inc} = i_{\text{earth}}$ $a = a_{\text{earth}}$ $e = e_{\text{earth}}$ $t = t_{\text{earth}}$

$T_{\text{os}} = T_{\text{os}}$ $i = 0..73$ $t_j = i/5\text{-day}$

$\text{Eearth}_i = \text{Efcn}(t_j, T_{\text{os}}, t, e)$ $\text{vearth}_i = a \cos\left(\frac{\cos(\text{Eearth}_i) - e}{1 - e \cos(\text{Eearth}_i)}\right)$

$r\text{earth}_i = a_{\text{earth}} (1 - e_{\text{earth}} \cos(\text{Eearth}_i))$

$x\text{e}_i = a \cdot 1 \cdot 1(\Omega, e, \text{inc}) \cos(\text{Eearth}_i) + b(a, e) \cdot 1 \cdot 2(\Omega, e, \text{inc}) \sin(\text{Eearth}_i) - a \cdot e \cdot 1 \cdot 1(\Omega, e, \text{inc})$
 $y\text{e}_i = a \cdot m \cdot 1(\Omega, e, \text{inc}) \cos(\text{Eearth}_i) + b(a, e) \cdot m \cdot 2(\Omega, e, \text{inc}) \sin(\text{Eearth}_i) - a \cdot e \cdot m \cdot 1(\Omega, e, \text{inc})$
 $z\text{e}_i = a \cdot n \cdot 1(e, \text{inc}) \cos(\text{Eearth}_i) + b(a, e) \cdot n \cdot 2(e, \text{inc}) \sin(\text{Eearth}_i) - a \cdot e \cdot n \cdot 1(e, \text{inc})$

$i = 0..61$ $j = 0..128$ $k = 0..189$ $l = 0..73$

APPENDIX C - LINK BUDGET CALCULATIONS

A. FORMULAS

This procedure for performing the link budget analysis follows the procedure from the *Mars Observer Telecommunications Design Control Document*, pp. 5 -2 through 5-17.

1. Free Space Loss

Space loss is due to signal divergence with range and the frequency dependence of the receiving antenna capture area.

$$L = [4\pi d/\lambda]^2 = [4\pi fd/c]^2 \quad (1)$$

Where: d = diameter of receiving antenna on spacecraft
 $c = 3 \times 10^8$ m/s
 f = appropriate frequency
 λ = wavelength

2. Effective Isotropic Radiated Power (EIRP)

To express the transmitted power of an earth station or a spacecraft, the effective isotropic radiated power is employed. The EIRP is the power generated time the gain of the sending antenna.

$$\text{EIRP} = P_T G_T \quad (2)$$

Where: P_T = power transmitted
 G_T = gain of transmitting antenna

3. Antenna Gain

$$G = \eta [\pi D/c]^2 \quad (3)$$

Where: η = efficiency of antenna
 D = diameter of circular antenna
 f = frequency being utilized

4. Power Received

$$(P_R)_{dB} = (EIRP)_{dBm} + (G_R)_{dBi} - (L_{total})_{dB} \quad (4)$$

Where: $(G_R)_{dB}$ = gain of receiving antenna in dBi
 $(L_{Total})_{dB}$ = total losses in dB

5. Conversion to Decibels

Whenever it is necessary to have a quantity y expressed in dB, it can be found from the basic quantity using the following equation:

$$y = 10 \log_{10}(x) \quad (5)$$

6. Conversion from dB or dBm

When it is necessary to obtain a basic quantity from a quantity y expressed in dB, the following equation can be used:

$$x = 10^{\frac{y}{10}} \quad (6)$$

A basic power in watts is calculated from an input y in dBm as follows:

$$P(\text{watts}) = \frac{10^{y/10}}{1000} \quad (7)$$

7. Nominal Receiver Noise Spectral Density

Nominal receiver noise spectral density in dBm / Hz is computed from:

$$N_0 = 10 \log_{10}(K) - 10 \log_{10}(T) \text{dBm / Hz} \quad (8)$$

Where: $K = \text{Boltzmann's constant} - 1.38 \times 10^{-20} \text{ mW/ Hz -K}$
 $T = \text{total effective ground or spacecraft system noise temperature in degrees K.}$

8. Command Performance

a. Power Allocation with Command Only:

$$\frac{P_c}{P_T} = J_0^2(\text{CMI}) \quad (9)$$

$$\frac{P_{\text{cmd}}}{P_T} = 2 J_1^2(\text{CMI}) \quad (10)$$

b. Power Allocation with Command and Ranging:

$$\frac{P_c}{P_T} = J_0^2(\text{CMI}) \cos^2 \theta_{\text{RG}} \quad (11)$$

$$\frac{P_{\text{cmd}}}{P_T} = 2 J_1^2(\text{CMI}) \cos^2 \theta_{\text{RG}} \quad (12)$$

$$\frac{P_{\text{RG}}}{P_T} = 2 J_1^2(\text{CMI}) \sin^2 \theta_{\text{RG}} \quad (13)$$

where: $P_c = \text{power in uplink RF carrier}$
 $P_{\text{cmd}} = \text{power in command data with sinusoidal wave subcarrier}$
 $P_{\text{RG}} = \text{power in ranging}$
 $P_T = \text{total uplink signal power}$
 $\text{CMI} = \text{peak modulation index of command}$
 $\theta_{\text{RG}} = \text{peak modulation index of ranging}$
 $J_0 \text{ and } J_1 = \text{Bessel Functions of Integer Order 0 and 1}$

9. Telemetry Performance

a. Power Allocation with Telemetry Only:

$$\frac{P_c}{P_T} = \cos^2 \theta_{\text{tlm}} \quad (14)$$

$$\frac{P_{\text{tlm}}}{P_T} = \sin^2 \theta_{\text{tlm}} \quad (15)$$

b. Power Allocation with Telemetry and Ranging

$$\frac{P_c}{P_T} = J_0^2 \cos^2 \theta_{\text{tlm}} \quad (16)$$

$$\frac{P_{\text{tlm}}}{P_T} = J_0^2 \sin^2 \theta_{\text{tlm}} \quad (17)$$

$$\frac{P_{\text{RG}}}{P_T} = J_0^2 J_1^2 \cos^2 \theta_{\text{tlm}} \quad (18)$$

Where: θ_{tlm} = peak modulation index of telemetry
 P_{tlm} = power in telemetry data with square wave subcarrier
 P_c = power in downlink RF carrier
 P_{RG} = power in ranging

10. Carrier Margin

Carrier Margin in either uplink or downlink is defined as:

$$M_c = \frac{P_c}{2B_{\text{LO}}N_o} \quad (19)$$

where: P_c = RF carrier power
 B_{LO} = one-sided threshold loop noise bandwidth
 N_o = one sided noise spectral density

11. Required Downlink Signal Power

The total signal power to noise spectral density ratio P_T / N_o to meet the required carrier and telemetry margins is computed as follows:

$$\frac{E_b}{N_o} = \frac{P_{t/m}}{N_o R_b} \quad (20)$$

since

$$\frac{P_{t/m}}{N_o} = \frac{P_T}{N_o} \sin^2 \theta_{t/m} \quad (21)$$

then

$$\frac{E_b}{N_o} = \frac{P_T}{N_o R_b} \sin^2 \theta_{t/m} \quad (22)$$

also since

$$\frac{P_c}{N_o} = \frac{P_T}{N_o} \cos^2 \theta_{t/m} \quad (23)$$

combine with (eqns. 14- 15) to get an expression for the carrier margin:

$$M_c = \frac{P_T \cos^2 \theta_{t/m}}{N_o 2B_{LO}} \quad (24)$$

Add sine and cosine square in (eqns 16-18) to obtain an expression of P_T / N_o with respect to required telemetry and carrier margins:

$$\frac{P_T}{N_o} = \frac{E_b R_b}{N_o} + M_c 2B_{LO} \quad (25)$$

B. UPLINK PARAMETERS

Parameter	Comments/Values
Modes	Command and Ranging
Ground Antenna	34 m (HEF) DSN Gain= 67.1 dB
Ground Transmitter Power	20.0 K Watts
Frequency	Carrier: 7.17 GHz Sine Subcarrier: 16.0 kHz
Modulation	PCM (NRL-Z)/PSK/PM
Modulation Index	Command: 1.0 Radian Ranging: .3 Radians
Constants:	Jo (CMI): .7652 COS(RMI)^2: .9127 J1(CMI): .4400 SIN(RMI)^@: .0873

C. DOWNLINK PARAMETERS

Parameter	Comment/Values
Modes	Telemetry, Ranging and Commands
Ground Antenna	34 m (HEF) DSN Gain: 68.1 dB 70 m Gain: 73.77 dB
Frequency	Carrier: 8.419 GHz
Coding	1/2 R Convolutional Reed-Solomon 18.92 ksps
Modulation	PCM/PM
Modulation Index	TLM data: 1.4 radians
Ranging mode	square wave
Ranging Modulation Index	.3 radians
Effective Ranging Mod. Index	.12 radians
Effective Noise Mod. Index	.27 radians .92745
Command Modulation	PCM(NRZ-L)/BPSK/PM
Command Modulation Index	1 radian
Constants	Jo: .76519 J1: .44005

1) Uplink Budget: LGA at 1AU

#	Parameter	Value	Comments
1	Ground Transmitter Power	73.0 dBm	34 m HEF
2	Ground Antenna Gain	67.1 dBi	
3	EIRP	140.1 dBm	1 + 2
4	Free Space Loss	-273.05 dB	
5	Atmospheric Loss	-2 dB	
6	Pointing Loss	-1 dB	
7	Polarization Loss	-2 dB	
8	S/C Passive Loss	-1.5 dB	
9	S/C Antenna Gain	1.0dB	
10	Max Total Received Power	-133.95 dB	3 + 4 + 5 + 6 + 7 + 8 + 9
11	S/C Antenna Null Depth	0.0 dB	
12	Total Received Power	-133.95 dB	10 + 11
13	Receiver Noise Temperature	225.7 deg - K	NF=2.5 dB
14	S/C Antenna Temperature	100 deg-K	
15	System Noise Density	-173.5 dBm/Hz	
16	Carrier/Total Power	-2.7 dB	
17	Received Carrier Power	-136.65 dBm	12 + 16
18	Carrier Loop Noise BW	13 dB-Hz	20 Hz
19	Noise Power	-160.5 dBm	15+18
20	Carrier / Noise Power	23.85 dB	17-19
21	Required Carrier /Noise Power	10 dB	Required DSN
22	Carrier Margin	13.85 dB	
23	Command/ Total Power	-4.5 dB	
24	Received Command Power	-138.45 dBm	12+23
25	Predetection Noise BW	45.1 dB-Hz	32000 Hz
26	Predetection Noise Power	-128.4 dBm	15+25
27	Predetection SNR	-10.1 dB	24-26
28	Command Data Rate (90 bps)	19.55 dB	24-15-29
29	Available E/Bit / Noise Density	15.5 dB	24-15-28
30	Decoder Degradation	2.0 dB	
31	Required E/Bit/Noise Density	10.6 dB	BER 10E-6
32	Available Command Margin	2.9 dB	29-31-30
33	Ranging/Total Power	-12.9 dB	
34	Received Ranging Power	-146.85 dBm	12+33
35	Ranging Noise BW	61.8 dB-Hz	1.5 x10E6 Hz
36	Received SNR Power	-35.15 dB	34-15-35

2) Uplink Budget: HGA at 2 AU

#	Parameter	Value	Comments
1	Ground Transmitter Power	73.0 dBm	34 m HEF
2	Ground Antenna Gain	67.1 dBi	
3	EIRP	140.1 dBm	1 + 2
4	Free Space Loss	-279.07 dB	
5	Atmospheric Loss	-2 dB	
6	Pointing Loss	-1 dB	
7	Polarization Loss	-2 dB	
8	S/C Passive Loss	-1.5 dB	
9	S/C Antenna Gain	40 dBi	
10	Max Total Received Power	-101.97 dB	3 + 4 + 5 + 6 + 7 + 8 + 9
11	S/C Antenna Null Depth	0.0 dB	
12	Total Received Power	-101.97	10+11
13	Receiver Noise Temperature	225.7 deg - K	NF=2.5 dB
14	S/C Antenna Temperature	100 deg-K	
15	System Noise Density	-173.5 dBm/Hz	
16	Carrier/Total Power	-2.7 dB	
17	Received Carrier Power	-104.67 dBm	12 + 16
18	Carrier Loop Noise BW	13 dB-Hz	20 Hz
19	Noise Power	-160.5 dBm	15+18
20	Carrier / Noise Power	55.83 dB	17-19
21	Required Carrier /Noise Power	10 dB	Required DSN
22	Carrier Margin	45.83 dB	
23	Command/ Total Power	-4.5 dB	
24	Received Command Power	-106.47 dBm	12+23
25	Predetection Noise BW	45.1 dB-Hz	32000 Hz
26	Predetection Noise Power	-128.4 dBm	15+25
27	Predetection SNR	21.93 dB	24-26
28	Command Data Rate 2000 bps	33 dB-Hz	24-15-29
29	Available E/Bit / Noise Density	34 dB	24-15-28
30	Decoder Degradation	2.0 dB	
31	Required E/Bit/Noise Density	10.6dB	BER 10E-6
32	Available Command Margin	21.4 dB	29-31-30
33	Ranging/Total Power	-12.9 dB	
34	Received Ranging Power	-114.87 dBm	12+33
35	Ranging Noise BW	61.8 dB	1.5 x10E6 Hz
36	Received SNR Power	-3.17 dB	34-15-35

3) Uplink Budget: LGA at 2 AU

#	Parameter	Value	Comments
1	Ground Transmitter Power	73.0 dBm	34 m HEF
2	Ground Antenna Gain	67.1 dBi	
3	EIRP	140.1 dBm	1 + 2
4	Free Space Loss	-279.07 dB	
5	Atmospheric Loss	-2 dB	
6	Pointing Loss	-1 dB	
7	Polarization Loss	-2 dB	
8	S/C Passive Loss	-1.5 dB	
9	S/C Antenna Gain	1 dBi	
10	Max Total Received Power	-139.97 dBm	3 + 4+5+6+7+8+9
11	S/C Antenna Null Depth	0.0 dB	
12	Total Received Power	-139.97 dBm	10+11
13	Receiver Noise Temperature	225.7 deg. - K	NF=2.5 dB
14	S/C Antenna Temperature	100 deg.-K	
15	System Noise Density	-173.5 dBm/Hz	
16	Carrier/Total Power	-2.7 dB	
17	Received Carrier Power	-142.67 dBm	12+16
18	Carrier Loop Noise BW	13 dB-Hz	20 Hz
19	Noise Power	-160.5 dBm	15+18
20	Carrier /Noise Power	17.83 dB	17-19
21	Required Carrier /Noise Power	10 dB	Required DSN
22	Carrier Margin	7.83 dB	
23	Command/ Total Power	-4.5 dB	
24	Received Command Power	-144.47 dBm	12+23
25	Predetection Noise BW	45.1 dB-Hz	32000 Hz
26	Predetection Noise Power	-128.4 dBm	15+25
27	Predetection SNR	-16.07 dB	24-26
28	Command Data Rate 22.5 bps	13.53 dB-Hz	24-15-29
29	Available E/Bit / Noise Density	15.5 dB	24-15-28
30	Decoder Degradation	2.0 dB	
31	Required E/Bit/Noise Density	10.6 dB	BER 10E-6
32	Available Command Margin	2.9 dB	29-31-30
33	Ranging/Total Power	-12.9 dB	
34	Received Ranging Power	-152.87 dBm	12+33
35	Ranging Noise BW	61.8 dB-Hz	1.5 x10E6 Hz
36	Received SNR Power	-41.17 dB	34-15-35

4) Uplink Budget: HGA at 3 AU

#	Parameter	Value	Comments
1	Ground Transmitter Power	73.0 dBm	34 m HEF
2	Ground Antenna Gain	67.1 dBi	
3	EIRP	140.1 dBm	1 + 2
4	Free Space Loss	-282.6 dB	
5	Atmospheric Loss	-2 dB	
6	Pointing Loss	-1 dB	
7	Polarization Loss	-2 dB	
8	S/C Passive Loss	-1.5 dB	
9	S/C Antenna Gain	40 dBi	
10	Max Total Received Power	-104.5 dBm	3 + 4+5+6+7+8+9
11	S/C Antenna Null Depth	0.0 dB	
12	Total Received Power	-104.5 dBm	10+11
13	Receiver Noise Temperature	225.7 deg. - K	NF=2.5 dB
14	S/C Antenna Temperature	100 deg.-K	
15	System Noise Density	-173.5 dBm/Hz	
16	Carrier/Total Power	-2.7 dB	
17	Received Carrier Power	-107.2 dBm	12 + 16
18	Carrier Loop Noise BW	13 dB-Hz	20 Hz
19	Noise Power	-160 dBm	15+18
20	Carrier / Noise Power	52.8 dB	17-19
21	Required Carrier /Noise Power	10 dB	Required DSN
22	Carrier Margin	42.8 dB	
23	Command/ Total Power	-4.5 dB	
24	Received Command Power	-109 dBm	12+23
25	Predetection Noise BW	45.1 dB-Hz	32000 Hz
26	Predetection Noise Power	-127.9 dBm	15+25
27	Predetection SNR	18.9 dB	24-26
28	Command Data Rate 1000 bps	30 dB-Hz	24-15-29
29	Available E/Bit / Noise Density	34 dB	24-15-28
30	Decoder Degradation	2.0 dB	
31	Required E/Bit/Noise Density	10.6 dB	BER 10E-6
32	Available Command Margin	21.4 dB	29-31-30
33	Ranging/Total Power	-12.9 dB	
34	Received Ranging Power	-117.4 dBm	12+33
35	Ranging Noise BW	61.8 dB-Hz	1.5 x10E6 Hz
36	Received SNR Power	-6.2 dB	34-15-35

5) Uplink Budget: LGA at 3 AU

#	Parameter	Value	Comments
1	Ground Transmitter Power	73.0 dBm	34 m HEF
2	Ground Antenna Gain	67.1 dBi	
3	EIRP	140.1 dBm	1 + 2
4	Free Space Loss	-282.6 dB	
5	Atmospheric Loss	-2 dB	
6	Pointing Loss	-1 dB	
7	Polarization Loss	-2 dB	
8	S/C Passive Loss	-1.5 dB	
9	S/C Antenna Gain	1 dBi	
10	Max Total Received Power	-143.5 dBm	3 + 4 + 5 + 6 + 7 + 8 + 9
11	S/C Antenna Null Depth	0.0 dB	
12	Total Received Power	-143.5 dBm	10 + 11
13	Receiver Noise Temperature	225.7 deg. - K	
14	S/C Antenna Temperature	100 deg-K	
15	System Noise Density	-173.5 dBm/Hz	
16	Carrier/Total Power	-2.7 dB	
17	Received Carrier Power	-146.2 dBm	12 + 16
18	Carrier Loop Noise BW	13 dB-Hz	20 Hz
19	Noise Power	-160.5 dB-Hz	15 + 18
20	Carrier / Noise Power	14.3 dB	17-19
21	Required Carrier / Noise Power	10 dB	Required DSN
22	Carrier Margin	4.3 dB	
23	Command/ Total Power	-4.5 dB	
24	Received Command Power	-148 dBm	12 + 23
25	Predetection Noise BW	45.1 dB-Hz	32000 Hz
26	Predetection Noise Power	-128.4 dBm	15 + 25
27	Predetection SNR	-19.6 dB	24-26
28	Command Data Rate	10 bps	24-15-29
29	Available E/Bit / Noise Density	15.5 dB	24-15-28
30	Decoder Degradation	2.0 dB	
31	Required E/Bit/Noise Density	10.6 dB	BER 10E-6
32	Available Command Margin	2.9 dB	29-31-30
33	Ranging/Total Power	-12.9 dB	
34	Received Ranging Power	-156.4 dBm	12 + 33
35	Ranging Noise BW	61.8	1.5 x 10E6 Hz
36	Received SNR Power	-44.7 dB	34-15-35

6) Uplink Budget: HGA at 3.6 AU

#	Parameter	Value	Comments
1	Ground Transmitter Power	73.0 dBm	34 m HEF
2	Ground Antenna Gain	67.1 dBi	
3	EIRP	140.1 dBm	1 + 2
4	Free Space Loss	-284.17 dB	
5	Atmospheric Loss	-2 dB	
6	Pointing Loss	-1 dB	
7	Polarization Loss	-2 dB	
8	S/C Passive Loss	-1.5 dB	
9	S/C Antenna Gain	40 dBi	
10	Max Total Received Power	-106.07 dBm	3 + 4 + 5 + 6 + 7 + 8 + 9
11	S/C Antenna Null Depth	0.0 dB	
12	Total Received Power	-106.07 dBm	10 + 11
13	Receiver Noise Temperature	225.7 deg. - K	
14	S/C Antenna Temperature	100 deg-K	
15	System Noise Density	-173.5 dBm/Hz	
16	Carrier/Total Power	-2.7 dB	
17	Received Carrier Power	-108.77 dBm	12 + 16
18	Carrier Loop Noise BW	13 dB-Hz	20 Hz
19	Noise Power	-160.5 dBm	15 + 18
20	Carrier / Noise Power	51.73 dB	17-19
21	Required Carrier / Noise Power	10 dB	Required DSN
22	Carrier Margin	41.73 dB	
23	Command/ Total Power	-4.5 dB	
24	Received Command Power	-110.57 dBm	12 + 23
25	Predetection Noise BW	45.1 dB-Hz	32000 Hz
26	Predetection Noise Power	-132 dBm	15 + 25
27	Predetection SNR	21.43 dB	24-26
28	Command Data Rate	781 bps	24-15-29
29	Available E/Bit / Noise Density	34 dB	24-15-28
30	Decoder Degradation	2.0 dB	
31	Required E/Bit/Noise Density	10.6 dB	BER 10E-6
32	Available Command Margin	21.4 dB	29-31-30
33	Ranging/Total Power	-12.9 dB	
34	Received Ranging Power	-118.97 dBm	12 + 33
35	Ranging Noise BW	61.8 dB-Hz	1.5 x 10E6 Hz
36	Received SNR Power	-7.27 dB	34-15-35

7) Uplink Budget: LGA at 3.6 AU

#	Parameter	Value	Comments
1	Ground Transmitter Power	73.0 dBm	34 m HEF
2	Ground Antenna Gain	67.1 dBi	
3	EIRP	140.1 dBm	1 + 2
4	Free Space Loss	-284.17 dB	
5	Atmospheric Loss	-2 dB	
6	Pointing Loss	-1 dB	
7	Polarization Loss	-2 dB	
8	S/C Passive Loss	-1.5 dB	
9	S/C Antenna Gain	1 dBi	
10	Max Total Received Power	-145.07 dBm	3 + 4+5+6+7+8+9
11	S/C Antenna Null Depth	0.0 dB	
12	Total Received Power	-145.07 dBm	10+11
13	Receiver Noise Temperature	225.7 deg. K	NF = 2.5 dB
14	S/C Antenna Temperature	100 deg. K	
15	System Noise Density	-173.5 dBm/Hz	
16	Carrier/Total Power	-2.7 dB	
17	Received Carrier Power	-147.77 dBm	12 + 16
18	Carrier Loop Noise BW	13 dB-Hz	20 Hz
19	Noise Power	-160.5 dBm	15+18
20	Carrier / Noise Power	12.73 dB	17-19
21	Required Carrier / Noise Power	10 dB	Required DSN
22	Carrier Margin	2.73 dB	
23	Command/ Total Power	-4.5 dB	
24	Received Command Power	-149.57 dB	12+23
25	Predetection Noise BW	45.1 dB-Hz	32000 Hz
26	Predetection Noise Power	-128.2 dBm	15+25
27	Predetection SNR	-21.73 dB	24-26
28	Command Data Rate	6.65 bps	24-15-29
29	Available E/Bit / Noise Density	15.5 dB	24-15-28
30	Decoder Degradation	2.0 dB	
31	Required E/Bit/Noise Density	10.6 dB	BER 10 E-6
32	Available Command Margin	2.9 dB	29-31-30
33	Ranging/Total Power	-12.9 dB	
34	Received Ranging Power	-157.97 dBm	12+33
35	Ranging Noise BW	61.8 dB-Hz	1.5 x10E6 Hz
36	Received SNR Power	-46.27 dB	34-15-35

8) Downlink Budget: HGA at 1 AU

#	Parameter	Value	Comments
1	S/C Transmitter	37 dBm	5 W
2	S/C Passive Loss	-1.5 dB	
3	S/C Antenna Gain	40 dBi	
4	EIRP	75.5 dBm	1+2+3
5	Free Space Loss	-274.44 dB	
6	Atmospheric Loss	-2 dB	
7	Polarization Loss	-2 dB	
8	Ground Receive Antenna Gain	68.1 dB	34 m (DSN)
9	Receiver Passive Loss	0.0 dB	
10	Pointing Loss	-1 dB	
11	Remodulation Noise Loss	-3 dB	
12	Total Received Power	-131.64 dBm	4+5+6+7+8+9+10+11
13	Ground System G/T (DSN)	52.8 dB	
14	Antenna Noise Temperature	0.0 deg.K	Sun in Side Lobes
15	System Noise Temperature	34.0 deg.K	
16	System Noise Density	-183.3 dBm/Hz	
17	Carrier Power/Total Power	-17.8 dB	
18	Carrier Power Received	-149.44 dBm	12+17
19	Carrier Tracking BW	10.3 dB-Hz	10.8 Hz
20	CNR Power Received	23.56 dB	18-16-19
21	CNR Power Required	10 dB	Eb/No
22	Carrier Margin	13.56 dB	
23	telemetry Data Pwr/Total Pwr	-2.5 dB	
24	Tlm Pwr Received	-134.04 dBm	12+23
25	TLM Data Rate	21,183 bps	24-16-26
26	TLM Pwr/Noise Pwr	6.0 dB	24-16-25
27	Detector Loss	5 dB	DSN
28	Data Pwr/Noise Pwr Required	2.5 dB	BER=10E-6
29	TLM Data Margin	3.0	
30	Range Pwr/Total Pwr	-36.1 dB	
31	Received Ranging Power	-167.74 dBm	30+12
32	Ranging Noise BW	-9.0 dB-Hz	1.25 Taq
33	Ranging SNR	24.56 dB	
34	Required Ranging SNR	-5 dB	
35	Ranging Margin	29.56 dB	

9) Downlink Budget: LGA at 1 AU

#	Parameter	Value	Comments
1	S/C Transmitter	40 dBm	10W
2	S/C Passive Loss	-1.5 dB	
3	S/C Antenna Gain	5 dB	
4	EIRP	43.5 dBm	1+2+3
5	Free Space Loss	-274.44 dB	
6	Atmospheric Loss	-2 dB	
7	Polarization Loss	-2 dB	
8	Ground Receive Antenna Gain	73.77 dB	70 m (DSN)
9	Receiver Passive Loss	0.0 dB	
10	Pointing Loss	-1 dB	
11	Remodulation Noise Loss	-3 dB	
12	Total Received Power	-157.97 dBm	4+5+6+7+8+9+10+11
13	Ground System G/T (DSN)	52.8 dB	
14	Antenna Noise Temperature	0.0 deg-K	Sun in Side Lobes
15	System Noise Temperature	34.0 deg-K	
16	System Noise Density	-183.3 dBm/Hz	
17	Carrier Power/Total Power	-17.8 dB	
18	Carrier Power Received	-159.9 dBm	12+17
19	Carrier Tracking BW	10.3 dB-Hz	10.8 Hz
20	Carrier Threshold Power	-163.3 dB	16+19+21
21	CNR Power Required	10 dB	Eb/No
22	Carrier Margin	3.4 dB	18-20
23	Telemetry Data Pwr/Total Pwr	-2.5 dB	
24	Tlm Pwr Received	-160.47 dBm	12+23
25	TLM Data Rate 48 bps	16.83 dB-Hz	24-16-26
26	TLM Pwr/Noise Pwr	6.0 dB	24-16-25
27	Detector Loss	5 dB	DSN
28	Data Pwr/Noise Pwr Required	2.5 dB	BER=10E-6
29	TLM Data Margin	3.0 dB	
30	Range Pwr/Total Pwr	-36.1 dB	
31	Received Ranging Power	-194.07 dBm	30+12
32	Ranging Noise BW	-9.0 dB-Hz	125 Tscq
33	Ranging SNR	-1.77 dB	
34	Required Ranging SNR	-5 dB	
35	Ranging Margin	3.23 dB	

10) Downlink Budget: HGA at 2 AU

#	Parameter	Value	Comments
1	S/C Transmitter	37 dBm	5 W
2	S/C Passive Loss	-1.5 dB	
3	S/C Antenna Gain	40 dBi	
4	EIRP	75.5 dBm	1+2+3
5	Free Space Loss	-280.5 dB	
6	Atmospheric Loss	-2 dB	
7	Polarization Loss	-2 dB	
8	Ground Receive Antenna Gain	68.1 dB	34 m (DSN)
9	Receiver Passive Loss	0.0 dB	
10	Pointing Loss	-1 dB	
11	Remodulation Noise Loss	-3 dB	
12	Total Received Power	-137.7 dBm	4+5+6+7+8+9+10+11
13	Ground System G/T (DSN)	52.8 dB	
14	Antenna Noise Temperature	0.0 deg-K	Sun in Side Lobes
15	System Noise Temperature	34.0 deg-K	
16	System Noise Density	-183.3 dBm/Hz	
17	Carrier Power/Total Power	-17.8 dB	
18	Carrier Power Received	-155.5 dBm	12+17
19	Carrier Tracking BW	10.3 dB-Hz	10.8 Hz
20	CNR Power Received	17.5 dB	18-16-19
21	CNR Power Required	10 dB	Eb/No
22	Carrier Margin	7.5 dB	
23	Telemetry Data Pwr/Total Pwr	-2.5 dB	
24	Tlm Pwr Received	-140.2 dBm	12+23
25	TLM Data Rate 5000 bps	37 dB-Hz	24-16-26
26	TLM Pwr/Noise Pwr	6.0 dB	24-16-25
27	Detector Loss	5 dB	DSN
28	Data Pwr/Noise Pwr Required	2.5 dB	BER=10E-6
29	TLM Data Margin	3.0 dB	
30	Range Pwr/Total Pwr	-36.1 dB	
31	Received Ranging Power	-173.8 dBm	30+12
32	Ranging Noise BW	-9.0 dB-Hz	125 Tscq
33	Ranging SNR	18.5 dB	
34	Required Ranging SNR	-5 dB	
35	Ranging Margin	23.5 dB	

11) Downlink Budget: LGA at 2 AU with 70m (DSN)

#	Parameter	Value	Comments
1	S/C Transmitter	40 dBm	10W
2	S/C Passive Loss	-1.5 dB	
3	S/C Antenna Gain	5 dB	
4	EIRP	43.5 dBm	1+2+3
5	Free Space Loss	-280.5 dB	
6	Atmospheric Loss	-2 dB	
7	Polarization Loss	-2 dB	
8	Ground Receive Antenna Gain	73.77 dB	70 m (DSN)
9	Receiver Passive Loss	0.0 dB	
10	Pointing Loss	-1 dB	
11	Remodulation Noise Loss	-3 dB	
12	Total Received Power	-163.83 dBm	4+5+6+7+8+9+10+11
13	Ground System G/T (DSN)	52.8 dB	
14	Antenna Noise Temperature	0.0 deg-K	Sun in Side Lobes
15	System Noise Temperature	34.0 deg-K	
16	System Noise Density	-183.3 dBm/Hz	
17	Carrier Power/Total Power	-17.8 dB	
18	Carrier Power Received	-181.63 dBm	12+17
19	Carrier Tracking BW	10.3 dB-Hz	10.8 Hz
20	Carrier Threshold Power	-152 dB	16+19+21
21	CNR Power Required	10 dB	Eb/No
22	Carrier Margin	-29.63 dB	18-20
23	Telemetry Data Pwr/Total Pwr	-2.5 dB	
24	Tlm Pwr Received	-166.33 dBm	12+23
25	TLM Data Rate	12.5 bps	24-16-26
26	TLM Pwr/Noise Pwr	6.0 dB	24-16-25
27	Detector Loss	.5 dB	DSN
28	Data Pwr/Noise Pwr Required	2.5 dB	BER=10E-6
29	TLM Data Margin	3.0	
30	Range Pwr/Total Pwr	-36.1 dB	
31	Received Ranging Power	-199.93 dBm	30+12
32	Ranging Noise BW	-9.0 dB-Hz	.125 Tacq
33	Ranging SNR	-7.63 dB	
34	Required Ranging SNR	-5 dB	
35	Ranging Margin	-2.63 dB	

12) Downlink Budget: HGA at 3 AU with 34m (DSN)

#	Parameter	Value	Comments
1	S/C Transmitter	40 dBm	10 W
2	S/C Passive Loss	-1.5 dB	
3	S/C Antenna Gain	40 dB	
4	EIRP	78.5 dBm	1+2+3
5	Free Space Loss	-283.4 dB	
6	Atmospheric Loss	-2 dB	
7	Polarization Loss	-2 dB	
8	Ground Receive Antenna Gain	68.1 dB	34m (DSN)
9	Receiver Passive Loss	0.0 dB	
10	Pointing Loss	-1 dB	
11	Remodulation Noise Loss	-3 dB	
12	Total Received Power	-137.6 dBm	4+5+6+7+8+9+10+11
13	Ground System G/T (DSN)	52.8 dB	
14	Antenna Noise Temperature	0.0 deg-K	Sun in Side Lobes
15	System Noise Temperature	34.0 deg-K	
16	System Noise Density	-183.3 dBm/Hz	
17	Carrier Power/Total Power	-17.8 dB	
18	Carrier Power Received	-155.4 dBm	12+17
19	Carrier Tracking BW	10.3 dB-Hz	10.8 Hz
20	CNR Power Received	17.9 dB	18-16-19
21	CNR Power Required	10 dB	Eb/No
22	Carrier Margin	7.9 dB	
23	Telemetry Data Pwr/Total Pwr	-2.5 dB	
24	Tlm Pwr Received	-140.1 dBm	12+23
25	TLM Data Rate	5200 bps	24-16-26
26	TLM Pwr/Noise Pwr	6.0 dB	24-16-25
27	Detector Loss	.5 dB	DSN
28	Data Pwr/Noise Pwr Required	2.5 dB	BER=10E-6
29	TLM Data Margin	3.0	
30	Range Pwr/Total Pwr	-36.1 dB	
31	Received Ranging Power	-173.7 dBm	30+12
32	Ranging Noise BW	-9.0 dB-Hz	.125 Tacq
33	Ranging SNR	18.6 dB	
34	Required Ranging SNR	-5 dB	
35	Ranging Margin	23.6 dB	

13) Downlink Budget: HGA at 3 AU with 70m (DSN)

#	Parameter	Value	Comments
1	S/C Transmitter	40 dBm	10 W
2	S/C Passive Loss	-1.5 dB	
3	S/C Antenna Gain	40 dBi	
4	EIRP	78.5 dBm	1+2+3
5	Free Space Loss	-283.4 dB	
6	Atmospheric Loss	-2 dB	
7	Polarization Loss	-2 dB	
8	Ground Receive Antenna Gain	73.77 dB	70 m (DSN)
9	Receiver Passive Loss	0.0 dB	
10	Pointing Loss	-1 dB	
11	Remodulation Noise Loss	-3 dB	
12	Total Received Power	-137.6 dBm	4+5+6+7+8+9+10+11
13	Ground System G/T (DSN)	52.8 dB	
14	Antenna Noise Temperature	0.0 deg-K	Sun in Side Lobes
15	System Noise Temperature	34.0 deg-K	
16	System Noise Density	-183.3 dBm/Hz	
17	Carrier Power/Total Power	-17.8 dB	
18	Carrier Power Received	-155.4 dBm	12+17
19	Carrier Tracking BW	10.3 dB-Hz	10.8 Hz
20	CNR Power Received	17.9 dB	18-16-19
21	CNR Power Required	10 dB	Eb/No
22	Carrier Margin	7.9 dB	
23	Telemetry Data Pwr/Total Pwr	-2.5 dB	
24	Tlm Pwr Received	-134.43 dBm	12+23
25	TLM Data Rate	19.4 kbps	24-16-26
26	TLM Pwr/Noise Pwr	6.0 dB	24-16-25
27	Detector Loss	5 dB	DSN
28	Data Pwr/Noise Pwr Required	2.5 dB	BER=10E-6
29	TLM Data Margin	3.0	
30	Range Pwr/Total Pwr	-36.1 dB	
31	Received Ranging Power	-168.03 dBm	30+12
32	Ranging Noise BW	-9.0 dB-Hz	.125 Tseq
33	Ranging SNR	24.27 dB	
34	Required Ranging SNR	-5 dB	
35	Ranging Margin	29.27 dB	

14) Downlink Budget: LGA at 3 AU with 70m (DSN)

#	Parameter	Value	Comments
1	S/C Transmitter	40 dBm	10W
2	S/C Passive Loss	-1.5 dB	
3	S/C Antenna Gain	5 dB	
4	EIRP	43.5 dBm	1+2+3
5	Free Space Loss	-283.4 dB	
6	Atmospheric Loss	-2 dB	
7	Polarization Loss	-2 dB	
8	Ground Receive Antenna Gain	73.77 dB	70 m (DSN)
9	Receiver Passive Loss	0.0 dB	
10	Pointing Loss	-1 dB	
11	Remodulation Noise Loss	-3 dB	
12	Total Received Power	-166.73 dBm	4+5+6+7+8+9+10+11
13	Ground System G/T (DSN)	52.8 dB	
14	Antenna Noise Temperature	0.0 deg-K	Sun in Side Lobes
15	System Noise Temperature	34.0 deg-K	
16	System Noise Density	-183.3 dBm/Hz	
17	Carrier Power/Total Power	-17.8 dB	
18	Carrier Power Received	-184.53 dBm	12+17
19	Carrier Tracking BW	10.3 dB-Hz	10.8 Hz
20	Carrier Threshold Power	-163.3 dB	16+19+21
21	CNR Power Required	10 dB	Eb/No
22	Carrier Margin	-21.23 dB	18-20
23	Telemetry Data Pwr/Total Pwr	-2.5 dB	
24	Tlm Pwr Received	-169.23 dBm	12+23
25	TLM Data Rate	6.4 bps	24-16-26
26	TLM Pwr/Noise Pwr	6 dB	24-16-25
27	Detector Loss	5 dB	DSN
28	Data Pwr/Noise Pwr Required	2.5 dB	BER=10E-6
29	TLM Data Margin	3.0	
30	Range Pwr/Total Pwr	-36.1 dB	
31	Received Ranging Power	-202.83 dBm	30+12
32	Ranging Noise BW	-9.0 dB-Hz	.125 Tseq
33	Ranging SNR	-10.53 dB	
34	Required Ranging SNR	-5 dB	
35	Ranging Margin	-5.53 dB	

15) Downlink Budget: HGA at 3.6 AU with 34m (DSN)

#	Parameter	Value	Comments
1	S/C Transmitter	40 dBm	10 W
2	S/C Passive Loss	-1.5 dB	
3	S/C Antenna Gain	40 dBi	
4	EIRP	78.5 dBm	1+2+3
5	Free Space Loss	-285.57 dB	
6	Atmospheric Loss	-2 dB	
7	Polarization Loss	-2 dB	
8	Ground Receive Antenna Gain	68.1 dB	34m
9	Receiver Passive Loss	0.0 dB	
10	Pointing Loss	-1 dB	
11	Remodulation Noise Loss	-3 dB	
12	Total Received Power	-139.77 dB	4+5+6+7+8+9+10+11
13	Ground System G/T (DSN)	52.8 dB	
14	Antenna Noise Temperature	0.0 deg-K	Sun in Side Lobes
15	System Noise Temperature	34.0 deg-K	
16	System Noise Density	-183.3 dBm/Hz	
17	Carrier Power/Total Power	-17.8 dB	
18	Carrier Power Received	-157.57 dBm	12+17
19	Carrier Tracking BW	10.3 dB-Hz	10.8 Hz
20	CNR Power Received	15.43 dB	18-16-19
21	CNR Power Required	10 dB	Eb/No
22	Carrier Margin	5.43 dB	
23	Telemetry Data Pwr/Total Pwr	-2.5 dB	
24	Tlm Pwr Received	-142.27 dBm	12+23
25	TLM Data Rate	35.03 dB=Hz	24-16-26
26	TLM Pwr/Noise Pwr	6 dB	24-16-25
27	Detector Loss	-5 dB	DSN
28	Data Pwr/Noise Pwr Required	2.5 dB	BER=10E-6
29	TLM Data Margin	3.0	
30	Range Pwr/Total Pwr	-36.1 dB	
31	Received Ranging Power	-175.87 dBm	30+12
32	Ranging Noise BW	-9.0 dB-Hz	125 Tseq
33	Ranging SNR	16.43 Db	
34	Required Ranging SNR	-5 dB	
35	Ranging Margin	21.43 dB	

16) Downlink Budget: HGA at 3.6 AU with 70m (DSN)

#	Parameter	Value	Comments
1	S/C Transmitter	40 dBm	10W
2	S/C Passive Loss	-1.5 dB	
3	S/C Antenna Gain	40 dBi	
4	EIRP	78.5 dBm	1+2+3
5	Free Space Loss	-285.57 dB	
6	Atmospheric Loss	-2 dB	
7	Polarization Loss	-2 dB	
8	Ground Receive Antenna Gain	73.77 dB	70 m
9	Receiver Passive Loss	0.0 dB	
10	Pointing Loss	-1 dB	
11	Remodulation Noise Loss	-3 dB	
12	Total Received Power	-134.1 dBm	4+5+6+7+8+9+10+11
13	Ground System G/T (DSN)	52.8 dB	
14	Antenna Noise Temperature	0.0 deg-K	Sun in Side Lobes
15	System Noise Temperature	34.0 deg-K	
16	System Noise Density	-183.3 dBm/Hz	
17	Carrier Power/Total Power	-17.8 dB	
18	Carrier Power Received	-151.9 dBm	12+17
19	Carrier Tracking BW	10.3 dB-Hz	10.8 Hz
20	CNR Power Received	21.1 dB	18-16-19
21	CNR Power Required	10 dB	Eb/No
22	Carrier Margin	11.1 dB	
23	Telemetry Data Pwr/Total Pwr	-2.5 dB	
24	Tlm Pwr Received	-136.6 dBm	12+23
25	TLM Data Rate	11.7 kbps	24-16-26
26	TLM Pwr/Noise Pwr	6 dB	24-16-25
27	Detector Loss	5 dB	DSN
28	Data Pwr/Noise Pwr Required	2.5 dB	BER=10E-6
29	TLM Data Margin	3.0	
30	Range Pwr/Total Pwr	-36.1 dB	
31	Received Ranging Power	-170.2 dBm	30+12
32	Ranging Noise BW	-9.0 dB-Hz	125 Tseq
33	Ranging SNR	22.1 dB	
34	Required Ranging SNR	-5 dB	
35	Ranging Margin	27.1 dB	

17) Downlink Budget: LGA at 3.6 AU with 70m (DSN)

#	Parameter	Value	Comments
1	S/C Transmitter	40 dBm	10W
2	S/C Passive Loss	-1.5 dB	
3	S/C Antenna Gain	5 dB	
4	EIRP	43.5 dBm	1+2+3
5	Free Space Loss	-285.57 dB	
6	Atmospheric Loss	-2 dB	
7	Polarization Loss	-2 dB	
8	Ground Receive Antenna Gain	73.77 dB	70 m (DSN)
9	Receiver Passive Loss	0.0 dB	
10	Pointing Loss	-1 dB	
11	Remodulation Noise Loss	-3 dB	
12	Total Received Power	-168.9 dBm	4+5+6+7+8+9+10+11
13	Ground System G/T (DSN)	52.8 dB	
14	Antenna Noise Temperature	0.0 deg.K	Sun in Side Lobes
15	System Noise Temperature	34.0 deg.K	
16	System Noise Density	-183.3 dBm/Hz	
17	Carrier Power/Total Power	-17.8 dB	
18	Carrier Power Received	-186.7 dBm	12+17
19	Carrier Tracking BW	10.3 dB-Hz	10.8 Hz
20	Carrier Threshold Power	-163.3 dB	16+19+21
21	CNR Power Required	10 dB	Eb/No
22	Carrier Margin	-20.4 dB	18-20
23	Telemetry Data Pwr/Total Pwr	-2.5 dB	
24	Tlm Pwr Received	-171.4 Db	12+23
25	TLM Data Rate	5.9 dB	24-16-26
26	TLM Pwr/Noise Pwr	6 dB	24-16-25
27	Detector Loss	5 dB	DSN
28	Data Pwr/Noise Pwr Required	2.5 dB	BER=10E-6
29	TLM Data Margin	3.0	
30	Range Pwr/Total Pwr	-36.1 dB	
31	Received Ranging Power	-205 dB	30+12
32	Ranging Noise BW	-9.0 dB-Hz	125 Tseq
33	Ranging SNR	-12.7 dB	
34	Required Ranging SNR	-5 dB	
35	Ranging Margin	-7.7 dB	

APPENDIX D - ELECTRICAL POWER SUBSYSTEM

A. BATTERY DESIGN

First, a list defining the variables used in the design:

P_C = Power required for battery charging.

P_d = Power discharged.

P_{sar} = Power provided by solar array during recharging.

P_{sad} = Power provided by solar array during recharging.

P_X = Power required by entire system (excluding BCR) during transmission phase.

P_S = Power required by entire system (excluding BCR) during transmission phase.

C = Battery capacity.

t_r = Time for recharge.

t_d = Time of discharge.

η = Charging efficiency.

V_{bus} = Bus voltage (EOL).

V_{DB} = Minimum discharge voltage.

V_{BC} = Maximum charge voltage

V_{DD} = Voltage drop across bypass diode

V_D = Minimum discharge voltage of the battery cell

R = Charge rate

I_r = Recharge current

N = Number of battery cells

To determine the maximum charge voltage, it is assumed that the maximum allowable battery charge voltage is 1.5V per cell. Another assumption is that one cell became an open-circuit failure while charging and that it is accommodated by three series-connected diodes connected in parallel with the failed cell. Given 22 cells and a voltage drop of 0.8V for each diode

$$\begin{aligned} V_{BC} &= 1.5(N - 1) + 3V_{DD} \\ &= 1.5(21) + 3(0.8) \\ &= 33.9V \end{aligned}$$

The mass and dimensions of the solar array can be minimized by maximizing the power (P_d) provided by the battery to supplement the solar array during the entire transmission phase. However, this cannot exceed the amount of power the solar array can provide for powering the spacecraft and recharging the battery during the science phase. These are two of the primary factors driving the battery design.

During the discharge cycle ($t_d = 10$ hrs), the solar array must provide the peak power needed for the transmission phase minus the power being floated by the battery. This leads to

$$P_{srd} = P_x - P_d \quad (1)$$

However, during the time the battery is charging ($t_c = 14$ hrs), the solar array must provide adequate power for science data gathering and recharging the batteries. This gives the relationship

$$P_{sar} = P_s + P_c \quad (2)$$

The power delivered by the solar array in the transmission phase (P_{srd}) and the science phase (P_{sar}) must be equivalent; therefore,

$$P_c + P_s = P_x - P_d \quad (3)$$

The relationship between the power and the times associated with charging and discharging the battery is

$$P_d = \frac{t_r P_c \eta}{t_d} \quad (4)$$

Equations (3) and (4) give the criteria that restricts P_d and P_c . From the power profile, $P_x = 219W$ and $P_s = 169W$. Assuming a charging efficiency $\eta = 90\%$, and using t_r and t_d defined above, the two equations yield

$$P_c \approx 22W \text{ and } P_d \approx 27W.$$

Therefore, the maximum power the battery can provide to supplement the solar array during the transmission is 27W. The equation used to determine the capacity of the battery needed to provide this power is

$$C = \frac{P_d t_d}{V_{DB} (DOD)} \quad (5)$$

The minimum discharge voltage can be determined from the equation

$$V_{DB} = (N - 1) \times V_D - V_{DD} \quad (6)$$

For $N = 22$ cells, $V_D = 1.2V$, and $V_{DD} = 1.1V$, equation (6) gives

$$V_{DB} = 24.1V$$

Using a design DOD of 50% and the applicable values from above, the battery capacity found from equation (5) is

$$C = 22.4 \rightarrow 25AH.$$

In order to determine the charge rate needed to recharge the battery during the science phase, it is necessary to use the relationship between the power required to charge the battery and the charge rate.

$$P_c = I_r V_{BC} = \frac{C}{R} V_{BC} \quad (7)$$

By substituting equations (4) and (7) into equation (3), solving for C/R, and then substituting the appropriate values

$$\begin{aligned} \frac{C}{R} &= \frac{P_x - P_s}{V_{BC}} \cdot \frac{t_d}{t_d + t_r \times \eta} \\ &= \frac{219 - 169}{33.9} \cdot \frac{10}{10 + 14 \times 0.9} \\ &= 652.6 \text{ mA} \end{aligned}$$

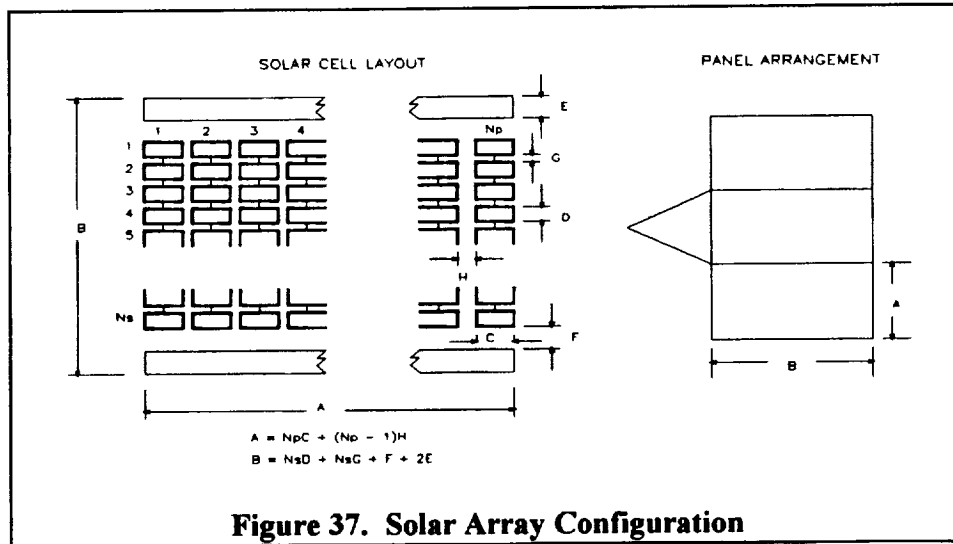
From this result, the charge rate for normal operation can be obtained by dividing the battery capacity, C, by the charge current which yields R = 38 for a capacity of 25AH.

B. SOLAR ARRAY DESIGN

The primary guidance for the design of the solar array came from the *Solar Cell Array Design Handbook* (JPL, 1976). The design procedure was established on a spreadsheet format (not shown) to facilitate updates due to changes mission description and refined design of other subsystems. The design was performed on four Spectrolab solar cells for comparison in order to determine the best combination of mass and dimensions. The cell selected is the K6700A silicon cell.

The solar array had to supply 33.9VDC at EOL in order to have adequate power to charge the battery. The design had to meet the mission requirements of all the four candidate asteroids. Because of the solar array voltage dependence on the array temperature, the voltage-sizing of the array must be determined for the "hot case" when the satellite is closest to the sun. The worst "hot case" occurs at the perihelion for Orpheus of 0.82AU. The resulting number of cells in series, N_s, is 104. The array current is more dependent on solar intensity, and therefore the current-sizing must be determined for when the satellite is furthest from the sun. This case occurs at the end of

mission of Selecus when the satellite is 2.75AU from the sun. The resulting number of strings needed in parallel, N_p , is 186. The relationships used to determine the substrate area are defined in the solar array layout diagram below. In addition the following tables provide the solar array design summary, the solar array mass breakdown, the EPS mass summary, and the solar array output at EOL and BOL.



CELL TYPE:	K6700A	K6700B	K7700A	GaAs/Ge
N_s	104	107	113	51
N_p	186	202	175	264
Number of panels	6	6	6	6
PANELS PER WING:	3	3	3	3
Corresponding number of cells in parallel	31	34	29	44
PANEL SIZE: (dimensions in meters)				
C = solar cell width (parallel)	0.040	0.040	0.040	0.040
H = cell gap (parallel)	0.001	0.001	0.001	0.001
D = cell length (series)	0.020	0.020	0.020	0.020
G = cell gap (series)	0.001	0.001	0.001	0.001
E = end contact bar width	0.005	0.005	0.005	0.005
F = end contact/cell gap	0.001	0.001	0.001	0.001
PANEL LENGTH:	1.27	1.39	1.19	1.80
PANEL WIDTH:	2.20	2.26	2.38	1.08
PANEL AREA:	2.79	3.15	2.83	1.95
ARRAY AREA:	16.73	18.87	16.99	11.71
TOTAL NUMBER OF CELLS	19344	21614	19662	13464
SUBSTRATE MASS:	12.29	13.87	12.49	8.60
CELL MASS:	8.51	4.15	8.65	10.77
COVERGLASS MASS:	5.19	5.80	5.28	3.61
TOTAL MASS:	26.00	23.82	26.42	22.99

Table 30. Solar Array Size and Layout

Component	Unit Mass	Qty of units	Total
Substrate (per panel)	2.050	6	12.30
Solar cells (per panel)	1.418	6	8.51
Coverglass (per panel)	0.865	6	5.19
Empty frame	9.400	2	18.80
Panel-Panel hinge	0.250	8	2.00
Yoke	2.750	2	5.50
Yoke-Panel hinge	0.270	4	1.08
Yoke-SADA hinge	1.360	2	2.72
Deployment system	-	-	4.48
Holddowns, cutters	0.470	12	5.64
Power harness	3.390	2	6.78
TOTAL			73.00

Table 31. Solar Array Mass Breakdown (kg)

	BOL (1AU)	EOL (2.75AU)
Pmax	1975.7	194.2
Vmp	45.9	34.2
Imp	43.0	5.7

Table 32. Solar Array Power Generation For Best and Worst Cases

APPENDIX E - ATTITUDE CONTROL CALCULATIONS

This appendix includes all of the MATLAB files used to model the satellite performance in three-axis stabilized mode. MATLAB 386 was the version used to develop the routines; small changes may be required to run these routines in other versions of MATLAB.

A. BUILDUP OF SOLAR TORQUE

```

% Iw is a property of the chosen wheel Iw=0.01592 N*M
  Iw=0.015992;   Omega=0*pi/180;
% The following parameters are variables
  Ixx=481; Iyy=310; Izz=559;
% The values below (Mn) are determined from the moment arm, thruster force and burn time of the
thruster.
  Mx=0.1068; My=0.1068; Mz=0.1246;
% Maximum Attitude errors
  PHImax=0.2*pi/180; THETAmx=0.2*pi/180; SImax=0.2*pi/180;
% System Time Constant
  e=2.71828182846;   Tsyphi=PHImax*Ixx*e/Msx;   Tsytheta=THETAmx*Iyy*e/Msy;
  Tsysi=SImax*Izz*e/Msz;
% Lead Time Constant
  Tphi=2*Tsyphi;   Ttheta=2*Tsytheta;   Tsi=2*Tsysi;
% Gain Constant
  Kphi=Ixx/(Tsyphi)^2;   Ktheta=Iyy/(Tsytheta)^2;   Ksi=Izz/(Tsysi)^2;
  tx=0:100:950400;
  NUMx=[Omega*Iw*Tsyphi^2 Tphi*Msx+Tphi*Omega*Iw Omega*Iw+Msx 0];
  DENx=[Tsyphi^2*Iw Tphi*Iw Iw 0 0];
  [y,x]=STEP(NUMx,DENx,tx);
  plot(tx/3600,y*30/pi);grid;xlabel('hours'); ylabel('RPMs');
  title('RPM (Momentum) Build up in Roll RWA due to solar pressure');
  ty=0:100:691200;
  NUMy=[Omega*Iw*Tsytheta^2 Ttheta*Msy+Ttheta*Omega*Iw Omega*Iw+Msy 0];
  DENy=[Tsytheta^2*Iw Ttheta*Iw Iw 0 0];
  [y,x]=STEP(NUMy,DENy,ty);
  plot(ty/3600,y*30/pi);grid;xlabel('hours'); ylabel('RPMs');
  title('RPM (Momentum) Build up in Pitch RWA due to solar pressure');
  tz=0:100:1036800;
  NUMz=[Omega*Iw*Tsysi^2 Tsi*Msz+Tsi*Omega*Iw Omega*Iw+Msz 0];
  DENz=[Tsysi^2*Iw Tsi*Iw Iw 0 0];
  [y,x]=STEP(NUMz,DENz,tz);
  plot(tz/3600,y*30/pi);grid;xlabel('hours'); ylabel('RPMs');
  title('RPM (Momentum) Build up in Yaw RWA due to solar pressure');
end

```

B. DESATURATION PERFORMANCE (1)

```
Iw=0.01592;   Omega=75*pi/180;
% The following parameters are variables
  Ixx=481; Iyy=310; Izz=559;
% The values below (Mn) are determined from the moment arm, thruster force and burn time of the
thruster.
  Mx=0.1068; My=0.1068; Mz=0.1246;
% Maximum Attitude errors
  PHImax=0.2*pi/180;   THETAmax=0.2*pi/180;   SImax=0.2*pi/180;
% System Time Constant
  e=2.71828182846;   Tsyphi=PHImax*Ixx*e/Mx;   Tsytheta=THETAmax*Iyy*e/My;
Tsyphi=PHImax*Izz*e/Mz;
% Lead Time Constant
  Tphi=2*Tsyphi;   Ttheta=2*Tsytheta;   Tsi=2*Tsyphi;
% Gain Constant
  Kphi=Ixx/(Tsyphi)^2;   Ktheta=Iyy/(Tsytheta)^2;   Ksi=Izz/(Tsyphi)^2;
% The equation for the reaction wheel angular momentum (and therefore
% speed) was also converted to a transfer function and plotted for
% a thruster firing interval to observe momentum desaturation.
WNUMx=[Omega*Iw*Tsyphi^2 Tphi*Mx+Tphi*Omega*Iw Omega*Iw*Mx 0];
WNUMy=[Omega*Iw*Tsytheta^2 Ttheta*My+Ttheta*Omega*Iw Omega*Iw*My 0];
WNUMz=[Omega*Iw*Tsyphi^2 Tsi*Mz+Tsi*Omega*Iw Omega*Iw*Mz 0];
WDENx=[Tsyphi^2*Iw Tphi*Iw Iw 0 0];
WDENZ=[Tsytheta^2*Iw Ttheta*Iw Iw 0 0];
WDENy=[Tsyphi^2*Iw Tsi*Iw Iw 0 0];
T2=Linspace (0,500);
WHSRADx=IMPULSE(WNUMx,WDENx,T2);
WHSRADz=IMPULSE(WNUMz,WDENZ,T2);
WHSRADy=IMPULSE(WNUMy,WDENy,T2);
% Converting radians per second to revolutions per minute (RPM).
WHSRPMx=WHSRADx*30/pi; WHSRPMz=WHSRADz*30/pi;
WHSRPMy=WHSRADy*30/pi;
plot (T2,WHSRPMx), grid,
title ('ROLL WHEEL SPEED DURING THRUSTER FIRING'),xlabel ('TIME sec.'),
ylabel ('WHEEL SPEED RPM');
plot (T2,WHSRPMz), grid,
title ('YAW WHEEL SPEED DURING THRUSTER FIRING'),xlabel ('TIME sec.'),
ylabel ('WHEEL SPEED RPM');
plot (T2,WHSRPMy), grid,
title ('PITCH WHEEL SPEED DURING THRUSTER FIRING'),xlabel ('TIME sec.'),
ylabel ('WHEEL SPEED RPM');
end
```

C. DESATURATION PERFORMANCE (2)

```
clear;clg;
Tx=86.89; Ty=55.78; Tz=173.3;Kx=0.2591; Ky=0.4035; Kz=0.07443; Ix=481; Iy=310;   Iz=559;
y2=[[0]; [.1246/Iz]];
```

```

[T2,Y2]=ode23('yawf',0,360,y2,0.00000001);
plot(T2/60,Y2(:,1)*180/pi);
y0=[[0]; [.1068/Iy]];
[T,Y]=ode23('pitchf',0,360,y0,0.00000001);
plot(T/60,Y(:,1)*180/pi);title('Error After Desaturation Firing');
xlabel('Minutes');ylabel('Error (deg)');
y1=[[0]; [.1068/Ix]];
[T1,Y1]=ode23('rollf',0,360,y1,0.00000001);
plot(T1/60,Y1(:,1)*180/pi);
Iw=0.01592; %This is assuming h=10 when nominal speed is 6000 RPM
h(1)=0.1068;
for i=2:length(T),
h(i)=h(i-1)-Ky*(Ty*Y(i-1,2)+Y(i-1,1))*(T(i)-T(i-1)); end;
RPM=30.*h./pi./Iw;
plot(T/60,RPM);
title('Wheel Speed After Desaturation');
xlabel('Minutes');ylabel('RPM');
h1(1)=0.1068;
for i=2:length(T1),
h1(i)=h1(i-1)-Kx*(Tx*Y1(i-1,2)+Y1(i-1,1))*(T1(i)-T1(i-1)); end;
RPM1=30.*h1./pi./Iw;
plot(T1/60,RPM1);
h2(1)=0.1246;
for i=2:length(T2),
h2(i)=h2(i-1)-Kz*(Tz*Y2(i-1,2)+Y2(i-1,1))*(T2(i)-T2(i-1)); end;
RPM2=30.*h2./pi./Iw;
plot(T2/60,RPM2);

```

D. SYSTEM STEP AND IMPULSE RESPONSE

The transfer functions for this routine are derived from the discussion in the Attitude Control section.

NUMsx=[0 0 1.569e-6]; NUMsy=[0 0 3.137e-6]; NUMsz=[0 0 1.542e-6];

NUMx=[0 0 0.1068]; NUMy=[0 0 0.1068]; NUMz=[0 0 0.1246];

% This is a property of the wheel chosen

Iw=0.01592; Ixx=481; Iyy=310; Izz=559;

% The values below (Mn) are determined from the moment arm, thruster force

% and burn time of the thruster.

Mx=0.1068; My=0.1068; Mz=0.1246;

% Maximum Attitude errors

PHIImax=0.2*pi/180; THETAmx=0.2*pi/180; SImax=0.2*pi/180;

% System Time Constant

e=2.71828182846; Tsyphi=PHIImax*Ixx*e/Mx; Tsytheta=THETAmx*Iyy*e/My;

Tsysi=SImax*Izz*e/Mz;

% Lead Time Constant

Tphi=2*Tsyphi; Tsi=2*Tsysi; Ttheta=2*Tsytheta;

% Gain Constant

Kphi=Ixx/(Tsyphi)^2; Ksi=Izz/(Tsysi)^2; Ktheta=Iyy/(Tsytheta)^2;

T=Linspace(0,400,400);

DENxx=[Ixx Kphi*Tphi Kphi];

```

DENzz=[Izz Ksi*Tsi Ksi];
DENyy=[Iyy Ktheta*Ttheta Ktheta];
IPERxx=IMPULSE(NUMx,DENxx,T);
IPERzz=IMPULSE(NUMy,DENzz,T);
IPERyy=IMPULSE(NUMz,DENzz,T);
SPERxx=STEP(NUMsx,DENxx,T);
SPERzz=STEP(NUMsy,DENzz,T);
SPERyy=STEP(NUMsz,DENyy,T);
% Converting radians to degrees.
IPExx=IPERxx*180/pi; IPEzz=IPERzz*180/pi; IPEyy=IPERyy*180/pi;
SPExx=SPERxx*180/pi; SPEzz=SPERzz*180/pi; SPEyy=SPERyy*180/pi;
plot(T,IPExx), grid,xlabel('TIME sec. '), ylabel('ROLL AXIS ERROR - deg');
title('ROLL AXIS ERROR IMPULSE RESPONSE TO THRUSTER FIRING')
plot(T,IPEzz), grid,xlabel('TIME sec. '), ylabel('YAW AXIS ERROR - deg');
title('YAW AXIS ERROR IMPULSE RESPONSE TO THRUSTER FIRING')
plot(T,IPEyy), grid,xlabel('TIME sec. '), ylabel('PITCH AXIS ERROR - deg');
title('PITCH AXIS ERROR IMPULSE RESPONSE TO THRUSTER FIRING')
plot(T,SPExx), grid, title('ROLL AXIS ERROR SOLAR STEP RESPONSE')
xlabel('TIME sec. '), ylabel('ROLL AXIS ERROR - deg. ');
plot(T,SPEyy), grid, title('PITCH AXIS ERROR SOLAR STEP RESPONSE')
xlabel('TIME sec. '), ylabel('PITCH AXIS ERROR - deg. ');
plot(T,SPEzz), grid, title('YAW AXIS ERROR SOLAR STEP RESPONSE')
xlabel('TIME sec. '), ylabel('YAW AXIS ERROR - deg. ');
end

```

E. REORIENTATION

```

y0=[[-30*pi/180];[ 0]];
[T, Y]=ode23('pitchf',0,240,y0,0.00000001);
plot(T/60, Y(:,1)*180/pi);
y10=[[-30*pi/180];[ 0]];
[T1, Y1]=ode23('rollf',0,240,y10,0.00000001);
plot(T1/60, Y1(:,1)*180/pi);
y20=[[-30*pi/180];[ 0]];
[T2, Y2]=ode23('yawf',0,240,y20,0.00000001);
plot(T2/60, Y2(:,1)*180/pi);
title('Response to Initial Error of 30 Degrees');
ylabel('Angular Error (Degrees)');xlabel('Minutes');

```

APPENDIX F - PROPULSION CALCULATIONS

Launch vehicle weight is 570 kg for the Delta-II 7925 rocket with a C3 of 40 km²/sec². The launch weight with a C3 of 36.5 km²/sec² is 605 kg. The estimated wet weight of the spacecraft is 725 kg, and all propulsion calculations assume this mass. The propellant weight is calculated to be 327.4 kg at an I_{sp} of 314 sec, using equation 1.

$$M_p = M_i \left[1 - e^{-\Delta v / I_{sp} g} \right] \quad (1)$$

With an oxidizer to fuel ratio of .77/1, the mass of oxidizer (N₂O₄) is 142.4 kg and the mass of fuel (N₂H₄) is 185.0 kg. Assuming 5 kg of N₂H₄ is required for attitude control, the final propellant masses are 142.4 kg of N₂O₄ and 190.0 kg of N₂H₄.

The density of N₂O₄ is 1477 kg/m³, giving a volume of 0.0964m³. Assuming 5% volume for screens for the propulsion management system and 5% ullage, the volume required is 0.1071m³. Using equal sized tanks, two tanks of 0.47m diameter are required. Using a density of 1011 kg/m³ for N₂H₄, the required propellant volume is 0.1879m³. Assuming the same margins (total margin of 10%), the tank volume required is 0.2088 m³. Two tanks of 0.59m diameter are required.

Pressurant volume is calculated based on propellant feed pressure of 200 psi, computed propellant tank volumes above, and a pressurant tank pressure of 4000 psi. Each pressurant tank is connected to an N₂H₄ tank and an N₂O₄ tank. Propellant tank volume for two tanks is 0.1457m³ (discounting ullage and screen volume). Using P₁V₁=P₂V₂, pressurant volume is calculated to be 0.007285 m³. Thus, each pressurant tank has a diameter of 0.24 meters. With a N₂ density of 1.2506 kg/m³, the total N₂ mass is 5.0 kg (2.50 kg/tank).

APPENDIX G - MASS BUDGET SPREADSHEET

The following pages are a listing of the spreadsheet used to formulate the mass budget.

SUB-SYSTEM COMPONENTS		MASS		TYPE		DIMENSIONS				LOCATION			MOMENTS OF INERTIA			PRODUCTS OF INERTIA				
		S	C	B	a	b	c	r	l	t2	l	X	Y	Z	lxx	lyy	lzz	lxy	lzx	lyz
Electric Power	2.13E+01	1			0.35	0.25	0.25					-0.41	-0.49	0.22	6.37E+00	4.94E+00	9.02E+00	4.28E+00	-1.92E+00	-2.30E+00
Battery (Ni-H)	1.00E+00	1						1.00	1.20			0.00	0.00	0.00	8.18E-01	8.18E-01	8.18E-01	0.00E+00	0.00E+00	0.00E+00
Battery Charge Regulator	3.40E+00	1						1.00	1.20			0.00	0.00	0.00	2.78E+00	2.78E+00	2.78E+00	0.00E+00	0.00E+00	0.00E+00
Power Distribution Unit	3.00E+00	1						1.00	1.20			0.00	0.00	0.00	2.45E+00	2.45E+00	2.45E+00	0.00E+00	0.00E+00	0.00E+00
Power Conditioning	6.95E+00	1			3.81	2.20	0.02					0.00	1.75	0.00	2.41E+01	8.41E+00	3.25E+01	0.00E+00	0.00E+00	0.00E+00
Empty Frame	6.95E+00	1			3.81	2.20	0.02					0.00	-1.75	0.00	2.41E+01	8.41E+00	3.25E+01	0.00E+00	0.00E+00	0.00E+00
(stowed)		1			1.27	0.09	2.20					0.00	0.76	0.30						
(stowed)		1			1.27	0.09	2.20					0.00	-0.76	0.30						
Solar array	2.39E+01	1			3.81	2.20	0.02					0.00	1.75	0.00	8.27E+01	2.89E+01	1.17E+02	0.00E+00	0.00E+00	0.00E+00
	2.39E+01	1			3.81	2.20	0.02					0.00	-1.75	0.00	8.27E+01	2.89E+01	1.17E+02	0.00E+00	0.00E+00	0.00E+00
(stowed)		1			1.27	0.09	2.20					0.00	0.76	0.30						
(stowed)		1			1.27	0.09	2.20					0.00	-0.76	0.30						
Solar array Drive Assemblies(2)	2.30E+00	1			0.1	0.1	0.1					0.00	0.59	0.00	8.04E-01	3.83E-03	8.04E-01	0.00E+00	0.00E+00	0.00E+00
	2.30E+00	1			0.10	0.10	0.10					0.00	-0.59	0.00	8.04E-01	3.83E-03	8.04E-01	0.00E+00	0.00E+00	0.00E+00
Panel Hinges (6)	1.80E+00	1						1.00	1.20			0.00	0.00	0.00	1.47E+00	1.47E+00	1.47E+00	0.00E+00	0.00E+00	0.00E+00
Yoke (2)	2.80E+00	1										0.00	0.64	0.00	1.15E+00	0.00E+00	1.15E+00	0.00E+00	0.00E+00	0.00E+00
	2.80E+00	1										0.00	-0.64	0.00	1.15E+00	0.00E+00	1.15E+00	0.00E+00	0.00E+00	0.00E+00
Yoke Hinge (2)	1.40E+00	1						1.00	1.20			0.00	0.00	0.00	1.14E+00	1.14E+00	1.14E+00	0.00E+00	0.00E+00	0.00E+00
Cable Wiring	6.00E+00	1						1.00	1.20			0.00	0.00	0.00	4.91E+00	4.91E+00	4.91E+00	0.00E+00	0.00E+00	0.00E+00
Harness	7.00E+00	1						1.00	1.20			0.00	0.00	0.00	5.72E+00	5.72E+00	5.72E+00	0.00E+00	0.00E+00	0.00E+00
Hold-down Mechanism (2)	9.00E+00	1						1.00	1.20			0.00	0.00	0.00	7.36E+00	7.36E+00	7.36E+00	0.00E+00	0.00E+00	0.00E+00
Pyros	5.00E-01	1						1.00	1.20			0.00	0.00	0.00	4.09E-01	4.09E-01	4.09E-01	0.00E+00	0.00E+00	0.00E+00
	1.26E+02																			
Structure																				
Central Tube	7.29E+00	1						0.23	0.23	0.93	0.00	0.00	0.00	0.00	7.17E-01	7.17E-01	3.82E-01	0.00E+00	0.00E+00	0.00E+00
Equipment Sides	3.51E+00	1			1.50	0.03	1.30					0.00	0.64	0.00	1.91E+00	1.13E+00	2.07E+00	0.00E+00	0.00E+00	0.00E+00
	3.51E+00	1			1.50	0.03	1.30					0.00	0.64	0.00	1.91E+00	1.13E+00	2.07E+00	0.00E+00	0.00E+00	0.00E+00
Center Deck	3.44E+00	1			1.50	1.24	0.02					0.00	0.00	0.00	4.41E-01	6.45E-01	1.09E+00	0.00E+00	0.00E+00	0.00E+00
Struts	1.60E+00	1						0.23	1.40			0.00	0.00	0.00	1.26E+00	1.26E+00	1.26E+00	0.00E+00	0.00E+00	0.00E+00
	1.60E+00	1						0.23	1.40			0.00	0.00	0.00	1.26E+00	1.26E+00	1.26E+00	0.00E+00	0.00E+00	0.00E+00
	1.60E+00	1						0.23	1.40			0.00	0.00	0.00	1.26E+00	1.26E+00	1.26E+00	0.00E+00	0.00E+00	0.00E+00
	1.60E+00	1						0.23	1.40			0.00	0.00	0.00	1.26E+00	1.26E+00	1.26E+00	0.00E+00	0.00E+00	0.00E+00
	1.60E+00	1						0.23	1.40			0.00	0.00	0.00	1.26E+00	1.26E+00	1.26E+00	0.00E+00	0.00E+00	0.00E+00
	1.60E+00	1						0.23	1.40			0.00	0.00	0.00	1.26E+00	1.26E+00	1.26E+00	0.00E+00	0.00E+00	0.00E+00
Strut Connections	3.00E+00	1						0.23	1.40			0.00	0.00	0.00	1.26E+00	1.26E+00	1.26E+00	0.00E+00	0.00E+00	0.00E+00
Thrust Cone	6.39E+00	1						0.68	0.70	0.53	0.00	0.00	0.00	-0.73	5.03E+00	3.04E+00	3.04E+00	0.00E+00	0.00E+00	0.00E+00

SUB-SYSTEM/COMPONENTS	MASS	TYPE	DIMENSIONS						LOCATION			MOMENTS OF INERTIA						PRODUCTS OF INERTIA					
			S	C	B	a	b	c	r1	r2	l	X	Y	Z	lxx	lxy	lzz	lyz	lxx	lxy	lzz	lyz	
Side panels	3.05E+00	1	0.02	1.30	1.30					0.00	0.00	0.76	2.62E+00	2.19E+00	4.30E-01	0.00E+00	0.00E+00	0.00E+00	0.00E+00	0.00E+00	0.00E+00	0.00E+00	
Rings (6)	1.57E+00	1					0.46	0.46	0.04	0.00	0.00	-0.76	2.62E+00	2.19E+00	4.30E-01	0.00E+00	0.00E+00	0.00E+00	0.00E+00	0.00E+00	0.00E+00		
tank	3.05E+00	1	0.02	1.30	1.30					0.00	0.00	0.76	2.62E+00	2.19E+00	4.30E-01	0.00E+00	0.00E+00	0.00E+00	0.00E+00	0.00E+00	0.00E+00		
center ring	1.57E+00	1					0.46	0.46	0.04	0.00	0.00	0.23	2.50E-01	2.50E-01	3.33E-01	0.00E+00	0.00E+00	0.00E+00	0.00E+00	0.00E+00	0.00E+00		
center ring	2.70E+00	1					0.46	0.47	0.04	0.00	0.00	-0.46	8.60E-01	8.60E-01	5.78E-01	0.00E+00	0.00E+00	0.00E+00	0.00E+00	0.00E+00	0.00E+00		
bottom ring	7.80E+00	1					0.46	0.48	0.06	0.00	0.00	-0.97	8.20E+00	8.20E+00	1.72E+00	0.00E+00	0.00E+00	0.00E+00	0.00E+00	0.00E+00	0.00E+00		
top ring	3.50E+00	1					0.46	0.48	0.04	0.00	0.00	0.49	1.23E+00	1.23E+00	7.74E-01	0.00E+00	0.00E+00	0.00E+00	0.00E+00	0.00E+00	0.00E+00		
Fuel and N2 Tank Mounts	5.00E+00	1											0.00E+00	0.00E+00	0.00E+00	0.00E+00	0.00E+00	0.00E+00	0.00E+00	0.00E+00	0.00E+00		
Top Deck	3.00E+00	1											0.00E+00	0.00E+00	0.00E+00	0.00E+00	0.00E+00	0.00E+00	0.00E+00	0.00E+00	0.00E+00		
Bottom Deck	3.00E+00	1											0.00E+00	0.00E+00	0.00E+00	0.00E+00	0.00E+00	0.00E+00	0.00E+00	0.00E+00	0.00E+00		
	7.69E+01																						
Thermal Control																							
MLI (.55kg/m ² x 8m ²)	4.40E+00	1					1.30	1.40		0.00	0.00	0.00	5.36E+00	5.36E+00	5.36E+00	0.00E+00	0.00E+00	0.00E+00	0.00E+00	0.00E+00	0.00E+00		
OSR (.55kg/m ² x 1.5m ²)	8.25E-01	1					1.30	1.40		0.00	0.00	0.00	1.00E+00	1.00E+00	1.00E+00	0.00E+00	0.00E+00	0.00E+00	0.00E+00	0.00E+00	0.00E+00		
Heaters, paint, etc	3.00E+00	1					1.30	1.40		0.00	0.00	0.00	3.65E+00	3.65E+00	3.65E+00	0.00E+00	0.00E+00	0.00E+00	0.00E+00	0.00E+00	0.00E+00		
	8.23E+00																						
Propulsion																							
Propellants:																							
NTO (delta v)	7.12E+01	1					0.00	0.23		0.00	0.00	0.23	5.27E+00	5.27E+00	1.51E+00	0.00E+00	0.00E+00	0.00E+00	0.00E+00	0.00E+00	0.00E+00		
	7.12E+01	1					0.00	0.23		0.00	0.00	-0.23	5.27E+00	5.27E+00	1.51E+00	0.00E+00	0.00E+00	0.00E+00	0.00E+00	0.00E+00	0.00E+00		
N2H4 (delta v) 178 6kg	9.50E+01	1					0.00	0.29		0.29	0.45	0.00	2.24E+01	1.12E+01	3.04E+01	1.24E+01	0.00E+00	0.00E+00	0.00E+00	0.00E+00	0.00E+00		
N2H4 (air cont) 5kg	9.50E+01	1					0.00	0.29		-0.29	-0.45	0.00	2.24E+01	1.12E+01	3.04E+01	1.24E+01	0.00E+00	0.00E+00	0.00E+00	0.00E+00	0.00E+00		
N2	2.35E+00	1					0.00	0.13		-0.55	-0.15	0.00	6.76E-02	7.26E-01	7.78E-01	1.94E-01	0.00E+00	0.00E+00	0.00E+00	0.00E+00	0.00E+00		
	2.35E+00	1					0.00	0.13		0.55	0.15	0.00	6.76E-02	7.26E-01	7.78E-01	1.94E-01	0.00E+00	0.00E+00	0.00E+00	0.00E+00	0.00E+00		
	3.37E+02																						
Thrusters																							
105 lbf (468N)	4.20E+00	1	0.20	0.20	0.30					0.00	0.00	-0.60	1.56E+00	1.56E+00	2.80E-02	0.00E+00	0.00E+00	0.00E+00	0.00E+00	0.00E+00	0.00E+00		
1 lbf (4.5N) 12 @ .33	3.96E+00	1					1.30	1.40					4.82E+00	4.82E+00	4.82E+00	0.00E+00	0.00E+00	0.00E+00	0.00E+00	0.00E+00	0.00E+00		
Pressure Vessels																							
NTO 45m dia 2 @ 5.0	5.00E+00	1					0.23	0.23		0.00	0.00	0.23	4.37E-01	4.37E-01	1.73E-01	0.00E+00	0.00E+00	0.00E+00	0.00E+00	0.00E+00	0.00E+00		
	5.00E+00	1					0.23	0.23		0.00	0.00	-0.23	4.37E-01	4.37E-01	1.73E-01	0.00E+00	0.00E+00	0.00E+00	0.00E+00	0.00E+00	0.00E+00		
N2H4 .55 dia 2 @ 7.0	7.00E+00	1					0.29	0.29		0.29	0.45	0.00	1.80E+00	9.74E-01	2.39E+00	9.14E-01	0.00E+00	0.00E+00	0.00E+00	0.00E+00	0.00E+00		
	7.00E+00	1					0.29	0.29		-0.29	-0.45	0.00	1.80E+00	9.74E-01	2.39E+00	9.14E-01	0.00E+00	0.00E+00	0.00E+00	0.00E+00	0.00E+00		
N2 24m dia 2 @ 1.5	1.50E+00	1					0.13	0.13		-0.55	-0.15	0.00	5.00E-02	4.70E-01	5.04E-01	1.24E-01	0.00E+00	0.00E+00	0.00E+00	0.00E+00	0.00E+00		
	1.50E+00	1					0.13	0.13		0.55	0.15	0.00	5.00E-02	4.70E-01	5.04E-01	1.24E-01	0.00E+00	0.00E+00	0.00E+00	0.00E+00	0.00E+00		

SUB-SYSTEM/COMPONENTS	MASS		TYPE		DIMENSIONS						LOCATION				MOMENTS OF INERTIA				PRODUCTS OF INERTIA			
	S	C	B	A	a	b	c	r1	r2	l	X	Y	Z	Ixx	Iyy	Izz	Ixy	Ixz	Iyz			
Misc: (subtotal of below)	5.67E+00		1					0.40	0.50		0.00	0.00	-0.50	2.20E+00	2.20E+00	7.81E-01	0.00E+00	0.00E+00	0.00E+00			
Filters 4 @ .166	6.64E-01																					
Pressure Transducer 4 @ .191	7.64E-01																					
F/D-F/V Valves 6 @ .076	4.56E-01																					
Isolation Valves 8 @ .286	2.29E+00																					
Plumbing	1.50E+00																					
	4.88E+01																					
Attitude Control																						
Star Camera	6.00E+00		1		0.10	0.20	0.10							2.50E-02	1.00E-02	2.50E-02	0.00E+00	0.00E+00	0.00E+00			
Gyros FOGS	2.00E+00		1					0.90	1.00					1.21E+00	1.21E+00	1.21E+00	0.00E+00	0.00E+00	0.00E+00			
Sun Sensors 3 @ .46	6.90E-01		1		0.05	0.05	0.01			1.91	2.85	0.00	0.00	5.60E+00	2.52E+00	8.12E+00	3.76E+00	0.00E+00	0.00E+00			
	6.90E-01		1		0.05	0.05	0.01			-1.91	-2.85	0.00	0.00	5.60E+00	2.52E+00	8.12E+00	3.76E+00	0.00E+00	0.00E+00			
Reaction Wheels 4 @ 3.78	1.51E+01		1		0.55	0.40	0.40			-0.13	-0.42	-0.20	0.00	3.68E+00	1.42E+00	3.49E+00	7.94E-01	3.78E-01	1.27E+00			
	2.45E+01																					
Integration																						
Electrical	2.00E+01		1					1.00	1.30					1.81E+01	1.81E+01	1.81E+01	0.00E+00	0.00E+00	0.00E+00			
Mechanical	8.00E+00		1					1.00	1.30					7.25E+00	7.25E+00	7.25E+00	0.00E+00	0.00E+00	0.00E+00			
	2.88E+01																					
Payload																						
Visible Imager	3.50E+00		1		0.20	0.20	0.20			0.65	0.00	-0.22	0.00	1.93E-01	1.67E+00	1.50E+00	0.00E+00	0.00E+00	-5.01E-01			
IR Spectrometer	1.60E+01		1		0.10	0.10	0.10			0.70	0.00	0.70	0.00	7.87E+00	1.57E+01	7.87E+00	0.00E+00	0.00E+00	7.84E+00			
Data and Control Sys Convrtr	1.00E+00		1					1.20	1.40					1.14E+00	1.14E+00	1.14E+00	0.00E+00	0.00E+00	0.00E+00			
Data and Control System	6.00E+00		1					1.20	1.40					6.83E+00	6.83E+00	6.83E+00	0.00E+00	0.00E+00	0.00E+00			
Laser Altimeter	5.00E+00		1		0.10	0.10	0.10			0.70	0.25	0.70	0.00	2.77E+00	4.91E+00	2.77E+00	8.75E-01	2.45E+00	8.75E-01			
Magnetometer	1.00E+00		1					1.20	1.40					1.14E+00	1.14E+00	1.14E+00	0.00E+00	0.00E+00	0.00E+00			
RF Communications																						
Parabolic Antennas (HGA)	5.00E+00		1					0.49	0.50	0.10	0.00	0.00	0.53	2.02E+00	2.02E+00	1.23E+00	0.00E+00	0.00E+00	0.00E+00			
Low Gain Antennas (4)	4.00E+00		1					1.30	1.50					5.27E+00	5.27E+00	5.27E+00	0.00E+00	0.00E+00	0.00E+00			
Power Amp (2)	5.00E+00		1					1.30	1.50					6.59E+00	6.59E+00	6.59E+00	0.00E+00	0.00E+00	0.00E+00			
Transponder (2)	5.00E+00		1					1.30	1.50					6.59E+00	6.59E+00	6.59E+00	0.00E+00	0.00E+00	0.00E+00			
DC/DC Converter (2)	5.00E+00		1					1.30	1.50					6.59E+00	6.59E+00	6.59E+00	0.00E+00	0.00E+00	0.00E+00			
Diplexer (2)	1.00E+00		1					1.30	1.50					1.32E+00	1.32E+00	1.32E+00	0.00E+00	0.00E+00	0.00E+00			
Coax Switches (2)	1.00E+00		1					1.30	1.50					1.32E+00	1.32E+00	1.32E+00	0.00E+00	0.00E+00	0.00E+00			
Coax Cables	1.00E+00		1					1.30	1.50					1.32E+00	1.32E+00	1.32E+00	0.00E+00	0.00E+00	0.00E+00			

REFERENCES

- Agrawal, B., *Design of Geosynchronous Spacecraft*, Englewood Cliffs: Prentice-Hall, 1986
- AIAA, *Supplemental Data Package for A Near-Earth Asteroid Rendezvous (NEAR) Mission*, AIAA Graduate Student Design Competition, 1992/ 1993.
- Applied Physics Laboratory, *Near Earth Asteroid Rendezvous - Report to Discovery Science Working Group NASA Solar System Exploration Division*, The John Hopkins University Applied Physics Laboratory, May 1991.
- Chetty, P.R.K., *Switch-Mode Power Supply Design*, Tab Books, Inc., 1986.
- Couch, L.W., *Digital and Analog Communication Systems*, 3rd ed., MacMillan Publishing Company, New York, 1990.
- Editors of Time-Life Books, *Understanding Computers: Space*, Time-Life 1991.
- Fortescue, P., and Stark, J., *Spacecraft Systems Engineering*, Wiley & Sons, New York, 1991.
- Griffin, M. D., and French, J. R., *Space Vehicle Design*, AIAA, Washington, D.C., 1991.
- Ha, T.T., *Digital Satellite Communications*, MacMillan Publishing Company, New York, 1986.
- Hirasawa, K. , *Analysis, Design, and Measurement of Small and Low-Profile Antennas*, Artech House, Inc., Mass., 1992.
- Jet Propulsion Laboratory Publication SP 43-38, *Solar Cell Array Design Handbook*, v. 1, Oct. 1976.
- Leonard & Levine, *Using Matlab to Analyze and Design Control Systems*, New York: Benjamin & Cummings, 1992
- Mars Observer-Telecommunications Design Control Document*, Doc. # 642-3309-TLC, Jet Propulsion Laboratory, California Institute of Technology, JPL D-8630, September 1991.
- Martin Marietta, *Discovery Program - Near Earth Object Spacecraft Study: Rendezvous Mission*, Martin Marietta, June 1991.

McDonnell Douglas Astronautics Company, *Delta II Commercial Spacecraft Users Manual*, 1987.

Rulf, B., *Understanding Antennas for Radar, Communications, and Avionics*, Van Nostrand Reinhold Company, New York, 1987.

Sortun, C., AE 4781 Spacecraft Design Project, *High Temperature Superconducting Infrared Imaging Satellite*, Monterey: Naval Postgraduate School, 1991

Tada, H.Y. et al., *Solar Cell Radiation Handbook*, Jet Propulsion Laboratory Publication 82-69, 3rd. ed., 1982.